A Laboratory Study on the Ability of Head Kinematics to Predict Brain Strains in Helmeted Head Impacts

by

Brooklynn Marie Knowles

A thesis submitted in partial fulfillment of the requirements for the degree of

Doctor of Philosophy

Department of Mechanical Engineering
University of Alberta

Abstract

Sports and recreation are a leading cause of traumatic brain injury (TBI) in North America, accounting for nearly 30% of TBI cases in youth in Canada. Contact sports, such as hockey and football, put athletes at greater risk of suffering mild traumatic brain injuries (mTBI, such as concussion), relative to the general population, despite mandated helmeted use. The ability of today's helmets to protect against brain injuries, is now under consideration. Nearly all modern helmets are certified against linear acceleration, which has been linked to severe focal injuries such as contusions or hemorrhages. In mitigating linear acceleration, today's helmets are credited with providing life-saving protection in direct head impacts.

Diffuse brain injury (of which concussion is one example) refers to widespread injury in the white matter of the brain. Angular kinematics are linked to diffuse brain injury, though helmet certification standards to date focus on limiting linear kinematics, with the exception of the National Operating Committee on Standards for Athletic Equipment (NOCSAE) that now also considers angular acceleration in helmet certification. Discussions surround how helmets may be assessed relative to kinematics linked to diffuse injury, however a consensus has not been reached regarding which kinematics this would include.

The objective of this thesis is to identify head kinematics that predict finite element model brain strain metrics and use the results to develop a kinematic metric that could be appropriate for use in helmet assessment.

Helmeted impacts were performed with a guided rail drop using the Hybrid III head and neck as well as with the Hybrid III head without a neck. Impacts were conducted at various

locations to ice hockey and football helmets at impact velocities ranging from 1.2 to 5.8 m/s and 3.9 to 6.1 m/s for hockey and football helmets, respectively, monitoring linear and angular head kinematics throughout each impact. Directional linear acceleration and angular velocity were input to the Improved Simulated Injury Monitor (SIMon) to compute brain strain metrics CSDM-15 and MPS.

Multiple regression techniques compared linear regression models based on different linear and angular kinematics from one single kinematic predictor to five kinematics in a single regression model. Adjusted R^2 was calculated for each model to determine which model best fit the data for each impact scenario. Comparing models that had similar R^2, the F-statistic was calculated to determine whether one of the compared models was significantly more descriptive of the data, than the other.

Peak resultant angular velocity (ω_R) overall yielded the greatest R^2 and F statistic values relative to other single kinematics as well as multi-kinematic regression models, for certification-style helmeted impacts with or without the Hybrid III neck. Arguably, ω_R could be chosen as a single kinematic predictor for strain. Choosing a single kinematic variable maximized the F-statistic as it required only a single variable to predict strain with $R^2>0.8$. This finding was consistent for impacts with and without the Hybrid III neck for hockey and football helmet impacts.

This study also found that the impact time duration for simulation influences maximum strain values for impacts without the Hybrid III neck. Strain values continued to increase after linear and angular impact kinematics had returned to zero or stabilized. Strain plots for no-neck impacts reached a local maximum at approximately 25 ms after initial impact and it was

noted that after impact, the headform continued to translate and rotate away from the impact site, an unlikely occurrence in a real human impact. Therefore, time duration for no-neck simulation was limited to 25 ms. It is noted that research groups conducting no-neck analyses should consider the effect of time duration.

This thesis documents which kinematics best predict brain strain metrics for certification style guided drop impacts using HybridIII test equipment for two plausible impact paradigms: a head tethered to a neck and a head free falling, absent a neck. Additionally, it documents that the time duration of simulated kinematics influence magnitude of brain strains. These findings will be of particular interest to the helmet assessment community which is currently discussing how certification methods might change. Therefore, this thesis also documents one possible approach to use the presented experimental methods and kinematics to identify a pass/fail threshold based on predicted brain strain.

Preface

This is an original work by Brooklynn Knowles. Much of the work surrounding methods and early results has been previously published as listed below.

B. M. Knowles, and C. R. Dennison, "Predicting cumulative and maximum brain strain measures from Hybrid III head kinematics: A combined laboratory study and post-hoc regression analysis". *Annals of Biomedical Engineering*. vol. 45, pp 2146-2158, 2017.

B. M. Knowles, S. R. MacGillivray, J. A. Newman, and C. R. Dennison, "Influence of rapidly successive head impacts on brain strain in the vicinity of bridging veins", *Journal of Biomechanics*, vol. 59, pp. 59–70, 2017.

B. M. Knowles, H. Yu, and C. R. Dennison, "Accuracy of a Wearable Sensor for Measures of Head Kinematics and Calculation of Brain Tissue Strain," *Journal of Applied Biomechanics*, vol. 33, pp 2-11, 2017.

The methods presented in this thesis were also used to advance the research presented in the following papers, which I co-authored:

H. Y. Yu, **B. M. Knowles**, and C. R. Dennison, "A Test Bed to Examine Helmet Fit and Retention and Biomechanical Measures of Head and Neck Injury in Simulated Impact", *JoVE Journal of Visualized Experiments*, no. 127, pp. e56288, Sep. 2017

R.C. Butz, **B.M. Knowles**, J.A. Newman, C.R. Dennison, "Effects of External Helmet Accessories on Biomechanical Measures of Head Injury Risk: An ATD Study Using the Hybrid III Headform". *Journal of Biomechanics*, vol. 48, pp 3816-3824, 2015.

Acknowledgements

I would like to first thank my supervisor Dr. Christopher Dennison for the countless hours he has spent providing guidance and support. From advice in research meetings, to extensive review of my written documents and any and all discussions in between, he has always aimed to make me a better researcher and I cannot thank him enough for his efforts.

I would also like to thank my supervisory committee: Dr. James Newman for his endless insight and motivation to improve the helmet community and Dr. Jason Carey and Dr. Albert Vette for their time and guidance throughout this entire process.

To everyone on my committee, I thank you for your discussion, ideas and feedback that have been absolutely invaluable.

I would also like to thank my fellow members of the Biomedical Instrumentation Lab for creating such a positive work environment.

And finally, thank you to my family and friends for all of their support over the years. Special thanks to Shari Neis, Brayden Wells, Abby Knowles and Katie Smith, for always being there for me with encouragement and love when I needed it most.

Table of Contents

List of Tables

List of Figures

1 Introduction

Traumatic brain injury (TBI) accounted for approximately 2.5 million emergency room visits, hospitalizations and deaths in one year in the United States [1]. The economic cost of TBI was estimated to be over $76.5 billion in 2010, including direct medical costs and indirect costs such as lost wages and productivity [2], while potential long-term effects on an individual's quality of life are immeasurable. The most common cause for TBI hospitalization behind falls and motor vehicle accidents is due to sport and recreation related injuries [3]. Nearly 30% of TBI cases in children and youth in Canada is related to sports and recreation [4]. Contact sports, such as football and hockey show considerable risk for brain injury, despite mandated helmet use. A study released in 2012 showed that while fatal brain injuries in football steadily decreased, brain injuries causing disability increased each year from 1984 to 2010 [5]. Hockey players are reported to experience brain injuries at rates (per 1000 exposures) of 0.54 for high school [6], 0.41-3.1 for collegiate [7], [8] and 1.81 for professional [9]. Discussions now surround head protection as one method for reducing risk of sport-related brain injury.

Today's helmets are credited with providing life-saving protection against severe head trauma that may otherwise cause death. Helmets have been designed and certified to limit the peak linear acceleration of one's head during an impact, which has led to the success of today's helmets in mitigating what are considered severe focal injuries such as contusions, hemorrhages or, in extreme cases, skull fracture. It may be perceived that helmets should also protect against injuries such as concussion, referred to as diffuse brain injury, however, this was not their original intent and at present, there is no method for quantifying a helmet's ability to do just that.

Research dating back decades has linked diffuse brain injury to angular kinematics. As will be discussed in detail in the next chapter, this has been done using surrogate gel models [10], studying animal response [11], [12], using cadavers [13] and evaluating human volunteer data [14], [15]. There is still no agreement, however, on which angular kinematic should be used as a method for predicting brain injury risk for helmeted impacts and most helmet certification methods do not include angular kinematic thresholds.

This thesis investigates one possible method for which helmets can be assessed based on kinematics that can ultimately be linked to brain injury risk. The method used in this study focuses on sport helmet impacts produced in a laboratory setting and do not reflect game reconstruction impacts. Hockey and football helmeted impacts are reconstructed, and impact kinematics are tracked to be used as inputs to a brain finite element model (BFEM) allowing the relationship between impact kinematics and computed strain metrics to be investigated. Guided linear drops provide impact conditions for an anthropomorphic test device (ATD) head and neck and the resulting linear and angular kinematics provide input to the BFEM to compute brain strain metrics. With the understanding of which kinematics are best correlated to computed brain strain in the helmeted impacts created here, a metric can be developed, based on the findings, that could be used to certify helmets using the methods presented in this thesis.

1.1 Thesis objectives

The overarching objective of this thesis is to identify head kinematics that predict finite element model brain strain metrics and secondarily to construct a kinematic metric based on these results that can be used during helmet assessment. This thesis will discuss in detail the experimental protocol for various test configurations and outline the data analysis process to identify ideal impact kinematics for predicting strain.

Successful completion of this thesis work will provide researchers and helmet manufacturers with a kinematic-based metric that correlates to computed strain metrics during certification-style helmeted impacts. Several impact test setups are explored in order to address long-standing questions and provide contributions regarding the following list of objectives:

- Identify the kinematic terms or individual kinematic that can predict brain strain metrics
- Determine whether there is need to consider direction-specific kinematics
- Understand the effect of the surrogate neck model on kinematic responses
- Identify one possible pass/ fail threshold for helmet certification

The overall objective of my thesis is achieved through three main stages:

- The first stage of this thesis is to design and execute an experimental process to simulate helmeted impacts in a certification-style drop test and acquire kinematic impact data.
- The second stage involves making use of the collected impact data for brain finite element modelling to determine strain metrics for each of the experimental drops.
- The third stage of this thesis uses multiple regression techniques to statistically describe correlations between impact kinematics and corresponding strain metrics.

Upon completion of all three stages, providing the following contributions:

- The key kinematic(s) to consider during future discussions regarding new helmet standards.
- The form in which kinematics should be considered and if this differs by impact configuration, helmet or impact location.
- The effect of removing the neck on resulting strain magnitudes and corresponding kinematic pass/ fail thresholds.
- One possible method for adopting the proposed kinematic metric as a pass/ fail criterion.

Through the completion of this thesis work, it is possible to report to researchers and manufacturers the optimum kinematic or set of kinematics for predicting strain in helmeted impacts for varying test configurations.

1.2 Thesis organization

The thesis begins by providing a brief overview of brain anatomy and details of head and brain injuries and injury biomechanics that will be referenced throughout the document. Helmets are then briefly described followed by their certification history and current certification methods. The progression of kinematics as predictors for injury and current efforts to improve helmet assessment methods will then be outlined. The role that finite element modelling plays in predicting injuries is discussed followed by details regarding various configurations for modelling impacts to complete the background review of this

thesis topic. A summary of the background information and an outline of the thesis objectives will also be provided.

The Methods chapter details the experimental configuration and data analysis protocol. The various impact scenarios considered in this study including headform, neck boundary conditions and helmet types are detailed in this section. The data collection and processing methods including calibration and validity investigations is then described followed by finite element modelling methods and statistical analysis techniques.

The Results chapter summarizes and provides the key findings for all scenarios under investigation, presenting results for impacts with the Hybrid III head and neck in full before presenting results for the free Hybrid III headform with no neck.

The Discussion chapter will explore the given results and provide insight into the importance of these findings for current and future researchers and the role these findings may play in future helmet assessment methods. Again, discussion surrounding impacts with the Hybrid III head and neck will be done before discussing findings specific to the Hybrid III head and no neck. A section outlining the process for applying the findings as a pass/ fail criterion for helmet certification will precede the limitations in the Discussion chapter. This section will detail the steps used to identify an acceptably injury type, risk level and corresponding kinematic limit.

Finally, the concluding chapter will summarize the results, discussion and contributions as well as provide suggestions for future work.

2 Background

2.1 Head and brain anatomy

To gain an understanding of head protection needs, this section discusses head and brain anatomy and the mechanics of injury. The skull and the brain are the two major structures of the head that are the focus for head protection efforts. It is imperative that the head be protected as any damage to the skull or brain can be fatal or have long-term sequelae.

The skull, or cranium, made up of multiple bones fused together, creates a protective shell around the brain. These bones include the frontal, parietal, and occipital bones forming the majority of the convex top of the skull, the temporal bones, and the sphenoid and ethmoid bones connecting to the anterior base of the skull [16]. Immediately below the skull are three membranes that separate and protect the brain from the skull: the dura mater, arachnoid mater and pia mater. The cerebrospinal fluid fills the subarachnoid space and protects the brain from mechanical shock [16].

The brain is divided into 4 main lobes including the frontal, temporal, occipital and parietal lobe. The frontal lobe, located at the front of the brain (Figure 2.1) is responsible for one's motor skills, reasoning, and higher cognitive functions. Damage to the frontal lobe can affect behavior and decision making. The temporal lobe, making up the bottom section of the brain, is responsible for hearing as well as forming memories. Memory, speech and language skills can be affected by damage to the temporal lobe. The middle portion of the brain is called the parietal lobe and is responsible for interpreting sensory feedback. The occipital lobe is located at the back of the brain and is responsible for processing visual information, resulting in vision problems if there is damage to this lobe [17]. Damage to any part of the brain can have lasting adverse effects on an individual's wellbeing [18].

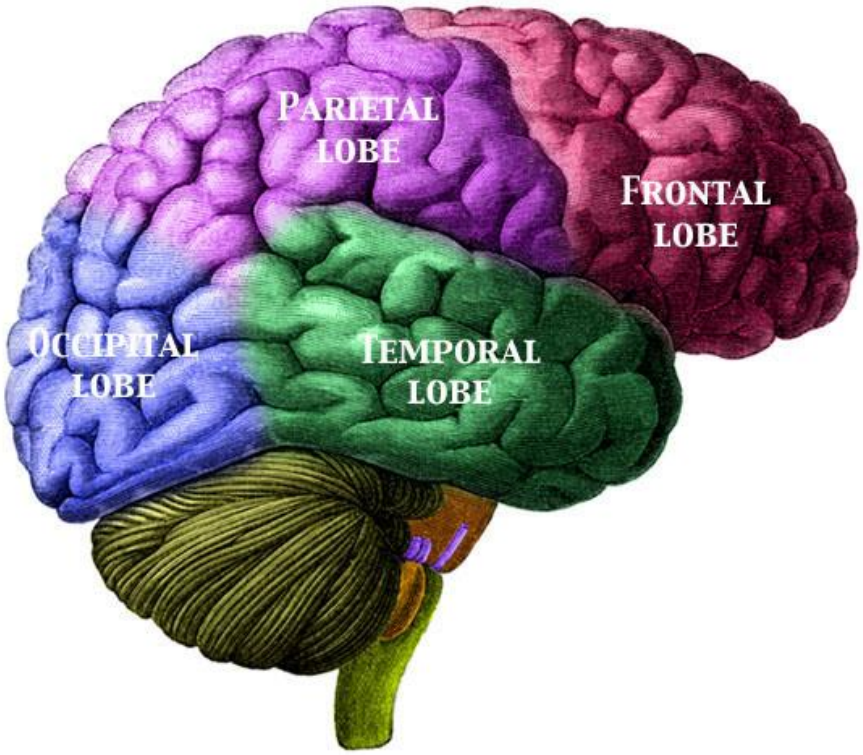

Figure 2.1: Brain anatomy: identifying the 4 main lobes of the brain. Brain Lobes Labelled. https://commons.wikimedia.org/wiki/File:BrainLobesLabelled.jpg. Image licensed under the Creative Commons Attribution 3.0 Unported license.

2.2 Head and brain injury biomechanics

Melvin and Lighthall eloquently describe brain injury biomechanics, explaining that injuries can be categorized as either focal or diffuse [19]. Energy transfer to the brain and skull can be caused by a direct load or impact to the head, which can lead to skull deformation and potentially skull fracture resulting in serious injury to the brain [19]. Focal injuries represent this type of energy transfer and refer to localized damage to the area surrounding an impact and include linear and depressed skull fractures as well as localized hematoma and contusion. Typically, focal injuries are associated with blunt force caused by direct loading. Contusion is caused by direct loading resulting in structural damage or bruising of the brain or skull. Brain contusions can occur at the location of loading or impact (coup) or opposite the initial loading site (contrecoup) [20]. Hematoma is typically the result of trauma to the skull causing rupture of veins below the surface. Focal injuries are considered serious brain injuries with high mortality rates [19].

Alternatively, brain injury may be present without direct loading to the skull causing skull deformation and rather as a result of head kinematics (accelerations or velocities) causing tissue damage in the brain. Diffuse brain injury (sometimes referred to as multi-focal injury) refers to widespread injury to the brain and is often the result of indirect loading causing acceleration or deceleration of the head. Diffuse injuries include a spectrum of injuries from mild traumatic brain injury (mTBI, of which concussion is one example) to severe trauma causing axon damage known as diffuse axonal injury (DAI). An early definition of diffuse brain injury was given by Strich in 1956, describing such brain trauma as "diffuse degeneration of the white matter" in head injury cases that were absent of skull fracture, intracranial hematomas and brain lacerations [21].

Motion of the head causing the brain inside the skull to deform can lead to widespread damaging shear strains within the brain. The casual mechanism of brain strains has been linked to rotational head motion for decades. Holbourn demonstrated this theory using a surrogate brain model, finding blows causing rotational motion resulted in shear strains or shear damage in locations corresponding to brain injuries noted in autopsies [10]. Ommaya et. al. later studied the effects of acceleration and impulse in rhesus monkeys [22] and experimentally confirmed the correlation between rotational acceleration and cerebral concussion [11]. Zhang et. al also proposed angular acceleration as a predictor for mTBI in 2004 [23]. Since the 1940s, and with decades of research, it has been acknowledged that rotational motion is a primary cause for diffuse brain injury.

Mild traumatic brain injury (mTBI), represents a spectrum of diffuse injuries that are considered mild relative to DAI and are often referred to as concussions. Although diffuse injuries can be less severe than focal injuries, multiple instances of sustaining a brain injury on the mild injury spectrum (multiple mTBI or multiple concussions) can lead to serious consequences including cognitive impairments. Furthermore, brain injuries considered to be in the category of mTBI are difficult to detect using conventional computed tomography (CT) [24]. For non-hemorrhagic, closed head injuries, magnetic resonance imaging (MRI) is able to better detect shear lesions that are present [25]. Mild diffuse injuries that do not include damage, or lesions, to axons may be difficult to detect using either CT or MRI.

Researchers suggest repeated brain injury can lead to chronic traumatic encephalopathy (CTE). The concept that multiple concussions or hits to the head could have lasting neurological effects was first presented by Martland in 1928, who gave it the name "punch drunk" [26]. Today, CTE has replaced punch drunk as a common reference for this condition. CTE is neurodegenerative disease that is diagnosed only during postmortem examination and there are currently no biomarkers for detecting CTE [27]. McKee et. al, notes that early symptoms of CTE include memory loss, problems with speech and cognitive abilities, confusion or potential for violent outbursts, among others [27]. Late stages of CTE can lead to Parkinsonism as well as dementia [27]. A review by Wilson et. al. considers numerous studies involving TBI and potential long-term effects. For those studies involving athletes exposed to multiple incidents of mTBI, there is a suggested link to neurodegenerative diseases, though it is noted that occurrence of neurodegenerative diseases is low [18].

Relative to the general public, individuals participating in contact sports such as hockey or football are at increased risk of suffering head and brain injuries. A study published in 2007 tracked all injuries for 15 sports in the National Collegiate Athletic Association (NCAA), collecting data over a 16-year period. It was found that hockey (men's and women's) and football had greater concussion rates per 1000 athlete exposures than all other sports (excluding women's soccer) [8]. Presently, sports that expose athletes to the risk of multiple concussions, such as hockey and football, are under a perceived spotlight by the media and the public, who seem to seek answers for the rate of concussions. One area that appears to be highlighted among the public is a helmet's ability to protect athletes against concussion.

2.3 Head protection: helmets

The helmet is designed to protect the head by attenuating energy such that energy is not transferred to the head directly during impact. Although helmet styles and construction can vary depending on the intended purpose, the main components typically include a hard, outer shell and a soft inner liner. The outer shell acts to distribute the load or forces applied to the skull, thereby reducing localized stress, while the compliant inner liner provides additional load distribution and energy attenuation as well as comfort. This section will briefly describe

function and design of modern helmets, though a much more in-depth and compelling description can be found in the book by Dr. Newman [28].

Head protection differs depending on the intended recreational activity. For example, cycling helmets are designed for single-use (i.e. should be replaced after one impact) and make use of relatively stiff foam to attenuate rare, but severe head impacts. Cycling helmets are typically made up of expanded polystyrene (EPS) covered by a thin polyethylene terephthalate (PET) plastic external liner (mainly for esthetics). EPS compresses to slow the head upon impact but is incapable of returning to its original form once deformed and therefore energy mitigating abilities are lost. Said differently, once these foams are crushed, they cannot be used again. Helmets manufactured for a single use (other examples include equestrian, ski/ snowboard and motorcycle helmets) should be replaced if ever an impact is sustained as its protective capabilities have been compromised.

Hockey and football helmets are examples of a multi-use helmets designed to withstand and protect the head against multiple impacts over the lifespan of the helmet. Generally, multi-use helmets use a more compliant liner to attenuate impact energy than that of single-use helmets. Hockey helmets are comprised of a hard plastic outer shell typically made of polyethylene, polycarbonate, or acrylonitrile–butadiene–styrene (ABS) often with an expanded polypropylene (EPP) or a vinyl nitrile (VN) foam liner [29]. Football helmet outer shells are made of a polycarbonate blend and commonly contain inflatable padding for the inner liner. An example of an inflatable padding includes vinyl, air-filled bladders. Other football helmet liners may use vinyl cases filled with soft foam. Levy et. al. details some of the history behind the football helmet [30]. Figure 2.2 displays examples of multi-use helmet constructions. Using foams such as EPP or inflatable padding is appropriate for multiple impacts as the liners can decompress shortly after a single impact. Liners that return to their initial state are capable of providing the same protection for future impacts. Hockey and football helmets are both designed for multiple impacts, although the frequency of impacts to the head is expected to be higher for football players relative to hockey players. A study by Crisco et. al. used instrumented football helmets to track head impact exposure to National Collegiate Athletic Association (NCAA) football players and quantified head impact frequency as 6.3 to 14.3 impacts per practice or game, respectively [31]. By comparison,

Brainard et. al. used instrumented ice hockey helmets to track impact exposure to collegiate hockey players and found that male athletes experienced 2.9 impacts per athlete exposure (exposure defined here as any organized play including practice, game and scrimmage) [32]. The difference in anticipated head impact frequency is reflected in the different designs for ice hockey and football helmets.

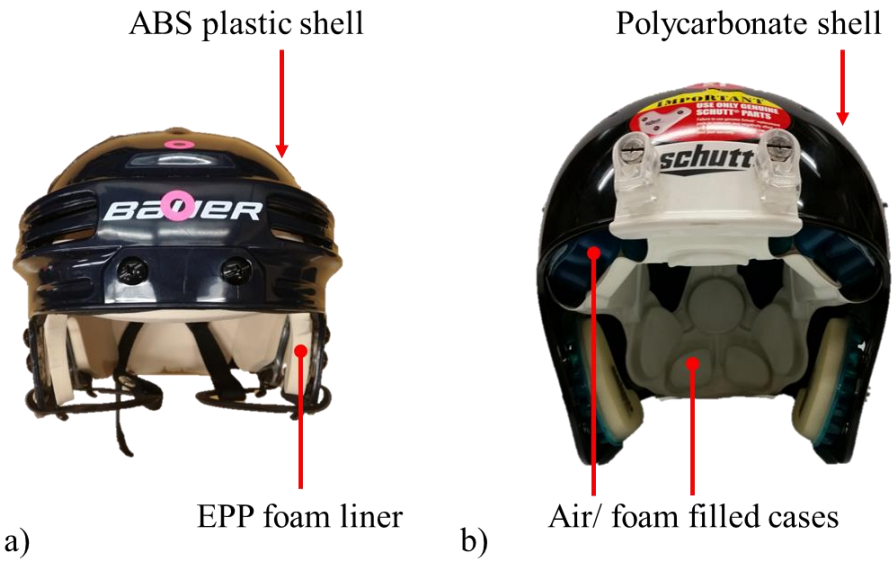

Figure 2.2: Outer shell and inner liner examples as shown on a) hockey and b) football helmet

Historical evidence and laboratory experiments have proven helmets to be effective in protecting against life-threatening head and brain injuries. A bicycle helmet study by Cripton et. al. presents calculated risk of severe brain injury, proving the presence of a bicycle helmet greatly reduces injury risk relative to impacts without a bicycle helmet [33]. Based on experiments using human cadavers and dogs, Gurdjian et. al. noted that the presence of a helmet preventing skull deformation could allow the human head to withstand nearly twice the linear acceleration needed to cause permanent damage to the brain than would otherwise be tolerable with no head protection [34]. Combining a rule change in American football with the introduction of the NOCSAE football helmet standard dramatically reduced the number of brain injury-related deaths observed in 5-year spans from 1945-1999 [35]. Additionally, the improvement in helmets, due in part to the implementation of a helmet standard, is credited with eliminating death due to cranial fracture [35]. Helmets have done

an effective job of mitigating life-threatening head injuries and are credited with all-but eliminating fatal focal injuries.

2.4 Helmet assessment and certification

The helmet remains a primary defense against head injury and any protective head gear marketed today is required to pass certification. Quantifying impact attenuation by measuring linear head acceleration continues to be fundamental during helmet certification. Linear acceleration thresholds are used in all helmet certification standards worldwide, where a helmeted impact resulting in peak linear acceleration below the chosen thresholds is considered to provide adequate impact attenuation.

The history of helmet certification standards can be traced back decades. Early impact simulations of an average head mass and helmet striking a fixed surface at 34 miles per hour (to apply 500 ft lbs force to the head and helmet) found that all but one of the helmets tested did not provide adequate protection of the skull [36]. Becker discussed early testing methods, describing the process, which involved technicians dropping a 10 lb block from 9 ft above a helmeted headform and measuring a force output from a gauge mounted beneath the headform [37]. The British Standards Institution (BSI) originally limited this exerted force to 5000 pounds [38]. In 1959, a swing-away method for testing was introduced where a headform was able to move upon impact [39]. In this method, the mass of the headform was known to be 12 lb and the acceleration of the headform was measured during impact. As the force exerted on the headform is the product of the headform mass and acceleration, the choice failure level of 4800 lb (below 5000 lb set by BSI) led to a failure criterion of 400 g (400 times the acceleration due to gravity) [39]. This early helmet testing, alongside research linking linear kinematics to fatal head injury (discussed further below) has provided the logic upon which today's helmet standards are based.

The pass/fail criterion in most of today's helmet performance standards is based solely on peak linear acceleration at impact, or peak g. The only exception to this is the recent NOCSAE football standard that considers both linear and angular acceleration. During certification drops, a helmeted magnesium headform is raised to a prescribed height and released in a linear drop to strike an anvil (Figure 2.3). The peak resultant linear acceleration

is monitored and if it does not exceed the corresponding standard threshold, the helmet passes and can be sold to consumers. For example, the Canadian Standards Association (CSA) states that a hockey helmet cannot exceed a pass/fail threshold of 275g in a linear drop test with an impact speed of 4.5m/s [40]. The Consumer Product Safety Commission (CPSC) requires that bicycle helmets do not exceed 300g for a 6.2 m/s impact [41].

Figure 2.3: An example of a hockey helmet certification set-up with a helmeted magnesium headform (EN960) and rigid neck, striking a modular elastic programmer (MEP) pad. The position shown is prior to release.

Helmet certifications are based on linear acceleration criteria determined during a drop impact for nearly all standards. Table 2.1 summarizes a selection of standards used in helmet certification, outlining typical impact velocities, surfaces and the given pass/ fail criteria for different helmet types.

Table 2.1 : A brief summary of helmet certification criteria for typical impact tests

	Helmet type	Minimum drop height	Impact velocity	Impact surface	Failure Threshold
CSA Z262.1-09	Ice Hockey	Based on impact velocity	4.5 m/s	modular elastomer programmer (MEP)	275 g
ASTM F1045-16	Ice Hockey	Based on impact velocity	4.5 m/s	modular elastomer programmer (MEP)	275 g
NOCSAE ND002-13m15	Football	Based on impact velocity	5.46 m/s	modular elastomer programmer (MEP)	1200 SI
NOCSAE ND002-17m17a	Football	Linear impactor	6.0 m/s	modular elastomer programmer (MEP)	1200 SI 6000 rad/s²
CPSC	Cycling	2 m (6.2 m/s) 1.2 m (4.8 m/s)	6.2 m/s (flat) 4.8 m/s (curb)	Steel anvil (flat and curbstone)	300 g
CEN EN1078	Cycling	1497 mm (flat) 1064 mm (curb)	5.42 m/s (flat) 4.57 m/s (curb)	Steel anvil (flat and curbstone)	250 g
ECE Reg 22	Motorcycle	Based on impact velocity	7.5 m/s	Steel anvil (flat and curbstone)	275 g HIC < 2400
Snell SA2015	Motorcycle	Based on impact velocity	8.5 m/s	Steel anvil (flat and hemispherical)	300 g
FIA 8860-2010	Protective	Linear impactor	9.5 m/s	Steel anvil (flat and hemispherical)	300 g HIC36 < 3500
NHTSA DOT FMVSS 571.218	Motorcycle	182.9 cm (6.0 m/s) 138.4 cm (5.2 m/s)	6.0 m/s (flat) 5.2 m/s (hemi)	Steel anvil (flat and curbstone)	400 g 200 g < 2.0 ms 150 g < 4.0 ms

CSA - Canadian Standards Association; ASTM - American Soctiety for Testing and Materials; NOCSAE - National Operating Committee on Standards for Athletic Equipment; CPSC - Consumer Product Safety Commission; CEN - European Committee for Standardization; ECE - Economic Commission for Europe; FIA - Federation Internationale de l'Automobile; NHTSA DOT - National Highway Traffic Safety Administration Department of Transportation

Certifying helmets by these methods, based on linear acceleration, has led to the design of recreational helmets that are credited with all-but eliminating fatal focal injury in sports. Currently, discussions now surround how helmet testing protocol may evolve to ensure helmet assessment considers both focal and diffuse injury.

2.5 Kinematics as head injury predictors

In the 1960s, based on work out of Wayne State University (WSU), a tolerance boundary known as the cerebral concussion tolerance curve (Figure 2.4) used cadaver impact data and incidents of skull fracture to develop a tolerance curve [13]. The curved decreasing line (from left to right) is interpreted as a representative boundary between safe (below and left of the line) and unsafe (anywhere above and to the right of the line) head impact.

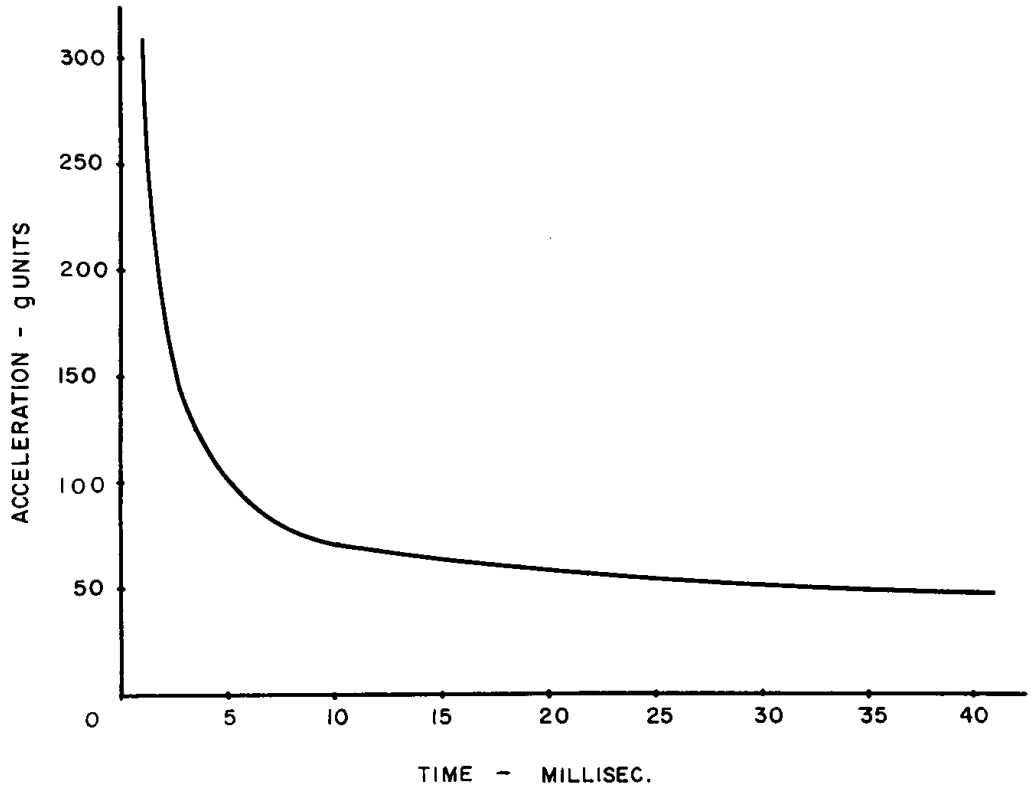

Figure 2.4: Wayne State Cerebral Concussion Tolerance curve [13].

Figure reproduced with permission from Gurdjian, Elisha S., V. L. Roberts, and L. Murray Thomas. Tolerance curves of acceleration and intracranial pressure and protective index in experimental head injury." Journal of Trauma and Acute Care Surgery 6.5 (1966): 600-604. https://journals.lww.com/jtrauma/Citation/1966/09000/TOLERANCE_CURVES_OF_ACCELERATION_AND_INTRACRANIAL.5.aspx

This curve provides a relationship between the average acceleration over the impact, the time duration of the acceleration pulse and the resulting risk of injury for an unprotected head. As an example, consider an impact resulting in 100 g acceleration. If 100 g is sustained for less than 5 ms, this could be considered a safe impact. However, if by moving to the right, and increasing time to 10 ms, one approaches and crosses the theoretical tolerance boundary, increasing head injury probability. Similarly, at a fixed time duration of 10 ms, as acceleration increases from 50 g to 100 g, one again approaches and crosses the curve, increasing head injury probability.

The Wayne State data was used to create the curve shown in Figure 2.4 to represent a tolerance limit between fatal and non-fatal impacts. This work also highlighted the important

effects of time duration. It is noted, however, that impacts conducted to the cadaver skull considered only forehead impacts and therefore specific tolerances may differ for other impact locations such as temporal or occipital impacts. Additionally, the effect of the location of the experimentally applied impact was only investigated using animal data and was not well defined for humans during the development of the Wayne State Tolerance Curve (WSTC). The data considered to create the WSTC is unlike sporting impacts and it is noted that it does not accurately represent helmeted impacts, however, the WSTC has been widely referenced in developing metrics for recreational head protection. Although there are limitations to this work, researchers aimed to create a functional that was capable of approximating the Wayne State data thereby assessing impact acceleration and estimating risk of fatal head injury. An initial formula was proposed that uses allowable average acceleration ($\overline{a}$) and time duration (T) so that an impact was considered safe if $\overline{a}^{2.5}T < 1{,}000$ (Equation 2.1).

$$\overline{a}^{2.5}T < 1{,}000 \tag{2.1}$$

The Gadd Severity Index (GSI) was developed using the constants from Equation 2.1 (i.e. 2.5 and 1000) and again including acceleration (a) and time duration (T) and was intended for use as threshold for serious head injury in frontal impact (Equation 2.2) [42]:

$$GSI = \int_T a^{2.5} dt < 1{,}000 \tag{2.2}$$

The National Operating Committee on Standards for Athletic Equipment (NOCSAE) was the first organization to use this concept and thereby introduce time duration, which is shown by the WSTC to be an important factor in head injury risk, into a helmet standard, known presently as the Severity Index (SI).

$$SI = \int_T a^{2.5} dt < N \tag{2.3}$$

Using SI as a helmet standard, N cannot exceed 1200 in football helmet impacts according to current NOCSAE specifications [43]. The start and end times for SI integration must be

chosen and depending on the technique used to define time duration, the magnitude of SI can vary considerably.

Versace challenged the validity of the SI [44] and another functional using linear acceleration was developed to quantify impact severity and relate severity with injury risk known as the Head Injury Criterion (HIC).

$$HIC=(t_2-t_1)\left[\frac{1}{(t_2-t_1)}\int_{t_1}^{t_2} a(t)dt\right]^{2.5} \quad (2.4)$$

HIC was developed primarily for short duration impacts with time duration (t_2-t_1) chosen as either 15ms or 36ms. HIC, introduced in 1971, was first used as part of the standard for motor vehicle crash worthiness, FMVSS-208 [45] and has become the most widely referenced head injury assessment function now also appearing in helmet standards [46][47].

Helmet assessment methods are simplified further to disregard time duration and consider only peak linear acceleration (with SI as an exception to this). For helmeted impacts, time duration is typically consistent ranging from approximately 10 – 15 ms [48], [49]. The time window consistency leads HIC to correlate with peak linear acceleration. It is noted that although current linear acceleration criteria (for example, peak g of 300 g or SI of 1200) were not chosen to represent a specific injury, it is now widely agreed that today's helmets passing these criteria save the lives of individuals that may otherwise be dead due to head impact.

With today's helmets protecting against fatal head injuries, debate among standards communities (Canadian Standards Association (CSA) and American Society for Testing and Materials (ASTM)) in relation to helmets now centers on whether or not today's helmets protect the wearer from mild traumatic brain injuries, or diffuse injuries (e.g. concussions). There is growing recognition that linear acceleration alone is not a reliable measure for determining diffuse injury and that angular kinematics should be considered for future helmet certification methods.

The notion that angular kinematics may predict diffuse injury can be traced back to the 1940s. Holbourn conducted experiments to understand how the brain responds to loading,

using a gelatin mixture to represent brain tissue and subjecting the mixture to impacts causing rotation [10]. Damaging shear strains were observed in the modelled brain in locations comparable to those of hemorrhages noted in autopsies for similar blows [10]. Yarnell and Ommaya investigated effects of rotation on brain injuries using rhesus monkeys. Rear impact conditions were simulated using forward-facing rhesus monkeys in a carriage causing them to experience whiplash conditions and confirming the significance of angular motion on brain injuries [11]. Gennarelli et.al. subjected squirrel monkeys to linear and angular motions, and noted a greater frequency of brain lesions under head rotation [12]. The results of these studies provide clear evidence that angular motion plays an important role in the occurrence of brain injuries.

2.5.1 Kinematic functions including angular kinematics

Although HIC is widely used, it does not account for angular rotation, leading Newman to develop the Generalized Acceleration Model for Brain Injury Threshold (GAMBIT), which was the first metric that considered the combined effects of linear and rotational kinematics [50]. The basis for GAMBIT is that brain injury can occur if the combined effects of linear and angular accelerations exceed a maximum allowable value (here G_{max}=1.0). GAMBIT is based on peak linear acceleration, a_{res}, and peak angular acceleration, α_{res} as well as critical limits on linear and angular acceleration, a_c and α_c, respectively (Equation 2.5).

$$G_{max} = \left[\left(\frac{a_{res}}{a_c}\right)^2 + \left(\frac{\alpha_{res}}{\alpha_c}\right)^2\right]^{1/2} \tag{2.5}$$

Considering cadaver injury points on a plot of linear acceleration versus angular acceleration, it is noted that a straight line intersecting 250 g and 10000 rad/s^2 creates a region of the plot where injury is unlikely to occur. The critical limits are therefore set at a_c=250 g and α_c=10000 rad/s^2 [50].

In 2000, Newman et. al. introduced the Head Impact Power (HIP) [51] as a detailed approach to assessing potential injury. HIP considers the rate of change of kinetic energy for six degrees of freedom.

$$HIP = ma_x \int a_x dt + ma_y \int a_y dt + ma_z \int a_z dt + I_x \alpha_x \int \alpha_x dt + I_y \alpha_y \int \alpha_y dt + I_z \alpha_z \int \alpha_z dt \qquad (2.6)$$

HIP considers acceleration, head mass and time duration as well as directional consideration and angular motion while taking into account inertial properties of the test headform. Through reconstruction of 12 injurious football impacts, including 24 players in head-to-head impacts, Newman et. al. evaluated the significance of numerous injury assessment functions including, peak linear acceleration, peak angular acceleration, SI, HIC, GAMBIT and HIP for predicting the occurrence of mTBI [52]. HIP was found to be the most significant predictor for concussive incidents among all functions investigated.

In addition to GAMBIT and HIP, another injury assessment function that incorporates angular kinematics is the Brain Injury Criterion (BrIC [14]).

$$BrIC = \frac{\omega}{\omega_c} \qquad (2.7)$$

BrIC is based on peak rotational velocity, ω, and a critical rotational velocity for brain injury, ω_c [14]. Impact tests were recreated using dummy models for front and side impacts and strain metrics were computed based on the impact data using the Simulated Injury Monitor [53]. BrIC was developed to establish a linear relationship between BrIC and the computed brain strain metric [53]. BrIC in the form presented in Equation 2.7 [14] is a simple diffuse injury predictor and was initially developed using automotive impact data, though is now being considered for helmet assessment as well.

By replacing linear acceleration in the HIC equation (Equation 2.4) with angular acceleration, the Rotational Injury Criterion is proposed (Equation 2.8) to approximate brain injury tolerance curves [54].

$$RIC = (t_2 - t_1)\left[\frac{1}{(t_2 - t_1)}\int_{t_1}^{t_2} \alpha(t) dt\right]^{2.5} \qquad (2.8)$$

A similar approach in developing RIC is applied to present the Power Rotational Head Injury Criterion, or PRHIC. In PRHIC, the linear acceleration term in HIC is replaced with the

rotational component of HIP as shown in Equation 2.9 below. Linear and angular acceleration data from football players was collected using instrumented helmets and applied to a finite element brain model computing cumulative strain damage measures (CSDM), discovering correlations between CSDM and PRHIC [54], [55].

$$PRHIC=(t_2-t_1)\left[\frac{1}{(t_2-t_1)}\int_{t_1}^{t_2} HIP_{rot}dt\right]^{2.5} \quad (2.9)$$

Related to helmet assessment, lack of linear kinematics in equations 2.7-2.9 raises concerns about neglecting severe focal injury risk if they are used in helmet certification. An ideal method metric will consider both diffuse and focal injury simultaneously.

HIP has incorporated all kinematics related to head injury and has proven capable of predicting diagnosed diffuse injury, however it is likely too complex to be adopted for use in helmet test methods. The use of HIP would require accurate measurement of many kinematics, though helmet assessment methods are typically developed around simple metrics with as few measures as possible. NOCSAE is the only certification test in use that considers angular kinematics during impact, presenting little opportunity to adopt any metric that includes angular measures. It is therefore important to identify an agreed upon kinematic metric that can be incorporated by multiple standards organizations.

2.6 Finite element head and brain models

Evaluating the correlation between kinematics and head injury was originally done using cadaver and animal data [13]. Over the years, brain finite element models (BFEM) have been developed to replace cadaver work as a technique for estimating injury that, if proven valid, could replace the need for complex experimental protocols involving cadavers or dummy models. Using impact kinematics as model inputs, BFEM compute tissue strain as a correlate to brain injury risk. Automotive researchers continue to develop kinematic injury predictors for diffuse injury using these numerical models as a tool to understand injury risk, as represented by BFEM strain metrics, and the relationship with kinematics.

One example of a brain finite element (FE) model is the Improved Simulated Injury Monitor (SIMon), developed by Takhounts et. al. SIMon models the cerebrum, cerebellum,

brainstem, ventricles, falx, tentorium, parasagittal blood vessels and a combined layer of cerebral spinal fluid (CSF) and pia arachnoid complex (PAC) (shown in Figure 2.5). To represent these components, SIMon uses 5153 (3790 rigid) shell elements, 14 beam elements and 40,708 solid elements, for a total of 45,875 elements and 42,500 nodes [56].

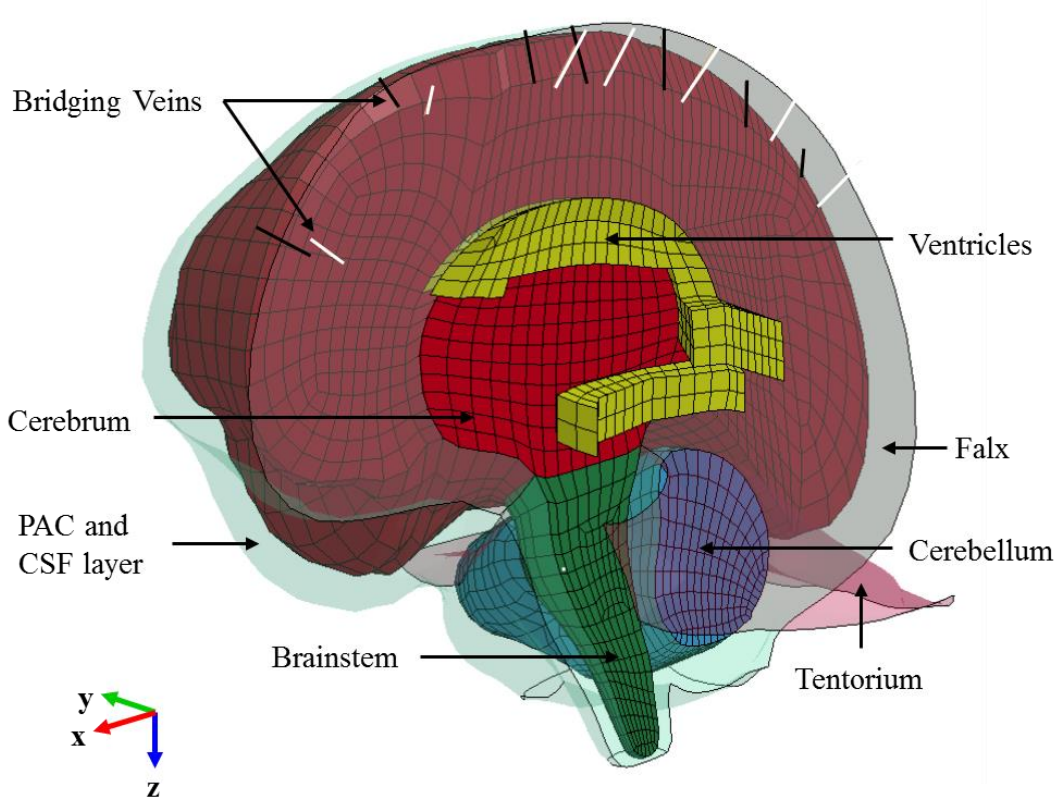

Figure 2.5: The Improved Simulated Injury Monitor brain finite element components. Modified from the Journal of Biomechanics [57]

Material properties were selected through a validation process comparing the SIMon model response to displacement-time history plots of neutral density targets (NDTs) [58]. NDTs were tracked at various points within a cadaver skull and their position, relative to the skull, was tracked and recorded. Nodes in the SIMon model closest to the location of the NDTs in the cadaver were chosen as points for comparison and the model properties were then adjusted to best fit the model response to the experimental data [58]. The SIMon skull is modelled as rigid, while all other brain structures are modelled as deformable, linear viscoelastic, isotropic and homogenous materials [58]. Table 2.2 summarizes the material properties of the Improved SIMon brain model components shown in Figure 2.5.

Table 2.2 : A summary of the materials used to model the Improved SIMon brain components

Material	Cerebrum/ Cerebellum/ Brain Stem	Ventricles	Blood Vessels (bridging veins)	Falx-Tentorium	PAC-CSF layer	Skull
Type	Kelvin-Maxwell Viscoelastic	Elastic fluid	Cable discrete beam	Elastic	Kelvin-Maxwell Viscoelastic	Rigid
Density, ρ (kg/m³)	1040	1000	5000	1130	1050	35200
Bulk modulus, K (MPa)	558.47	2100	-	-	4.966	-
Short time shear modulus, G_0 (MPa)	0.00166	-	-	-	0.1	-
Long time shear modulus, G_I (MPa)	0.000928	-	-	-	0.02	-
Decay constant, β	16.95	-	-	-	-	-
Decay constant, τ	-	-	-	-	0.01	-
Young's modulus, E (Mpa)	-	0	0.275	31.5	-	6900
Poisson's ratio, υ	-	0.5	-	0.45	-	0.3
Viscosity coefficient, VC	-	0.2	-	-	-	-

Other models currently being used include the Global Human Body Model Consortium (GHBMC), Wayne State University Head Injury Model (WSUHIM) and the University College Dublin Brain Trauma Model (UCDBTM). In addition to the components modelled by SIMon, these models also include representation of facial bones and skin as well as a differentiation between grey and white matter [59]–[61]. These more detailed models require an increased number of elements with as many as 270,552 in the case of GHBMC [61], which increases computing efforts required to solve these models. SIMon reports nearly identical strain metrics to those of the GHBMC under the same input conditions, though SIMon may be less computationally demanding as it includes less detail and fewer elements to solve relative to the GHBMC [14].

Pressure, stress and strain can all be considered to represent mechanical trauma to the human brain using finite element models. Intracranial pressure was proved to cause concussive effects when applied to the brain of anesthetized dogs [13] and many brain finite element models are validated against intracranial pressures, including SIMon [58]. Maximum strain values communicate the level of element deformation, indicating localized brain deformation and potential damage. To also consider widespread element strain, the cumulative strain damage measure (CSDM) represents the cumulative volume of the brain model exceeding a given strain level and is often used by researchers to predict risk of diffuse brain injury [14], [55], [62]. Another measure to represent diffuse injury, known as maximum axonal strain, is described by Sahoo et. al. as representing strain at the axonal level and a reliable predictor of DAI [63]. To understand both localized and widespread brain deformation and potential mechanical trauma, it is useful to consider measures that represent each. Here, cumulative strain damage and maximum principal strain were chosen for a comprehensive understanding of strain throughout the brain as well as local peaks during simulated impact.

SIMon-computed brain strain metrics that are focused on in this thesis include the cumulative strain damage measure (CSDM-15, specifically) and maximum principal strain (MPS). MPS indicates the single peak strain occurring within the brain model during impact simulation, while CSDM represents the volume fraction of the brain that exceeds a chosen strain threshold. For example, CSDM-15 indicates the volume fraction of the brain that meets or exceeds 15% strain. CSDM is meant to be a mechanical predictor of risk of diffuse axon injury (DAI) as it considers wide spread brain strain and using logistic regression and animal injury data, Takhounts et. al was able to establish correlations between CSDM levels and the experimental data [58]. Kleiven also determined a correlation between CSDM and brain injury by evaluating mild traumatic brain injuries through accident reconstruction of football impacts using the KTH brain model [64]. Kinematics recorded from animal heads, both linear and angular, were scaled to represent what would be experienced by a human and input to the SIMon brain model. Resulting CSDM values were compared to DAI injuries sustained by the animal and, using logistic regression, injury thresholds were established corresponding to 50% probability of injury [58]. It was also found that specifically CSDM-15 correlates best to DAI based on developmental work by Takhounts et. al. [58].

SIMon has been used previously to investigate impact kinematics and correlations to brain strain metrics. During development of the Improved SIMon model, head kinematics for football impacts were used as inputs to SIMon, identifying angular kinematics as better predictors for strain metrics than linear kinematics [56]. Furthermore, the study of these football helmet impacts found that CSDM and MPS correlated with diagnosed brain injuries [56]. As well, the brain injury criterion, or BrIC, was originally developed using SIMon for use in the automotive industry as an estimate for brain injury risk [14].

Brain finite element models have become a useful research tool for computing brain strain metrics and estimating injury, though do not align with typical helmet certification methods that aim for simple and efficient impact measures. In computing brain strains from impact kinematics, it is possible to identify kinematic measures capable of predicting strain metrics that represent injury risk. Research remains ongoing to discover a widely agreed-upon method for accurately estimating head and brain injury.

2.7 Head models and impact configurations for measuring impact mechanics

In addition to discussion surrounding suitable kinematics for helmet assessment, there is much debate over the most appropriate equipment. The Hybrid III head and neck was originally developed for the automotive industry and is widely used in impact assessments. However, it was designed to mimic human response during frontal impacts only. Therefore, there is discussion over whether this setup is a viable option to represent human response for helmeted impacts at various locations. There is also concern that the properties of the Hybrid III neck may change over time and as a result is cause for concern for equipment maintenance and test reproducibility. National Operating Committee on Standards for Athletic Equipment (NOCSAE) developed headforms with features appropriate for use with helmets and compliance to deform under significant loading [65], however there is a lack of published data on the NOCSAE headform mass and inertial properties as well as headform repeatability.

The method used to impose an impact on the chosen headform during helmet certification is commonly a guided drop focused on measuring linear kinematics [40], [41], [66]. A twin wire system generates headform impact by releasing a drop assembly from a given height to

strike the surface mounted to the anvil located at the drop system base [67]. Similarly, a guided monorail configuration also makes use of the falling headform striking an anvil [33]. Guided drop systems can be modified to accept a flexible neck, allowing both linear and angular impact kinematics to be determined [68]. Alternatively, a stationary headform linearly impacted by a horizontal striking arm (often pneumatically-driven) can allow linear and angular impact kinematics to be determined [69]. A pendulum system is another impact method which also keeps the headform stationary, using a pendulum arm falling from a prescribed height to strike the headform [70].

A suitable impact configuration for helmet certification will make it possible to measure all kinematics that have been identified as important for considering both focal and diffuse injury. Based on previous research, an appropriate system must allow for angular motion to consider diffuse injury.

2.8 Traumatic brain injury and future helmet assessment

Despite the widespread use of helmets, traumatic brain injuries (TBI) remain a concern for athletes participating in contact sports. Helmet use is understood to mitigate risks for severe focal injuries, and as a result, discussions are now centered upon what role the helmet plays in mitigating risks for diffuse brain injuries. Quantifiable helmet assessment relative to focal and diffuse injury, simultaneously, is an important progression in continued improvement of head protection.

Current helmet standards and impact methods that focus on linear acceleration do not account for diffuse injury during assessment and standards organizations seem to agree that pass/fail testing should move towards methods that assess a helmet's ability to prevent both focal and diffuse injury. However, there is currently no consensus on which kinematics a new metric considering diffuse injury should be based upon. Researchers worldwide are investigating methods for certifying helmets using rotational kinematics. Many European test setups use a helmeted headform unconstrained (without a neck) during impact tests [71], [72] in efforts to advance helmet assessment techniques.

As discussed previously, there are a number of kinematic functions that aim to estimate head and brain injury, though none that have been specifically developed for helmet testing. The

Summation of Tests for the Analysis of Risk (STAR) is a rating system that assesses helmet performance based on impact kinematics, taking into account head impact exposure. In a laboratory test setup, a helmet is impacted at various locations and each impact condition is associated with an estimated number of impacts per season and the probability that a concussion would occur from such an impact. Combining this information with approximated concussion risk, based on kinematics, provides the STAR rating for the helmet of interest. The Football STAR equation is based on linear acceleration while the Hockey STAR equation considers both linear and angular acceleration [73].

Biomechanical research suggests angular head kinematics are the best predictors for diffuse injury [14], while linear acceleration and time duration are important factors for severe or fatal focal head injury [13]. There is ongoing debate, over which specific kinematics should be used in future helmet certification methods. While it is known that angular kinematics are best for predicting brain injuries such as concussion, there is currently no test protocol that allows head rotation and consequently no functions used in certification that are capable of predicting diffuse injury.

3 Methods

The overall goal of this thesis work is to identify impact kinematics that can be measured and used to predict strain during certification-style helmeted impacts. The work presented here uses experimental impact data and finite element modelling of the brain to understand the relationship between impact kinematics and computed brain strain. Helmeted impacts, experimentally replicated, provide measured head kinematics for use as inputs to a brain finite element model to estimate the risk of brain injury. Statistical analyses determine which impact kinematics best predict brain strain metrics while also considering what is appropriate for future helmet assessment methods. Figure 3.1 shows a flow chart of the overall experimental protocol.

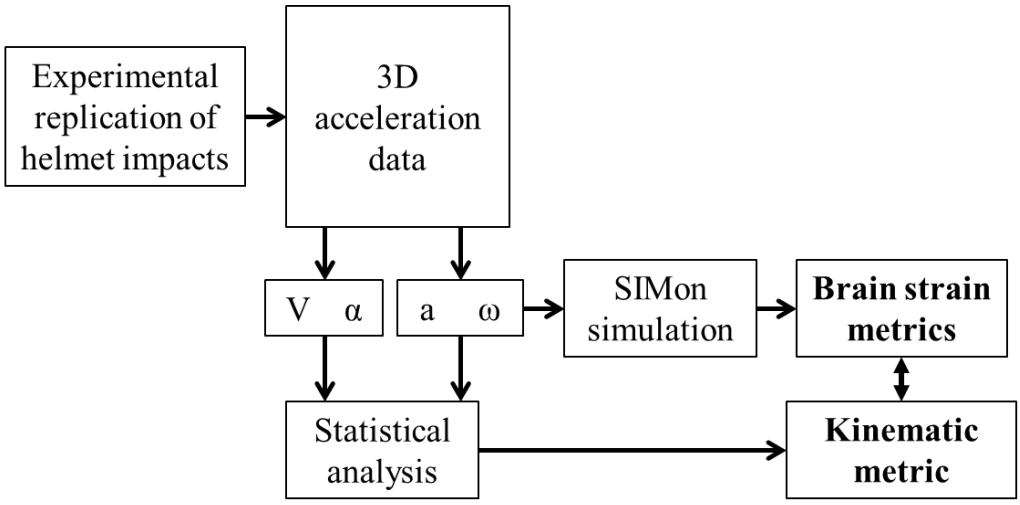

Figure 3.1: Experimental protocol flow chart. Here, linear and angular kinematics are represented by V (linear velocity), a (linear acceleration), ω (angular velocity) and α (angular acceleration).

3.1 Drop tower assembly and instrumentation

Conducting the necessary experiments to investigate correlations between head impact kinematics and potential brain injury requires appropriate testing equipment. The test setup chosen allows for repeatable impacts to a helmeted headform at variable impact speeds and the ability to record linear kinematics and calculate angular kinematics. Configuring the drop tower to accommodate helmeted headform impacts is the first step in completing the work for this thesis including assembly of the anthropomorphic test device (ATD) head and neck system and the gimbal components as well as mounting instrumentation and developing

acquisition and saving software. Assembly and calibration of the instrumentation along with data acquisition is discussed below.

3.1.1 50th Percentile Hybrid III headform and neck

The Hybrid III 50th percentile full-body dummy was developed for safety testing by researchers in the automotive industry. The components of the full-body model that will be used in this study are the Hybrid III head and neck. The Hybrid III head represents the circumference and mass of the average male head with a combined head and neck mass of 5 kg. The headform was validated during forehead impacts only, comparing headform response to that of cadavers [74]. The shape of the upper portion of the headform was designed to match the dimensions of humans, though the lower part of the headform and jawline were not designed to accommodate helmets. The Hybrid III head and neck was designed and validated exclusively for the automotive industry, though has been used widely for research involving sport helmets [15], [23], [75]. The Hybrid III head and neck with the positive coordinate system is shown in Figure 3.2.

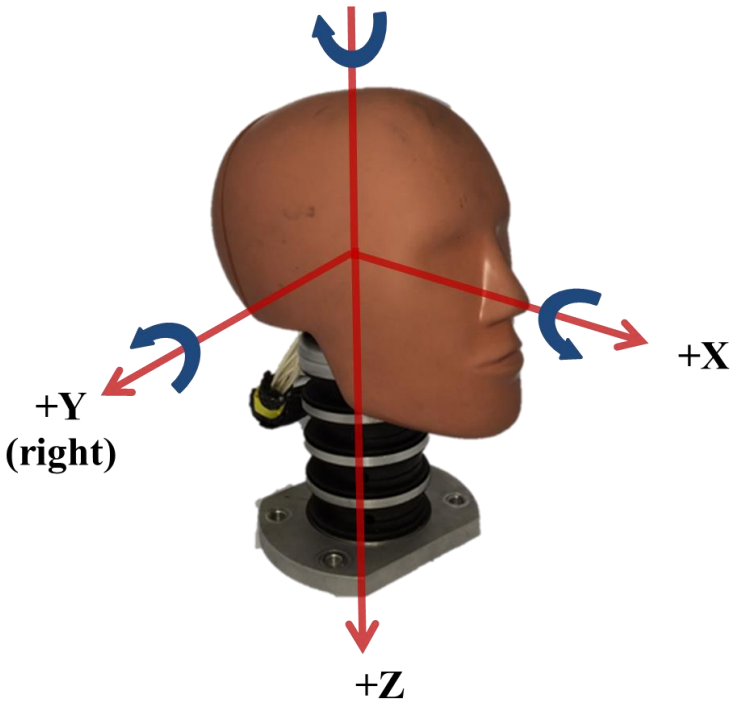

Figure 3.2: Hybrid III head and neck showing the positive coordinate system.

The Hybrid III headform is equipped with nine uniaxial accelerometers (Measurement Specialties Inc. Hampton VA, model 64C-2000-360) mounted in a 3-2-2-2 array allowing for the measurement of linear accelerations at the head center of mass and calculation of angular accelerations by applying equations presented by Padgaonkar [76]. At the head center of gravity is a mounting block with 3 accelerometers measuring in the x-, y-, and z-directions. The additional 6 accelerometers are mounted inside the headform with 2 on the left side (A), 2 at the front (B) and 2 at the crown (C). These outboard mounted accelerometer locations and the corresponding measured acceleration directions are shown in Figure 3.3.

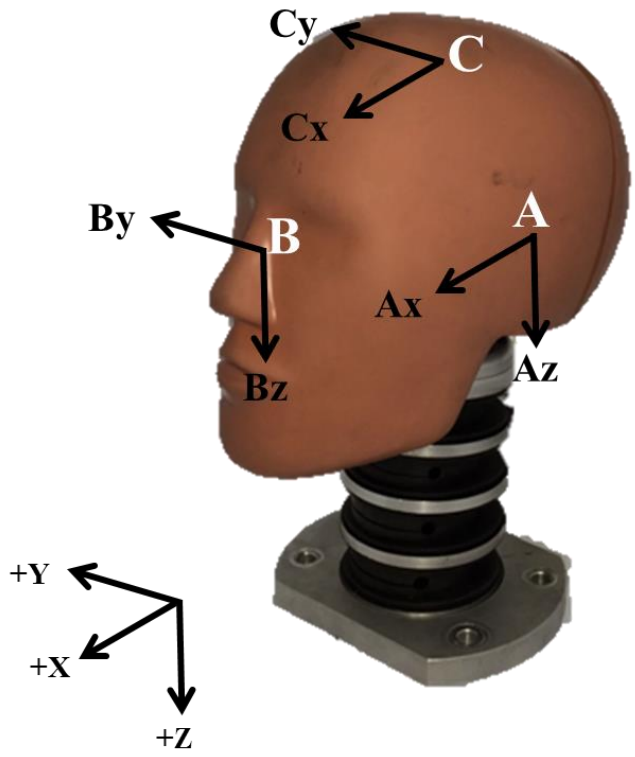

Figure 3.3: Hybrid III head and neck showing 2-2-2 accelerometer locations (of the 3-2-2-2 array) and coordinate directions. Mounting blocks are located inside the headform at A, B and C, each with 2 accelerometers reporting linear acceleration in the directions shown.

3.1.2 Data acquisition

Impact acceleration data is collected (acquisition rate of 100 kHz) and saved using National Instruments hardware and software (PXI 6251 and Labview v8.5, Austin TX). Analog voltages are first filtered using an anti-alias hardware filter (cut-off frequency 4 kHz) before

conducting post-process low-pass filtering (4^{th} order Butterworth with a cut-off frequency of 1650 Hz) using software per Channel Frequency Class (CFC) 1000 [77]. Impact speed is measured within 40 mm of impact using a purpose-built velocity gate. The velocity gate was calibrated during the initial configuration of the drop tower, confirming that correct peak g values occur at the corresponding impact speed requirements.

Upon completion of the drop tower assembly and accelerometer installation, the system is validated through trial drops and polarity checks performed as per instrumentation standards [77, p. 211]. During calibration impacts, the Labview software user interface is used to confirm realistic kinematic traces and correct acceleration directions for all 9 accelerometers.

An example of kinematics for impacts using the Hybrid III head and neck equipped with a hockey helmet can be seen in Figure 3.4. All impact kinematics were measured and computed relative to the Hybrid III head center of gravity.

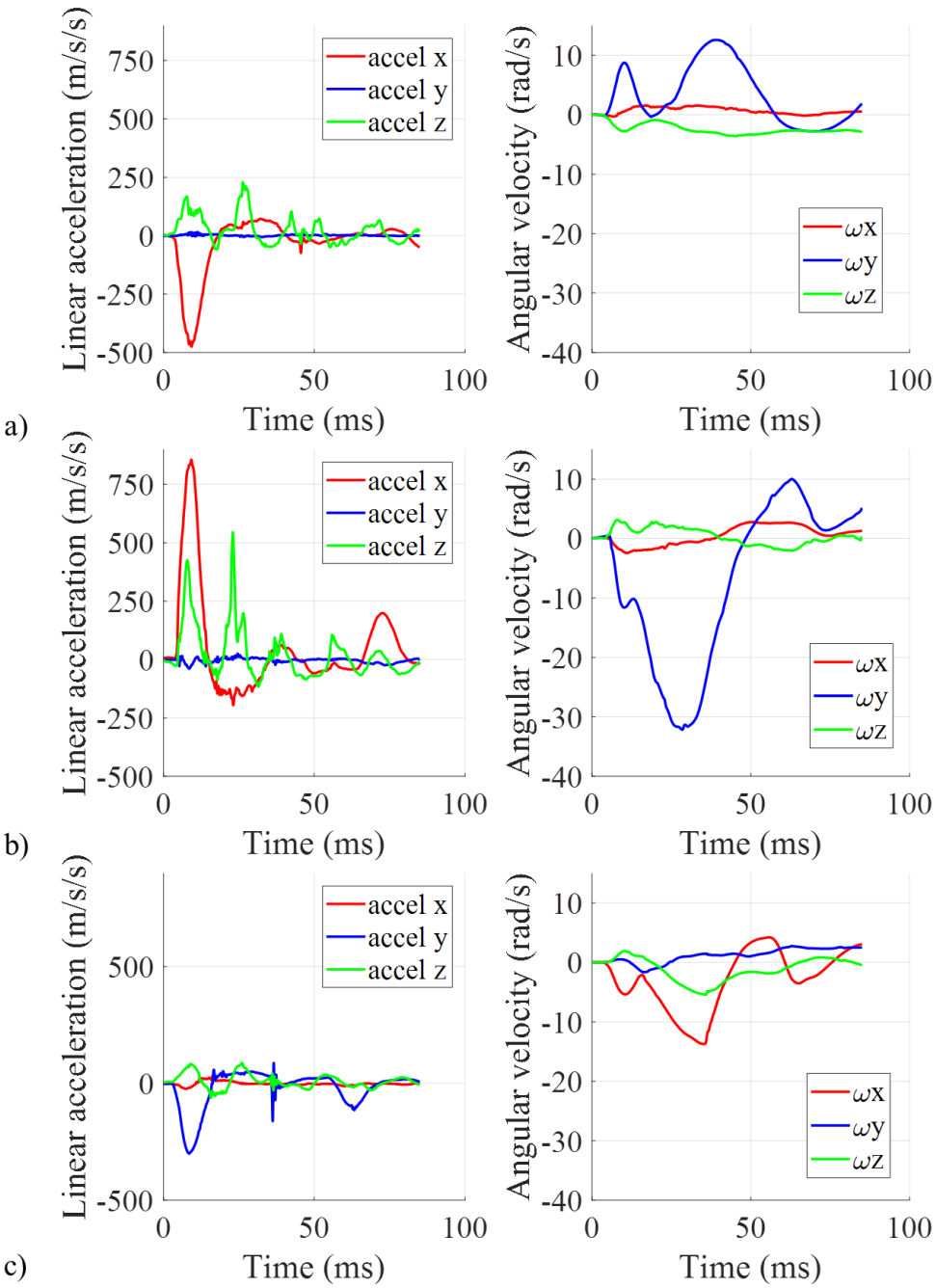

Figure 3.4: Directional linear acceleration (left) and angular velocity (right) for a helmeted Hybrid III head and neck impact to a hockey helmet a) front, b) back and c) right side. Impact time duration shown here is 80 ms with time scales adjusted to start at time=0, immediately prior to initial impact acceleration.

An impact to the helmet Hybrid III forehead (Figure 3.4a) shows the greatest linear acceleration in the negative x-direction and greatest angular velocity about the y-axis, consistent with the direction of impact as defined by the Hybrid III headform coordinate

system. This same observation regarding highest kinematic directions corresponding to correct impact location is consistent for all impact configurations.

A custom MATLAB script was written to digitally process the acquired accelerometer data. The software was used to read and filter the data and to visually represent kinematic traces as well as to determine kinematic values of interest. The kinematics extracted from the acceleration data included impact velocity, peak resultant linear and angular acceleration as well as resultant and direction-specific changes in linear velocity and resultant and direction-specific changes in angular velocity of the Hybrid III headform. The kinematics listed here are further detailed later in this chapter. The MATLAB script was also used to save and format linear acceleration and angular velocity data for use in finite element modelling, which will be discussed below.

3.1.3 Accelerometer compatibility check

Completing checks for polarity and compatibility confirms the instrumentation is functioning properly. Successful polarity checks show correct coordinate directions are being measured. This was done by striking the stationary, unprotected headform at the front, back and each side and confirming accelerometer responses corresponded to the striking location through correct coordinate direction and correct positive or negative magnitude.

To check for compatibility, each measured acceleration trace was also calculated using a set of rigid body constraint equations as described by Takhounts [78]. This system of equations allows measured accelerations to be compared to calculated ones, where calculated accelerations is considered correct based on rigid body motion of the Hybrid III head. Proper function of accelerometers displays direct overlap of measured and calculated accelerations, therefore if the measured acceleration does not identically match the calculated, it is considered incompatible and readings are questioned. Figure 3.5 shows example results for one compatibility test performed for a helmeted impact.

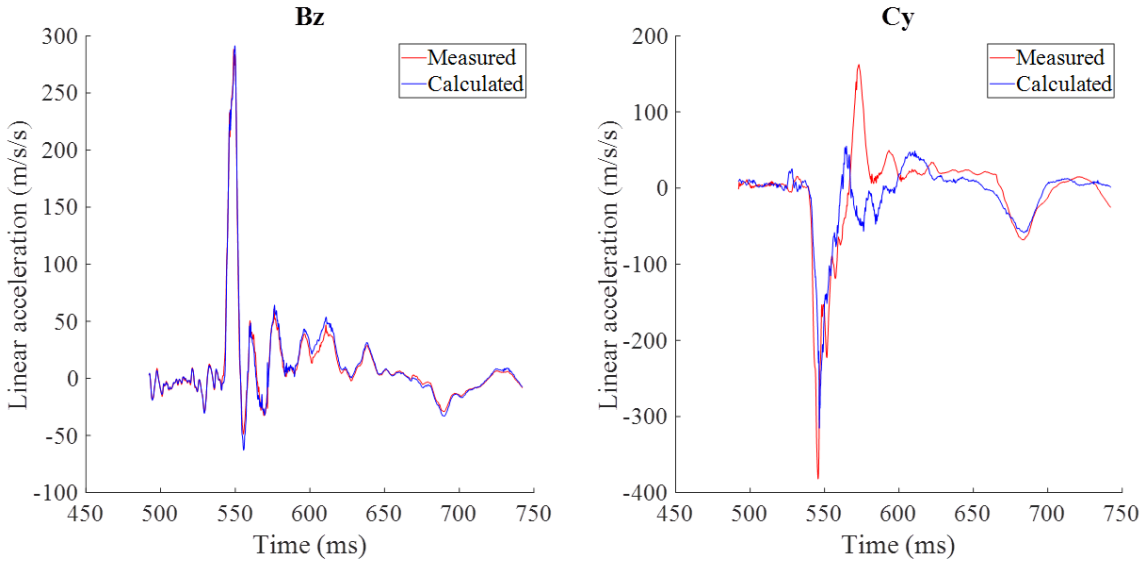

Figure 3.5: Example results for a compatibility check for a helmeted impact. Accelerometer Bz (left) shows an example of nearly identical acceleration curves and accelerometer Cy (right) is an example of few cases where acceleration curves do not perfectly match.

The compatibility checks completed for this thesis dataset overall show near-perfect agreement between measured and calculated acceleration curves, similar to what is shown on the left in Figure 3.5. The right plot in Figure 3.5 is an example of what is considered to be an erroneous or incompatible channel. In a case where an erroneous channel is suspected, the consequence of using the potentially incorrect acceleration trace was quantified by comparing resulting kinematics and computed strains for two cases: one using the measured acceleration values (red curve data) and the other using the calculated acceleration values (blue curve data). After using the kinematics shown in red as inputs to SIMon and then the kinematics shown in blue and computing the resulting strain metrics for each, the relative difference in computed strains is less than 1.5% of one another. These erroneous channels rarely occurred and in cases that it was noted, the effect on strain was within a relative 1.5% of the corrected measure. Therefore, the effect of a rare incompatible channel is negligible on the outcome of this study.

Furthermore, SIMon brain model videos showing head and brain motion correctly represent the impact scenario. For example, input kinematics for an impact to the front of the helmet result in a video of the brain rotating positively about the y-axis (backwards), which matches the motion experienced by the headform during impact.

3.2 Experimental design

Linearly guided drop impacts created the means for investigating headform impacts in this study. Helmeted impacts were performed using the Hybrid III head and neck as well the Hybrid III head without a neck. Impacts were conducted to the helmet front, back and sides for both hockey and football helmets with added crown impacts for football helmets to capture common impact scenarios for each sport. Impact kinematics from 60 hockey helmets and 6 football helmets formed the data base from which the impact data was drawn to achieve the listed sample sizes. Each hockey helmet was impacted a maximum of 18 times (as per CSA standard with maximum 3 impacts at 6 different impact sites), where each individual impact was treated as one sample. After each impact, a visual inspection of the helmet was done to confirm the helmet sustained no structural damage. Similarly, football helmets were impacted up to 25 times each (per NOCSAE requirements of maximum 5 impacts per 5 unique impact sites), resulting in multiple samples per helmet with a visual inspection conducted after each impact. Finally, impacts were conducted to the unprotected headform as a way of understanding the effect of a helmet on select impact kinematics for this drop configuration.

A summary of all impact scenarios investigated, corresponding impact duration times and the samples sizes for each is found in Table 3.1. The summary includes select linear and angular kinematic ranges, quantified by impact velocity (V_i), peak linear acceleration (peak g) and peak resultant angular velocity (ω_R). All impact setups will be described in detail following this table.

Table 3.1: Summary of impacts conducted and N-samples in the data set

Setup	Samples (N)	Time duration (ms)	Vi (m/s)	Peak g (g)	ωR (rad/s)
HybridIII head and neck					
Hockey					
All	255	80	1.2 - 5.8	19 - 138	6 - 40
Front	100	80	1.5 - 5.8	23 - 138	6 - 30
Back	85	80	1.4 - 5.1	21 - 110	14 - 40
Side	70	80	1.2 - 4.7	19 - 105	8 - 25
Football					
All	115	85	3.9 - 6.1	45 - 129	14 - 49
Crown	25	85	4.2 - 6.1	45 - 120	15 - 32
Front	45	85	3.9 - 6.1	51 - 129	18 - 32
Back	20	85	4.1 - 6.1	60 - 129	32 - 49
Side	25	85	4.1 - 6.1	55 - 128	18 - 38
Unprotected					
All	39	85	1.4 - 3.9	49 - 204	10 - 47
Front	15	85	1.4 - 3.7	50 - 176	10 - 31
Back	15	85	1.5 - 3.8	49 - 204	17 - 32
Side	9	85	1.7 - 3.9	71 - 197	19 - 47
HybridIII head, no-neck					
Hockey					
All	227	75	1.6 - 5.6	27 - 141	4 - 45
Front	82	75	1.8 - 5.6	27 - 134	6 - 27
Back	78	75	1.8 - 5.6	29 - 141	4 - 45
Side	67	75	1.6 - 5.2	38 - 119	7 - 21
Football					
All	117	90	3.8 - 6.0	42 - 126	4 - 43
Crown	25	90	4.1 - 6.0	73 - 126	6 - 23
Front	46	90	3.8 - 6.0	42 - 100	4 - 43
Back	25	90	4.2 - 6.0	67 - 109	5 - 31
Side	21	90	4.1 - 5.9	79 - 110	6 - 43
Unprotected					
All	37	65	1.5 - 3.0	61 - 171	2 - 44
Front	15	65	1.5 - 3.0	61 - 151	8 - 24
Back	14	65	1.5 - 3.0	63 - 135	2 - 30
Side	8	65	1.6 - 2.9	65 - 171	14 - 44

3.2.1 Hybrid III head and neck impact configuration

Various impact scenarios investigated use a customizable linearly-guided rail drop system as the basis for the experimental setup. A guided linear drop creates the impact velocity for the helmeted headform striking an anvil. Other methods for impacting the headform can include

a linear impactor or pendulum strikes. Using a drop-style impact avoids overlap with other research efforts while still providing a simple and feasible setup for helmet assessment.

The primary setup of the drop rail system includes a modular drop gimbal compatible with an anthropomorphic test device (ATD) head and neck impacting a stationary steel impact anvil [68], [79], [80] as shown in Figure 3.6.

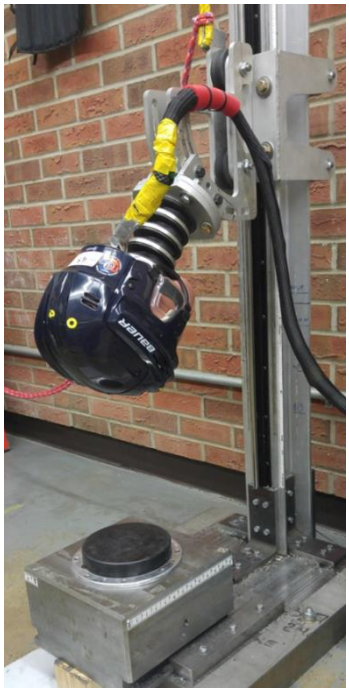

Figure 3.6: Drop tower configured for hockey helmet impact with 50th percentile Hybrid III head and neck mounted to a custom gimbal (total head, neck and gimbal falling mass is 10 kg).

The Hybrid III 50th Percentile dummy head and neck is chosen for the initial setup to represent one possible model for future helmet assessment methods that results in head rotation during impact.

3.2.2 Hybrid III head and no neck impact configuration

Helmeted impacts with a free headform, absent of a neck are also a consideration for future helmet assessment methods [71] and therefore helmeted impacts are simulated using the Hybrid III head without use of a surrogate neck (Figure 3.7). By avoiding directly duplicating others' methods, this work adds to the current database of work that studies sport impacts, providing additional insights. Should the findings here be similar to those that are

based on different impact methods, this could confirm the appropriate kinematics that could be considered for future helmet certification, regardless of the impact setup.

Figure 3.7: The drop tower configured for hockey helmet impacts with Hybrid III head without a neck. A custom gimbal attachment designed for no-neck impacts is used here.

Impacts without the use of the Hybrid III neck require a purpose-built gimbal attachment capable of guiding the headform to strike the anvil with no headform interference immediately following the impact. The design of substitute components to the drop gimbal and anvil allow for ATD head impacts to occur without a neck restraint during the guided drop.

The same range of impact speeds for hockey and football helmets will be used for the impact protocol with and without the neck. Repeating impacts without the Hybrid III neck make it possible to investigate different neck boundary conditions and understand the role the neck plays in the kinematic response of the head.

3.2.3 Helmeted impacts

The various drop scenarios that were explored include impacts using hockey helmets and football helmets mounted on the Hybrid III head. This study used one type each of hockey and football helmets and therefore it is recognized that the results may not necessarily extend

to all helmet types. Hockey helmets (CSA certified helmets, Bauer 4500, size medium) mounted on the Hybrid III headform were subject to impact speeds up to 5.8 m/s, exceeding the required impact speed for certification of 4.5 m/s [40]. Additionally, reference was made to a study that presents typical impacts for collegiate ice hockey players and the corresponding peak g range was achieved using the chosen impact speeds [32]. A modular elastomer programmer (MEP) provided the impact surface for hockey helmets, in compliance with certification and to represent an impact onto an ice surface.

Football helmet (NOCSAE certified helmets, Schutt VTD II and Z10, size medium) impacts reached impact speeds of 6.1 m/s, again exceeding certification requirements of 5.46 m/s [43]. However, in football game impact reconstructions, Pellman et. al. determined an average head impact velocity for both concussed and uninjured players to be approximately 8 m/s [81]. This work focuses on current certification impact speeds, however, future football helmet certification could identify and include typical head impact speeds observed in football. The impact surface atop the anvil for football helmet impacts was a low-friction plastic surface (Kydex Acrylic PVC, 1/8-inch thick) deemed representative of helmet-to-helmet impacts. A study of concussive impacts in the National Football League found that concussive injuries occur nearly evenly as a result of helmet-to-helmet, helmet-to-body, and helmet-to-ground impacts [82]. Helmet-to-helmet impacts are simulated in this study to represent a consistent and repeatable impact condition that accounts for approximately 1/3 of concussive injuries in football.

Helmet impact locations were equally represented during experiments including front, back, and side (left and right) locations, defined as four evenly distributed sections as shown in the upper left quadrant for each helmet in Figure 3.8. Additional crown impacts were conducted for football helmet impacts.

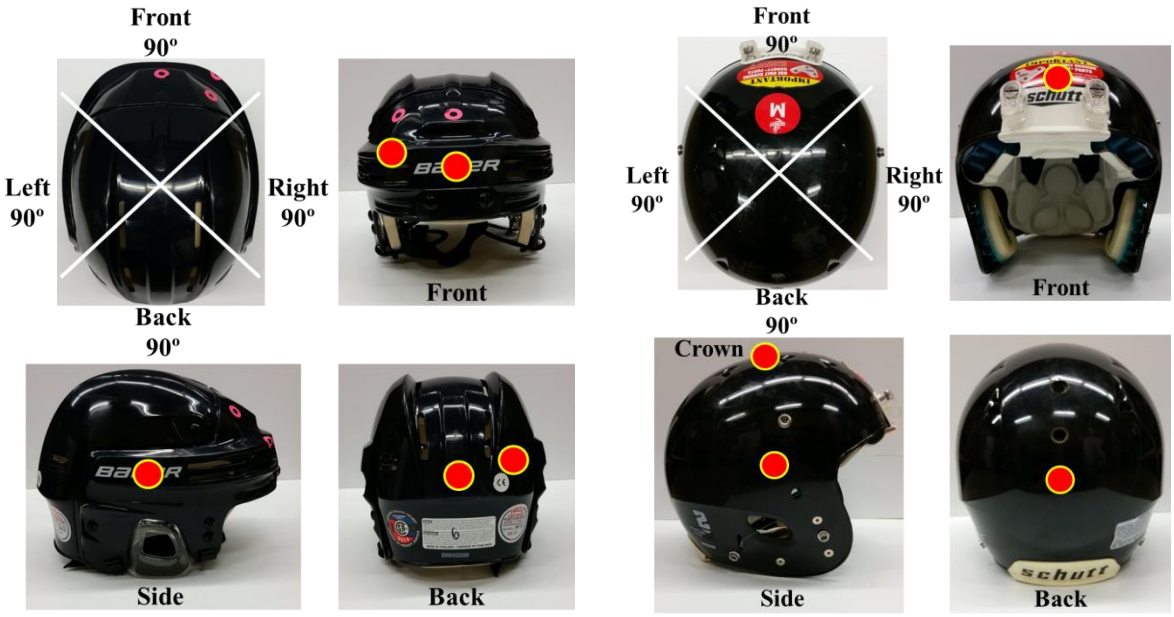

Figure 3.8: Impact location definitions (as indicated by red dots) as shown on a hockey (left) and football (right) helmet.

3.2.4 Unprotected headform consideration

Any kinematic chosen for helmet assessment should be of greatest magnitude when the headform is unprotected and lesser when the headform is helmeted, to confirm a helmet mitigates kinematics associated with injury risk. An unprotected headform with no helmet was subjected to drop impacts as an added comparison to evaluate the effect of using a helmet on the resulting impact kinematics. Unprotected headform impacts were conducted using the MEP surface at impact speeds up to 3.9 m/s for impacts with the neck and 3.1 m/s for impacts without a neck. Impact speeds for unprotected headform drops were not matched identically to the helmeted impacts to prevent breaking the headform or accelerometers as well as to ensure the safety of personnel during drops without use of the neck.

Kinematics from unprotected headform impacts were used to compute strain metrics, including cumulative strain and maximum principal strain, though were not subject to statistical analysis. Results from impacts to the unprotected headform are used to compare kinematics and strain metrics for the helmeted and unprotected headform under similar impact conditions. A helmet should effectively lower the risk of injury relative to no helmet at all. The impact kinematics deemed appropriate for certification through this thesis work

should reflect changes in brain strain metrics for both helmeted and unprotected headform impacts. Through the comparison of impact kinematics for the helmeted and unprotected Hybrid III headform, it is possible to ensure effective and reliable kinematics are identified for future helmet assessment.

Figure 3.9 summarizes the different impact setups investigated including impacts with and without the Hybrid III neck for the Hybrid III headform equipped with a hockey helmet, football helmet and the unprotected headform.

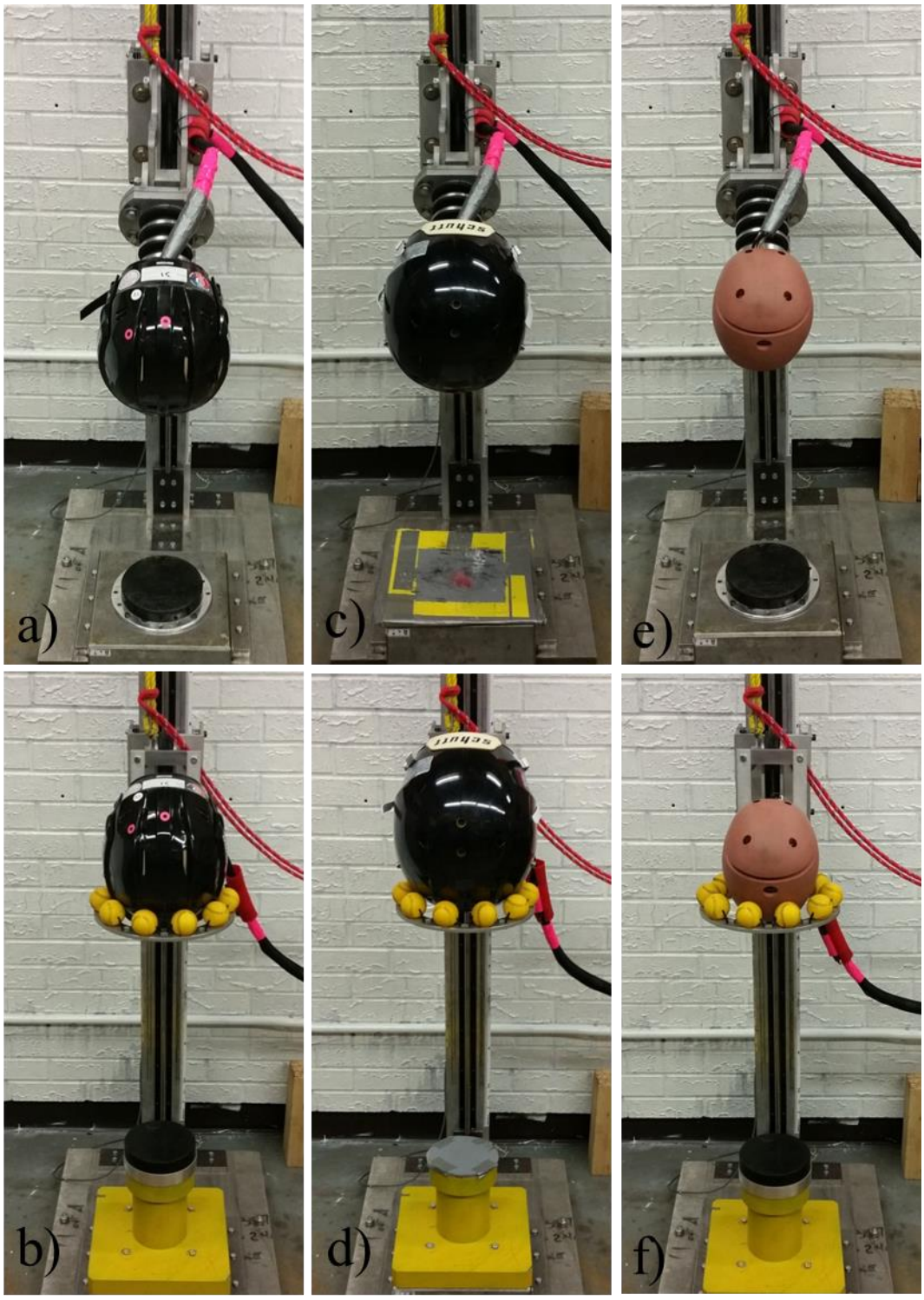

Figure 3.9: A summary of the impact configurations investigated. A 50th percentile Hybrid III head and neck was equipped with an a) hockey and c) football helmet. The Hybrid III head without a neck was also impacted, equipped with a b) hockey or d) football helmet. Finally, the unprotected Hybrid III headform was impacted e) with the Hybrid III neck and f) without a neck.

Oblique impacts with an angled anvil were not considered here as sufficient rotation about each axis was thought to be achieved for all impacts with the Hybrid III head and neck. It is recommended that oblique impacts be considered for no-neck protocols in the future to guarantee similar rotation for all no-neck impacts as well.

Using a drop configuration to induce impact presents one possible setup for helmet certification and aligns with many scenarios currently used in certification. Additionally, in using drop impacts, this work does not duplicate the efforts of other researchers using linear impactors or pendulums. This thesis presents a simple experimental setup up that does not overlap with the work of others and could be feasible for use in helmet assessment.

3.3 Brain finite element modelling

Following acquiring impact acceleration data, brain finite element modelling was used to compute brain strain using the measured impact kinematics. The MATLAB-processed directional linear acceleration and angular velocity served as input to the Improved Simulated Injury Monitor (SIMon [56]) brain-skull FE model (solved using multi-core processor, Core™ i7-4790 CPU 8GB RAM, Intel ®, Santa Clara). SIMon uses linear acceleration in the x, y, and z directions and angular velocity about the x, y, and z axes as kinematic inputs applied to the rigid skull of the model to compute and report mechanical strains experienced over the impact duration.

Maximum principal strain (MPS) and the cumulative strain damage measure (specifically CSDM-15) are two examples of measures that represent brain strain that were used for this thesis work. MPS is the maximum tensile strain reached at any location within the brain, while CSDM-15 represents the cumulative volume fraction of the brain that reaches or exceeds a maximum strain of 15%. Experiments conducted using animals and cadavers, tracking neutral density targets and intra-cranial pressures [83] were used to validate the SIMon brain model to ensure accurate depiction of human response [56]. CSDM has been correlated to diffuse brain injury, originally shown to correlate to injury based on animal injury data [58] and later shown to be an effective predictor for an injury dataset specific to automotive injury [14]. A study of reconstructed football impacts causing mild TBI also established a correlation between CSDM and brain injury [64]. During the development of

BrIC, Takhounts et. al. noted both CSDM-15 and CSDM-25 statistically fit injury data [14]. CSDM-15 is commonly used in literature and therefore will also be used in this study to represent diffuse brain injury risk. Furthermore, the SIMon model was used in developing and correlating CSDM and MPS with diagnosed injury [56] making these strain metrics appropriate for use to represent injury in this experimental process. It is to be noted that using SIMon-computed CSDM-15 and MPS as relative measures for brain strain indicates that an increase in strain metrics translates to an increase in brain injury risk.

Acquired acceleration data spanned a total of 1 s over the duration of the impact experiment, which exceeded the time necessary to capture the main impact event. The impact time window for consideration was narrowed using software to encompass the entire impact including 5 ms prior to and, for hockey helmet impacts, 80 ms following the time at which peak linear acceleration was achieved. For impacts using a football helmet, the time window extended to 85 ms following the time of peak linear acceleration. Choosing a duration of 80 ms for hockey helmet impacts and 85 ms in the case of football helmet impacts for use in SIMon simulations allowed both CSDM-15 and MPS to reach a stable maximum for impacts to the Hybrid III head and neck configuration. In impacts conducted without the use of a surrogate neck (no-neck impacts), the impact durations chosen provide enough time for the kinematics to return to zero or no longer increase. No-neck impact durations also exclude the later moment at which headform interference occurred (i.e. when the headform is restrained by experimenters following the impact). Impact durations of 75 ms and 90 ms are used for 'no-neck' hockey and football helmet impacts, respectively.

3.4 Statistical analysis

3.4.1 Multiple regression

Upon the compilation of impact kinematic data and corresponding brain strain metrics, a statistical analysis is performed to investigate correlations between the two. To determine an appropriate set of kinematics for predicting SIMon-computed brain strain, multiple regression techniques compare kinematic-based linear regression models. Equations 3.1 and 3.2 below present the linear form of the models to be investigated.

$$CSDM15 = a_0 + \beta_1 a_1 + \beta_2 a_2 + \beta_3 a_3 + \cdots + \beta_i a_i \quad (3.1)$$

$$MPS = c_0 + \gamma_1 c_1 + \gamma_2 c_2 + \gamma_3 c_3 + \cdots + \gamma_i c_i \quad (3.2)$$

In the above equations, beginning with a single predictor (i=1), statistical measures are computed including weighted coefficients (β_i, Υ_i) and whether the variable is significant in predicting strain ($p < 0.05$), the coefficient of determination (R^2) and the adjusted R^2 value. The linear model evolves by incrementally increasing the number of kinematic terms (a_i, c_i). As terms are added or replaced, new statistical values are determined.

Comparing models with the same number of predictor terms, the greatest magnitude of R^2 conveys which model best predicts variation in CSDM-15 and MPS. As R^2 will always increase with added terms, adjusted R^2 is computed as a way of accounting for the increased number of terms such that a decrease in adjusted R^2 indicates the most recently added term is not necessarily benefiting the model.

Calculating the F-statistic tests the null hypothesis that the regression coefficients are equal to zero (i.e. the regression model based on the chosen variables is as predictive as simply taking the intercept). Therefore, a significant F-statistic ($p<0.01$) indicates the variables in the regression model improve how well the model fits the data [84]. For cases where no decrease in adjusted R^2 is observed to clearly identify the maximum number of terms that can effectively predict strain, the F-statistic is calculated as a method to rank the models, as the F-statistic is considered here to represent how efficiently the model uses the included terms to predict the data set [85].

Similar to R^2, a higher F is favorable [84], [86]. A high adjusted R^2 value indicates the model predicts the variation in the data. A high F-statistic ensures the model is better than using the intercept only. Where two models achieve similar R^2, the model with the greater F-statistic would be a better choice as it indicates higher probability of being better than the intercept alone. The aim for this analysis is to identify a model that optimizes both R^2 and F.

A Multiple Regression analysis conducted for all impact scenarios allows comparing of the chosen models to identify which kinematics predictors are significant ($p < 0.05$), which model best fits the data (adjusted R^2) and the relative efficiency of that model (F) compared

to other models being investigated. The ideal model, for example, would have the greatest F-statistic value of all the models with R^2 close to 1 and all predictor variables showing significance. This statistical method will determine an appropriate number of kinematics and identify the specific kinematics to include in a metric for predicting strain. Prior to conducting this analysis, it is not known to the author whether multiple kinematic variables are required, or what those variables should be.

The technique described above was applied to all impact locations considered together in a single data set as well as each impact location separately in order to determine whether the best kinematic predictors based on statistics differs by impact location. Considering helmet location as a covariate or a confounding variable could be another method for confirming whether impact location alters the statistical findings for kinematic predictors. The method used in this study, however, was to apply multiple regression techniques to each individual location.

The list of kinematics that are considered individually and in combination include: peak resultant linear acceleration (peak g), peak resultant angular acceleration (α_R), impact velocity (V_i), resultant change in linear velocity (ΔV_R), peak resultant linear velocity (V_R), resultant change in angular velocity ($\Delta\omega_R$), directional change in angular velocity ($\Delta\omega_x$, $\Delta\omega_y$, $\Delta\omega_z$), peak resultant angular velocity (ω_R) and directional peak angular velocity (ω_x, ω_y, ω_z). Figure 3.10 demonstrates how each of the listed kinematics is determined.

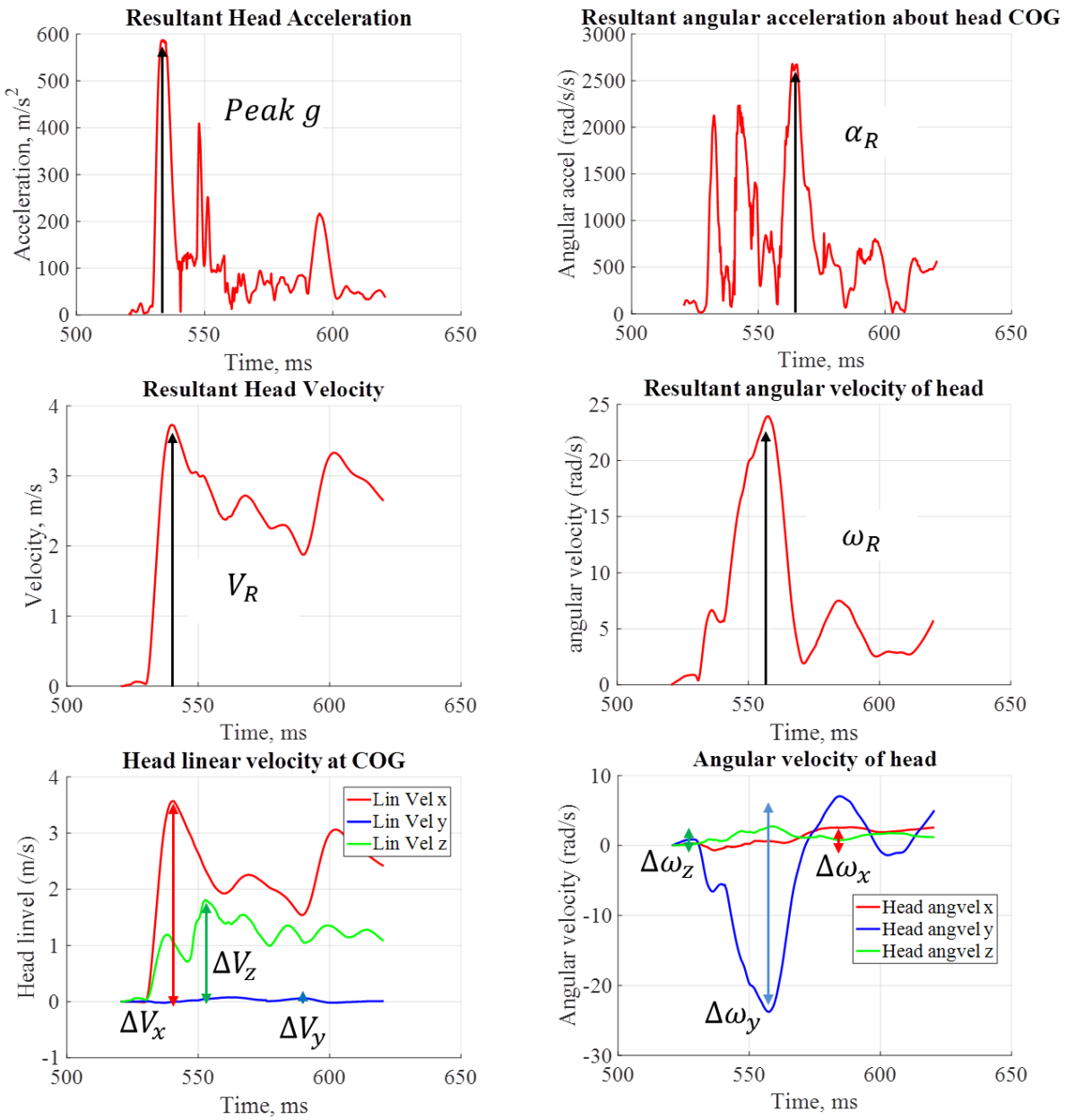

Figure 3.10: Examples of linear (left) and angular (right) impact kinematics to define the variables considered.

Resultant change in linear and angular velocity were calculated selecting the greatest magnitude of kinematic change about individual axes regrardless of the time at which this occurred within the impact duration as a way of capturing the maximum head motion during impact. These values were calculated using the following formulas:

$$\Delta V_R = \sqrt{\Delta V_x^2 + \Delta V_y^2 + \Delta V_z^2} \tag{3.3}$$

$$\Delta \omega_R = \sqrt{\Delta \omega_x^2 + \Delta \omega_y^2 + \Delta \omega_z^2} \tag{3.4}$$

The same practices are used for linear and angular kinematics for all impact setups including hockey and football helmet impacts with the Hybrid III head and neck and Hybrid III head with no neck.

3.4.2 Sample size

Determining an approriate sample size for multiple regression analysis can be complex. Some methods that have been presented require sufficient prior knowledge of correlation coefficents [87] that may not always be known to the researcher. Therefore, Green presented some rules of thumb that can be applied when using multiple regression that have been generally accepted when the number of predictors is less than N=7 [88]. These general guidelines suggest researchers apply the following equation to determine the number of samples required for multiple regression analysis, where N is the number of samples and *i* indicates the number of predictor terms.

$$N \geq 50 + 8i \tag{3.5}$$

In applying this formula, considering the maximum number of predictors (here *i*=5) requires a minimum sample size of 90. All sample sizes in this study exceeded 90 for helmeted impacts considering all impact locations together. For example, the smallest sample size is 115 for football helmet impacts with a neck when all impacts are considered together as one dataset. Considering impact locations separately, sample sizes become smaller than the minimum rule of thumb of 90 samples, and though the statistical significance of each individual kinematic may not be robust in this case, the additional analyses provide valuable insight regarding relative correlations.

It is recognized that interactions between predictor variables may be present, though they are not quantitatively explored here during the statistical analyses. The objective of this thesis is to identify a model for assessing helmets based on kinematics that correlate with strain

metrics. In practice, helmet assessment metrics are simple and contain few terms. Therefore, realistically, this will require a metric that is simple, containing as few elements as possible, while still sufficiently predicting injury. It is recognized that there may be correlations between individual predictor kinematics in addition to correlations with strain metrics, though the goal of this thesis is not to quantify individual effect sizes. Therefore, only statistical considerations relevant to the specific thesis objectives of developing a kinematic method for predicting strain during helmet assessment are analyzed.

By applying the statistical results to understand the kinematics that best correlate with injury measures, it is possible to identify the key kinematics to consider during future helmet assessment methods.

3.5 Test repeatability

A test for repeatability was conducted for this experimental setup with the Hybrid III head and corresponding instrumentation. Three impacts were considered to the hockey helmet front, and three to the football helmet side. The accelerometer measures in the dominant acceleration direction (CoGx, Ax and Cx for front impacts and CoGy, By, Cy) for side impacts) were compared and found to be repeatable (Figure 3.11), with an average root mean square deviation of 1.89 g. A comparison of average peak values and standard deviations for peak g, ω_R, CSDM-15 and MPS at multiple impact speeds and locations can be found in Appendix A. For the impacts presented in Appendix A, the average coefficient of variation is 0.03.

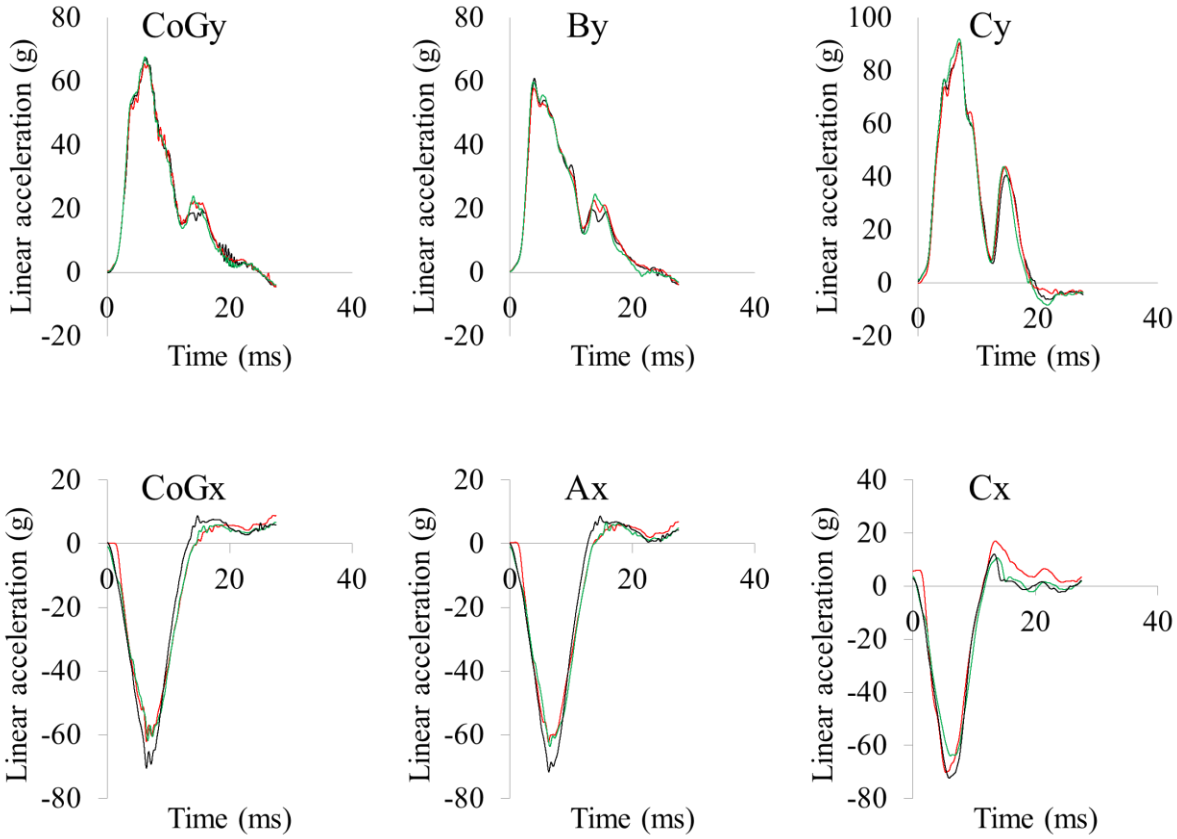

Figure 3.11: Comparison of accelerometer data for the same impact speed for a side impact with a football helmet (top) and a front impact with a hockey helmet (bottom).

4 Results

This chapter summarizes the statistical results for regression models focusing on adjusted R^2 and F-statistic to convey which models were most explanatory of CSDM-15 and MPS. A short discussion follows to identify which models could be viewed as most efficient (most explanatory, with least variables) and to understand what R^2 and F a simple kinematic model can achieve in predicting CSDM-15 and MPS. Results for impacts using the Hybrid III head and neck will be presented first, followed by results related to impacts with the Hybrid III head and no neck. Finally, the effect of a helmet on mitigating impact kinematics will be presented. Appendix B comprises summary tables for all regression results so that the interested reader may review all considered models.

4.1 Results for helmeted Hybrid III head and neck

4.1.1 SIMon-computed strain

Ensuring that the computed strain levels achieve a stable maximum with no further changes in strains indicates the entire impact event has been captured. The Improved SIMon-computed strain levels achieve a stable maximum for the chosen impact duration suggesting enough time was considered to capture the entire impact and strain event. Figure 4.1 displays the resulting SIMon-computed strain plots for a front hockey helmet impact. All impacts with the Hybrid III head and neck considered for statistical analysis show strain values achieving a stable maximum similar to the plots shown below.

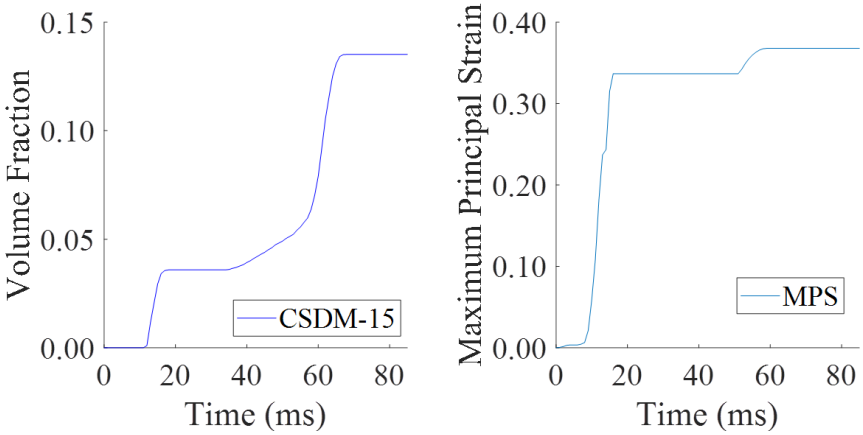

Figure 4.1: SIMon-computed CSDM-15 (left) and MPS (right) plotted against time for a helmeted Hybrid III head and neck impact to the helmet front.

4.1.2 Statistical analysis for helmeted Hybrid III head and neck

4.1.2.1 Single kinematics with highest adjusted R^2

For helmeted impacts with the Hybrid III head and neck, the single best kinematic predictor for strain, defined as the kinematic that simultaneously achieves the highest F-statistic and adjusted R^2, is angular velocity. For hockey helmet impacts, the choice single kinematic is peak resultant change in angular velocity ($\Delta\omega_R$), while football helmet impacts favor peak resultant angular velocity (ω_R). The kinematic achieving the highest F-statistic and adjusted R^2 among single predictors of CSDM-15 and MPS, is summarized in Table 4.1 and Table 4.2, respectively, organized by helmet type and impact location.

Table 4.1: The single best kinematic for predicting CSDM-15 for helmeted impacts with Hybrid III head and neck. Bold and italicized variables indicate that they are significant predictors.

Impacts	Variables		Adj R^2	F
Hockey				
All	$\boldsymbol{\Delta\omega_R}$		0.86	1629
Front	$\boldsymbol{\Delta\omega_R}$		0.83	522
Back	$\boldsymbol{\Delta\omega_R}$		0.96	2386
Side	$\boldsymbol{\Delta\omega_R}$		0.72	185
Football				
All		$\boldsymbol{\omega_R}$	0.83	679
Crown	$\boldsymbol{\Delta\omega_R}$		0.74	85
Front	$\boldsymbol{\Delta\omega_R}$		0.83	234
Back		$\boldsymbol{\omega_R}$	0.89	201
Side		$\boldsymbol{\omega_R}$	0.86	180

Table 4.2: The single best kinematic for predicting MPS for helmeted impacts with Hybrid III head and neck. Bold and italicized variables indicate that they are significant predictors.

Impacts	Variables		Adj R^2	F
Hockey				
All	$\Delta\omega_R$		0.89	2023
Front	$\Delta\omega_R$		0.83	479
Back	$\Delta\omega_R$		0.93	1072
Side	$\Delta\omega_R$		0.78	253
Football				
All		ω_R	0.64	234
Crown	α_R		0.77	64
Front	$\Delta\omega_R$		0.68	105
Back	$\Delta\omega_R$		0.87	158
Side		ω_R	0.85	169

4.1.2.2 Regression models achieving highest F-statistic value

Regression models resulting in the maximum F-statistic are almost exclusively based on angular velocity. Commonly, the greatest F-statistic model includes a single predictor variable, matching the models presented above with the greatest adjusted R^2 for single kinematic predictors for both hockey and football helmet impacts with the head and neck. The variables included in the regression model that achieves the maximum possible F-statistic for each impact scenario are shown in Table 4.3 and Table 4.4 for predicting CSDM-15 and MPS, respectively.

Table 4.3: A summary of regression models and the kinematic(s) included in each model achieving the maximum F-statistic for predicting CSDM-15 for helmeted impacts with Hybrid III head and neck. Bold and italicized variables indicate that they are significant predictors.

Impacts	No. of Variables	Variables included in model						Adj R^2	F
Hockey									
All	1		$\Delta\omega_R$					0.86	1629
Front	1		$\Delta\omega_R$					0.83	522
Back	1		$\Delta\omega_R$					0.96	2386
Side	1		$\Delta\omega_R$					0.72	185
Football									
All	1	ω_R						0.83	679
Crown	1		$\Delta\omega_R$					0.74	85
Front	1		$\Delta\omega_R$					0.83	234
Back	1	ω_R						0.89	201
Side	3			ω_x	ω_y	ω_z		0.96	236

Table 4.4: A summary of multi-variable regression models and the kinematic(s) included in each model achieving the maximum F-statistic for predicting MPS for helmeted impacts with Hybrid III head and neck. Bold and italicized variables indicate that they are significant predictors.

Impacts	No. of Variables	Variables included in model						Adj R^2	F
Hockey									
All	1			$\Delta\omega_R$				0.89	2023
Front	1			$\Delta\omega_R$				0.83	479
Back	1			$\Delta\omega_R$				0.93	1072
Side	1			$\Delta\omega_R$				0.78	253
Football									
All	1			ω_R				0.64	234
Crown	2	***Peak g***	α_R					0.92	115
Front	1			$\Delta\omega_R$				0.68	105
Back	1			$\Delta\omega_R$				0.87	158
Side	3				ω_x	ω_y	ω_z	0.96	244

4.1.2.3 Multi-variable regression models achieving highest possible adjusted R^2

Maximizing adjusted R^2 requires up to 5 predictor variables (the maximum number investigated) including linear and angular kinematics, although, as previous tables show, a single angular kinematic can predict strain metrics. A summary of the models that achieve maximum adjusted R^2 for models predicting CSDM-15 and MPS can be seen in Table 4.5 and Table 4.6, respectively, for head and neck impacts.

Table 4.5: A summary of multi-variable regression models and the kinematics included in each model achieving the maximum adjusted R^2 for predicting CSDM-15 for helmeted impacts with Hybrid III head and neck

Impacts	No. of Variables	Variables included in regression model								Adj R^2	F
Hockey											
All	4	***Peak g***	V_i	ΔV_R					$\Delta\omega_R$	0.89	525
Front	4	Peak g				ω_x	ω_y	ω_z		0.92	289
Back	2			V_R					$\Delta\omega_R$	0.98	2314
Side	4	***Peak g***	V_i	ΔV_R	α_R					0.81	75
Football											
All	4	Peak g				$\Delta\omega_x$	$\Delta\omega_y$	$\Delta\omega_z$		0.90	319
Crown	4	***Peak g***	V_i	V_R	α_R					0.92	53
Front	4	Peak g	V_i	ΔV_R					$\Delta\omega_R$	0.83	61
Back	3	Peak g		V_R					ω_R	0.94	123
Side	4	Peak g				ω_x	ω_y	ω_z		0.96	189

Table 4.6: A summary of multi-variable regression models and the kinematics included in each model achieving the maximum adjusted R^2 for predicting MPS for helmeted impacts with Hybrid III head and neck

Impacts	No. of Variables	Variables included in regression model								Adj R^2	F
Hockey											
All	5	***Peak g***		ΔV_R		ω_x	ω_y	ω_z		0.90	447
Front	5	***Peak g***		ΔV_R		ω_x	ω_y	ω_z		0.93	283
Back	3					$\Delta\omega_x$	$\Delta\omega_y$	$\Delta\omega_z$		0.94	473
Side	4	***Peak g***	V_i	ΔV_R	α_R					0.82	73
Football											
All	3					$\Delta\omega_x$	$\Delta\omega_y$	$\Delta\omega_z$		0.81	188
Crown	4	Peak g	V_i	V_R	α_R					0.94	78
Front	2				α_R				ω_R	0.80	78
Back	4	Peak g	V_i	V_R					$\Delta\omega_R$	0.90	52
Side	5	Peak g		ΔV_R		ω_x	ω_y	ω_z		0.97	166

Considering all impacts together as well as considering location-specific impacts individually for the helmeted Hybrid III head and neck, there are 6 different models to consider that achieve a maximum adjusted R^2 for predicting CSDM-15 and 5 different models for predicting MPS, depending on the location, compared to 2 different single predictor models for predicting CSDM-15 and 3 for predicting MPS. Additionally, considering all impacts together, the maximum possible adjusted R^2 for a model with multiple kinematic terms improves adjusted R^2 by an average of 10% relative to a model based on a single kinematic considering both CSDM-15 and MPS. By comparison, the F-statistic decreases by 55% on average from a single kinematic model to a model achieving the maximum adjusted R^2. All F-statistics for models including angular velocity only are significant (p-value<0.01) and R^2 is as high as 0.89, suggesting the modest increase in R^2 may not justify the decrease in F corresponding to a complex, multi-variable model.

4.1.3 Choosing one kinematic model

The set of kinematics that achieves the maximum adjusted R^2 is not the same for all impact scenarios. For example, a model including Peak g, ω_x, ω_y, and ω_z achieves a maximum adjusted R^2 of 0.92 for predicting CSDM-15 for front hockey helmet impacts, while a maximum adjusted R^2 of 0.98 for a model predicting CSDM-15 for back hockey helmet

impacts includes V_R and $\Delta\omega_R$. Similar results are found for predicting MPS, as well as predicting both CSDM-15 and MPS for football helmet impacts.

Adding predictor variables to a previous model always results in adjusted R^2 increasing or staying the same, though the F-statistic always decreases. Considering impact locations separately, as well as all together, on average, maximizing adjusted R^2 by adding kinematic variables to a model predicting CSDM-15 for helmeted impacts with the Hybrid III head and neck increases adjusted R^2 by 7% relative to a single kinematic predictor while the F-statistic decreases by an average of 42%. Similarly, for predicting MPS, adjusted R^2 increases by 10% on average with added terms, while the F-statistic decreases by 45% for helmeted impacts to the Hybrid III head and neck.

A single kinematic variable demonstrates capable of predicting strain metrics, meaning, contrary to many previously proposed metrics, a model need not include multiple predictors to achieve R^2 greater than 0.8 and significant F. Figure 4.2 and Figure 4.3 compares a single-kinematic model for predicting CSDM-15 and MPS to a multi-variable kinematic model including the same single kinematic with added terms for a greater adjusted R^2 value. Note that in Figure 4.2 and Figure 4.3, the horizontal axes are presented without units. In plots a) and c), the regression model is in units of rad/s such that a change in angular velocity corresponds to a change in strain. For plots b) and d), the use of multiple kinematics and regression coefficients indicates that a change in the model represents a relative change in strain. However, the magnitudes of the horizontal axes are not of interest here, but rather the resulting R^2 and F-statistic.

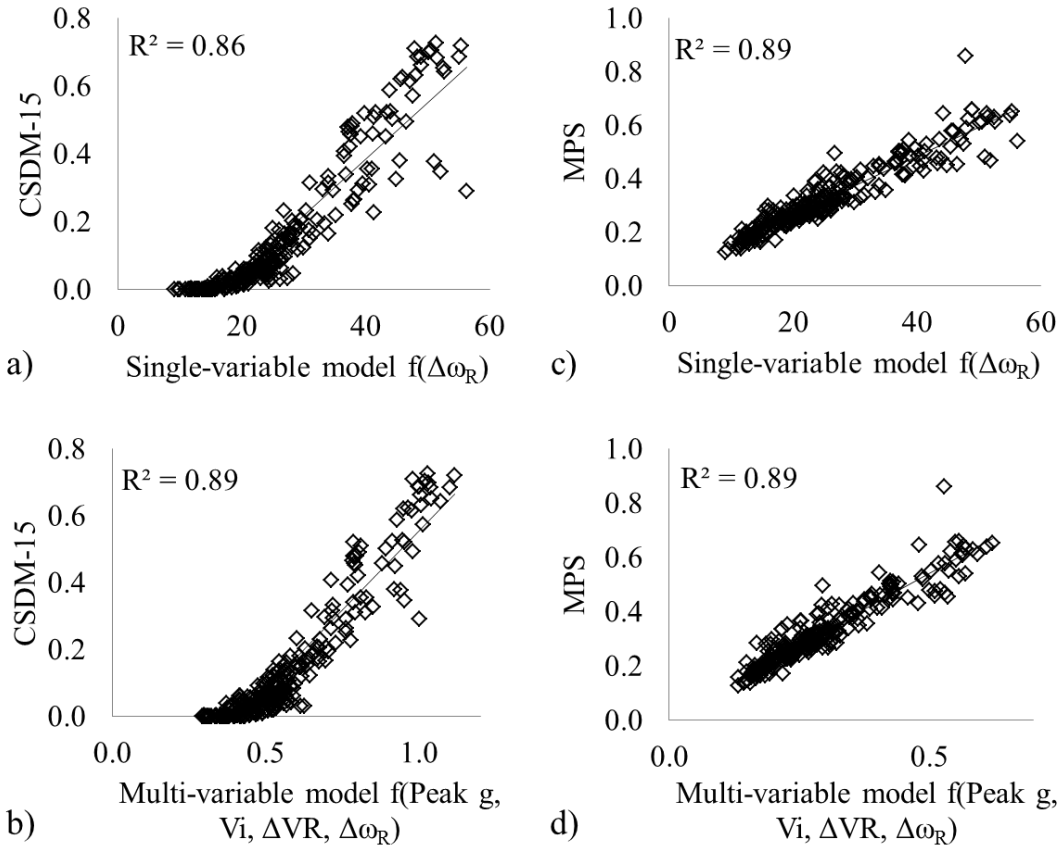

Figure 4.2: Scatter plot comparisons for hockey helmet impacts including a) a single-kinematic model, $\Delta\omega_R$, in units of rad/s, plotted against CSDM-15 and b) a multi-variable model including $\Delta\omega_R$ and added variables Peak g, V_i, and ΔV_R, in units of volume fraction, plotted against CSDM-15. Similarly, c) $\Delta\omega_R$, in units of rad/s, plotted against MPS and d) a multi-variable model including $\Delta\omega_R$, Peak g, V_i, and ΔV_R, in units of strain, plotted against MPS.

In Figure 4.2a, R^2 is 0.86 with the single kinematic predictor $\Delta\omega_R$, while in Figure 4.2b R^2 only increases to 0.89 using a regression model based on four kinematic variables. From Figure 4.2a to Figure 4.2b, the F-statistic decreases, though both remain significant ($p<0.01$) and therefore it may not be necessary to include four predictor terms. In Figure 4.2c and Figure 4.2d, R^2 does not change at all, though F decreases. Similar results are presented in Figure 4.3 for football helmet impacts. It can therefore be argued that four kinematics are not required for a regression model to correlate to strain and achieve significant F.

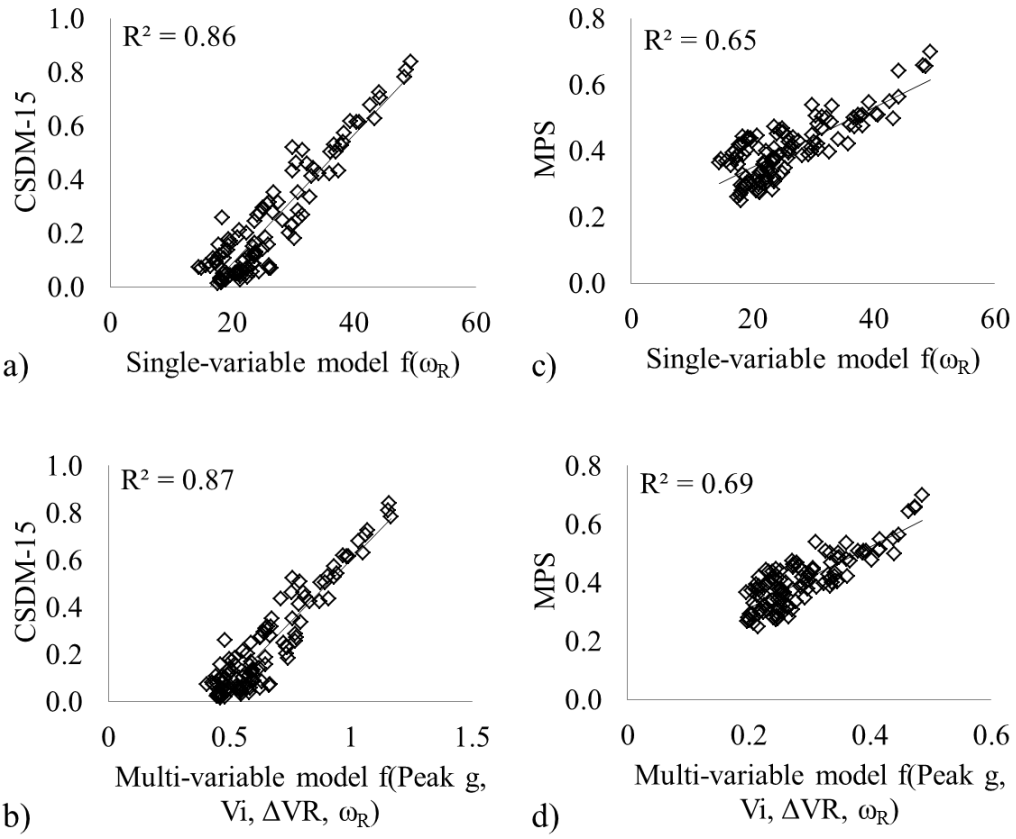

Figure 4.3: Scatter plot comparisons for football helmet impacts including a) a single-kinematic model, ω_R, in units of rad/s, plotted against CSDM-15 and b) a multi-variable model including ω_R and added variables Peak g, V_i, and ΔV_R, in units of volume fraction, plotted against CSDM-15. Similarly, c) ω_R, in units of rad/s, plotted against MPS and d) a multi-variable model including ω_R, Peak g, V_i, and ΔV_R, in units of strain, plotted against MPS.

Based on Figure 4.2 and Figure 4.3, once the individual kinematic with the greatest R^2 for predicting strain is identified ($\Delta\omega_R$ for hockey helmets and ω_R for football helmets), adding terms achieves nearly identical predicted variance (R^2) though decreases F.

Overall, peak resultant angular velocity gives a greater adjusted R^2 for predicting strain when considering all impacts together for both football and hockey helmets. Considering all impact locations together to the helmeted Hybrid III head and neck, using ω_R to predict CSDM-15 and MPS achieves an average adjusted R^2 of 0.84 and 0.74, respectively, averaging individual adjusted R^2 values for hockey and football helmet impacts. Similarly, adjusted R^2 for predicting CSDM-15 and MPS using $\Delta\omega_R$ is 0.78 and 0.67, respectively when

averaging adjusted R^2 values for hockey and football helmet impacts. Overall, ω_R as a strain predictor for helmeted impacts achieves the greatest value of R^2.

All impact locations considered together and combining hockey and football helmet impact data into one data set, ω_R achieves greater R^2 values than $\Delta\omega_R$. In all but one case, the single best kinematic predictor was either ω_R or $\Delta\omega_R$. All impacts considered together, $\Delta\omega_R$ is the choice single kinematic to predict strain for hockey helmet impacts, while ω_R is the choice kinematic for football impacts. Figure 4.4 compares the variance in predicting CSDM-15 and MPS using ω_R and $\Delta\omega_R$.

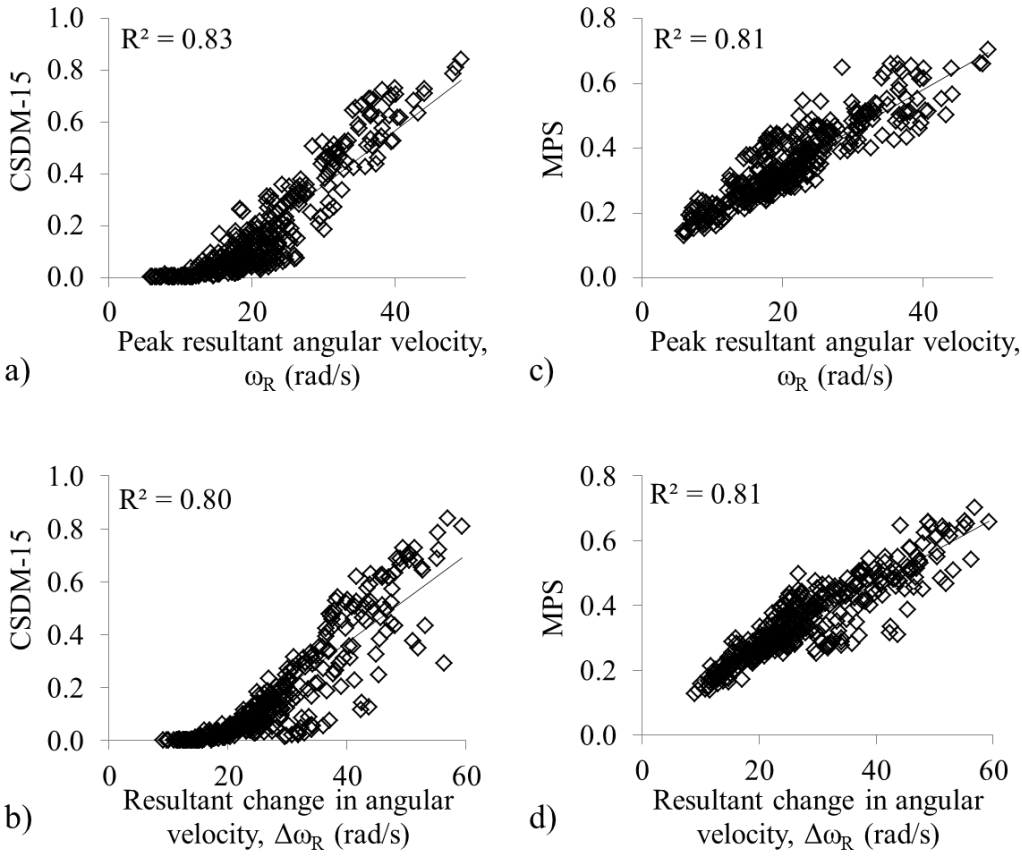

Figure 4.4: CSDM-15 plotted against a) peak resultant angular velocity, ω_R, and b) resultant change in angular velocity, $\Delta\omega_R$. Similarly, MPS plotted against c) ω_R and d) $\Delta\omega_R$. The plots above are for hockey and football impacts combined and all impacts considered together in a single data set.

Using ω_R in place of $\Delta\omega_R$ to predict strain for hockey helmet impacts reduces adjusted R^2 on average for CSDM-15 and MPS by 6%. Alternatively, using $\Delta\omega_R$ to predict strain for football helmet impacts decreases adjusted R^2 by 25% relative to using ω_R. In all cases, the

F-statistic remains significant. Furthermore, when all football and hockey helmeted impacts are considered as a single dataset, plotting CSDM-15 against ω_R results in less variance than CSDM-15 plotted against $\Delta\omega_R$ (Figure 4.4). For predicting MPS, nearly identical variance is observed. Overall, ω_R is the best single kinematic for predicting strain for helmeted impacts with the Hybrid III head and neck.

Peak resultant angular velocity, ω_R, achieves greater R^2 than linear acceleration when plotted against strain metrics. Figure 4.5 and Figure 4.6 show CSDM-15 and MPS, respectively, plotted against each of peak g and ω_R for all helmeted impacts. Comparing R^2 and F, ω_R results in R^2 of 0.83 and F of 1829 when plotted against CSDM-15, while peak g results in R^2 of 0.33 and F of 189 when also plotted against CSDM-15. Similarly, ω_R results in R^2 of 0.81 and F of 1569 when plotted against MPS, while peak g results in R^2 of 0.42 and F of 262. This shows ω_R increases R^2 and F on average by 122% and 682%, respectively, relative to peak g.

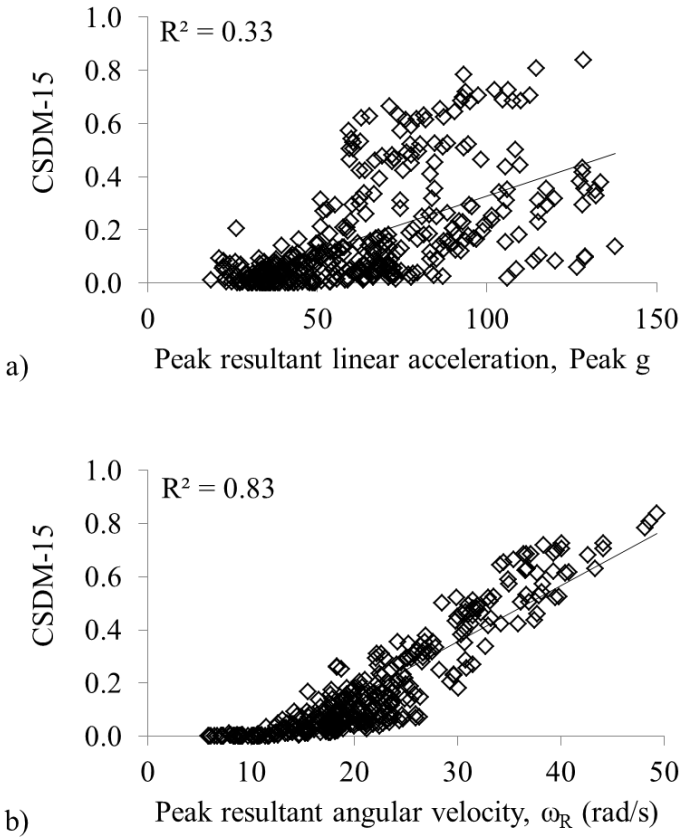

Figure 4.5: CSDM-15 plotted against a) peak linear acceleration and b) peak resultant angular velocity for all helmeted impacts.

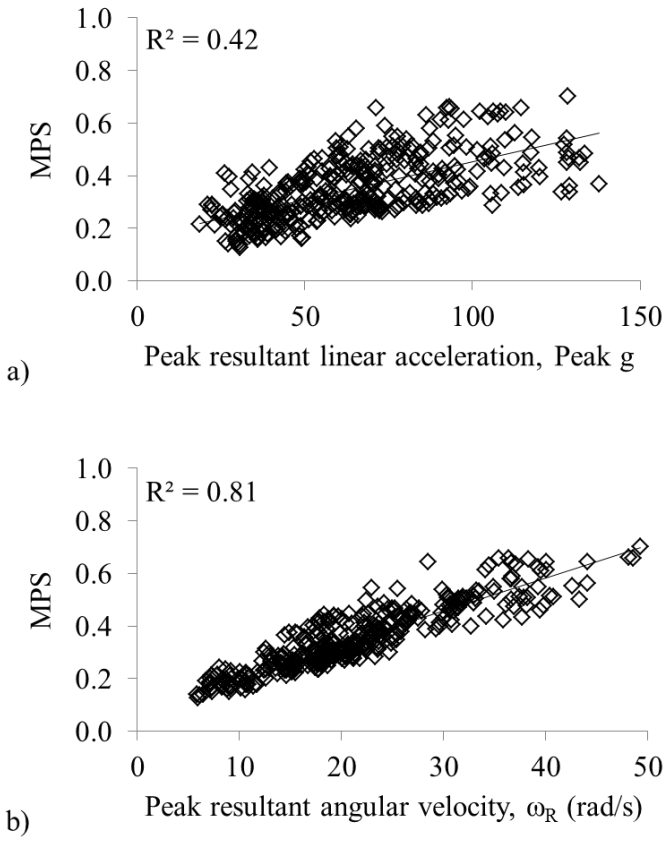

Figure 4.6: MPS plotted against a) peak linear acceleration and b) peak resultant angular velocity for all helmeted impacts

Linear acceleration is used in current helmet standards [40], [43], [66] though is shown in this study to be a poor predictor for strain metrics. Angular velocity achieves a greater adjusted R^2 and F-statistic than current helmet certification metric, peak g, though a positive correlation was found between peak g and ω_R, as shown by the relationship displayed in Figure 4.7. Overall, an increase in ω_R corresponds to an increase in peak g.

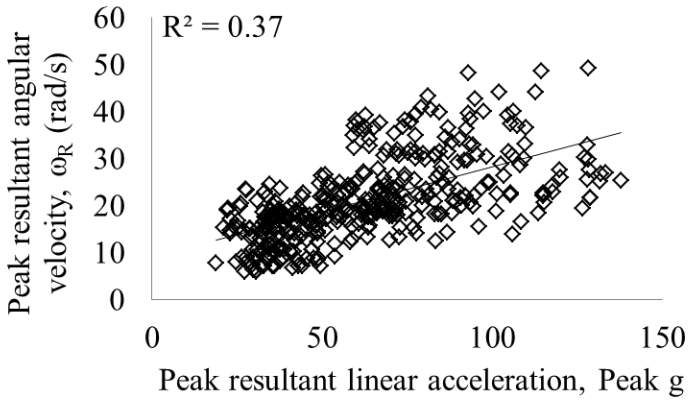

Figure 4.7: Correlation between peak resultant angular velocity and linear acceleration for all helmeted impacts together with the Hybrid III head and neck.

Though there is scatter noted in the plot of peak g vs ω_R, the trend shows an overall positive correlation between the two kinematics. As ω_R correlates with strain metrics that are considered here to be indicative of diffuse brain injury risk, by limiting ω_R, and indirectly peak g, it may be possible to account for both focal and diffuse injury with a single kinematic.

4.2 Results for helmeted Hybrid III head and no neck

4.2.1 Effect of time duration on kinematics and strain

The kinematic response for impacts with the Hybrid III head with no neck is different from those with the Hybrid III head and neck in that late in the impact the headform continues to rotate at a seemingly constant speed, rather than return to rest. This is reflected in the acceleration curves, which reach a peak value and return to zero without crossing the x-axis or changing direction. As linear and angular acceleration returns to zero without changing direction or coordinate sign, the corresponding velocities do not return to zero, but rather stabilize. Figure 4.8 displays an example of linear acceleration and angular velocity plots for front, back and side impacts with a hockey helmet mounted on the Hybrid III headform.

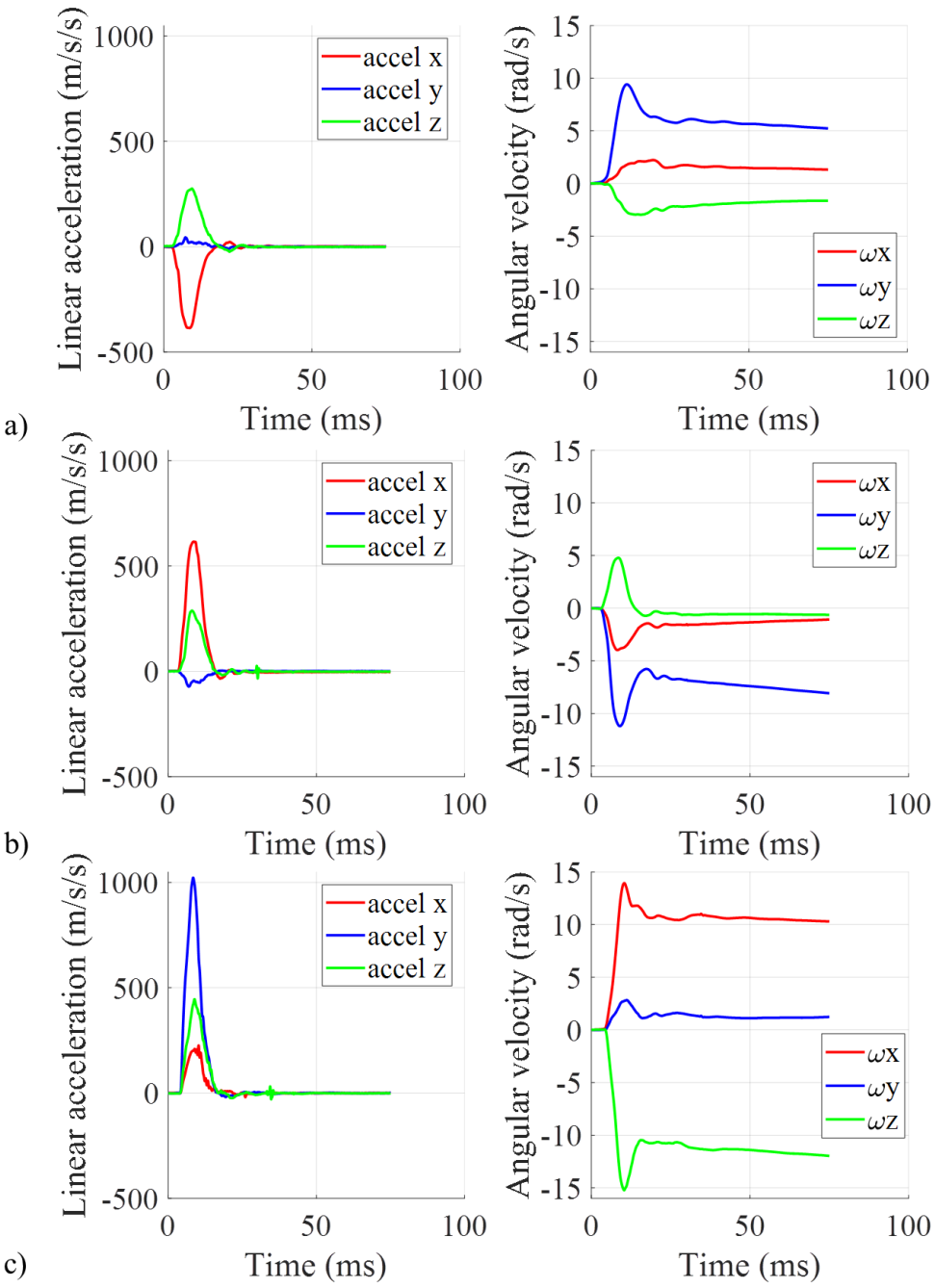

Figure 4.8: Directional linear acceleration (left) and angular velocity (right) for impacts to a helmeted Hybrid III head with no neck for an impact to a hockey helmet a) front, b) back and c) left side. Impact time duration shown here is 75 ms with time scales adjusted to start at time=0, immediately prior to initial impact acceleration.

Although velocities do not return to zero by the end of the selected 75 ms time window, it is noted in Figure 4.8 that they are no longer dramatically increasing or decreasing and have

slopes at approximately zero, aligning with the zeroed acceleration curves. By the end of the impact duration for no-neck impacts, all kinematics have stabilized

SIMon-computed strain metrics from no-neck impact kinematics often do not reach a stable maximum within 75 ms and appear to increase beyond the value at the final time step (as noted in Figure 4.9), though kinematics no longer increase. As noted above, kinematics reach a steady-state while strain magnitudes continue to increase after the main impact event has ended. In some impacts, strains do achieve a stable maximum without increasing further, however, many of the impacts display a continued increase in strain throughout the time frame and seemingly beyond it. Figure 4.9 shows examples of CSDM-15 and MPS plotted over time for a back impact. As a result, it is difficult to confirm the proper peak strain value as it may vary over the 75 ms time duration.

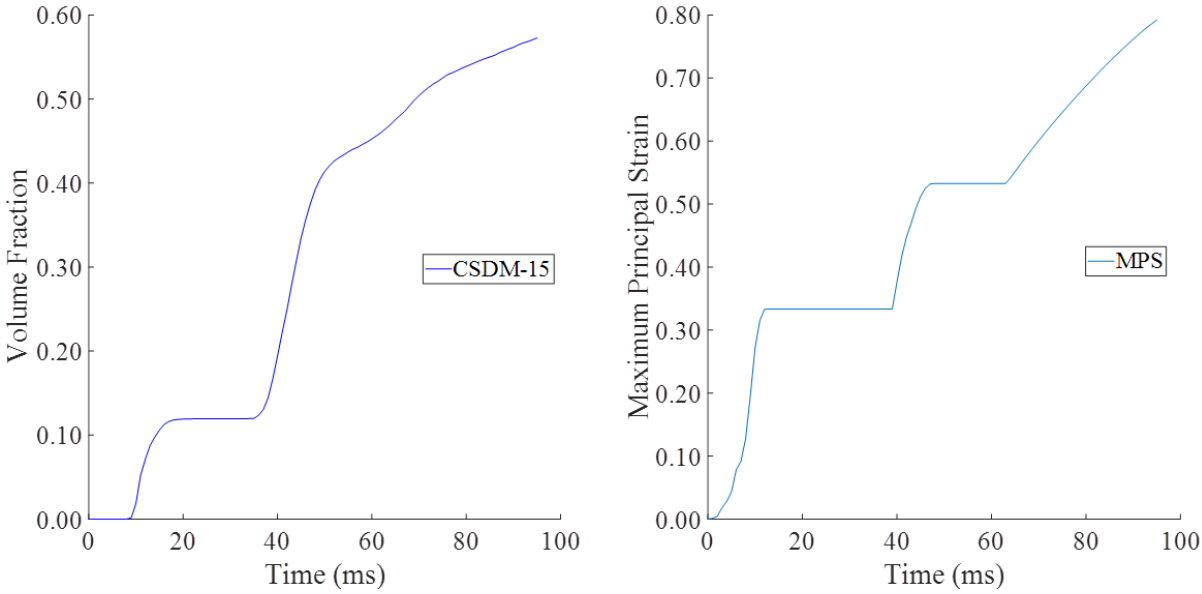

Figure 4.9: Example plots of CSDM-15 (left) and MPS (right) over time showing strain values increase after an initial plateau.

Investigating the effect of time duration on the resulting strain curves revealed that a plateau in both the CSDM-15 and the MPS curve was almost always reached at approximately 25 ms, leading to a shorter time duration being considered. It is noted that strain begins to increase within milliseconds and reaches a first plateau within 25 ms. Strain then begins to increase again after about 40 ms. The first plateau at 25 ms is what is referred to in this text

as the local maximum. Each impact has corresponding strain metrics that achieve a local maximum at 25 ms and therefore, CSDM-15 and MPS are determined within the first 25 ms.

Investigating time durations up to 200 ms gave unchanging kinematics following the initial acceleration pulse, though increasing strains were still observed. During the experimental drop, kinematic data is acquired for 1 s from which the shorter time windows (typically 75-90 ms for no-neck impacts) are used for analysis and referred to as the impact duration. Changing impact duration refers to increasing or reducing the time considered after the initial acceleration pulse. The kinematic pulse duration, or the width of the acceleration pulse, is not modified in any way. To investigate longer durations for no-neck impacts, adjustments were simply made to the post-processing step to include more time after the initial impact. Including more time after the impact was thought to allow the steady-state kinematics to be reflected in the strain metrics in that strains would reach a stable maximum. Longer time durations input to SIMon, however, did not result in strains reaching a maximum. Considering more time after the impact event than the initial 75 ms time duration showed the same result of continued strain increase.

The finding that strains continue to increase under constant velocity and zero acceleration could be due to the properties of the chosen brain finite element model. Angular velocity of the headform, applied to the rigid skull of the brain model, causes body forces within the brain finite elements. The free headform continues to rotate after impact resulting in constant angular velocity input and persisting body forces, which continue to deform the viscoelastic elements. The viscoelastic elements are deformed by the initial change in angular velocity, and as angular velocity does not return to zero, deformation and strain continue to increase over the impact duration. This hypothesis was tested by inputting formulated kinematic data into SIMon that included zero linear accelerations and angular velocity that increased steadily to a constant maximum of 30 rad/s for a total impact duration of 100 ms, arbitrarily chosen to investigate strain response, about the x, y and z axes in a series of 3 tests. For each simulation, the strain curves displayed similar findings in that they continued to increase over the entire duration, providing support for the hypothesis that constant, non-zero angular velocity causes continuous strain increase. Depending on the specific properties of the material, it is possible that time beyond 200 ms is necessary to allow elements to reform.

Based on the continually increasing strain plots, the elements are still deforming within the chosen time frame.

As strain metrics do not reach a stable maximum, it is impossible to confidently identify the peak strain value for a time duration greater than 25 ms. Selecting 25 ms captures the entire impact pulse, allows SIMon-computed strain values to achieve a local maximum, and omits arguably unrealistic head rotation that may occur beyond 25 ms. Figure 4.10 displays front impact kinematics for a 25 ms time window with the corresponding strain plots shown in Figure 4.11.

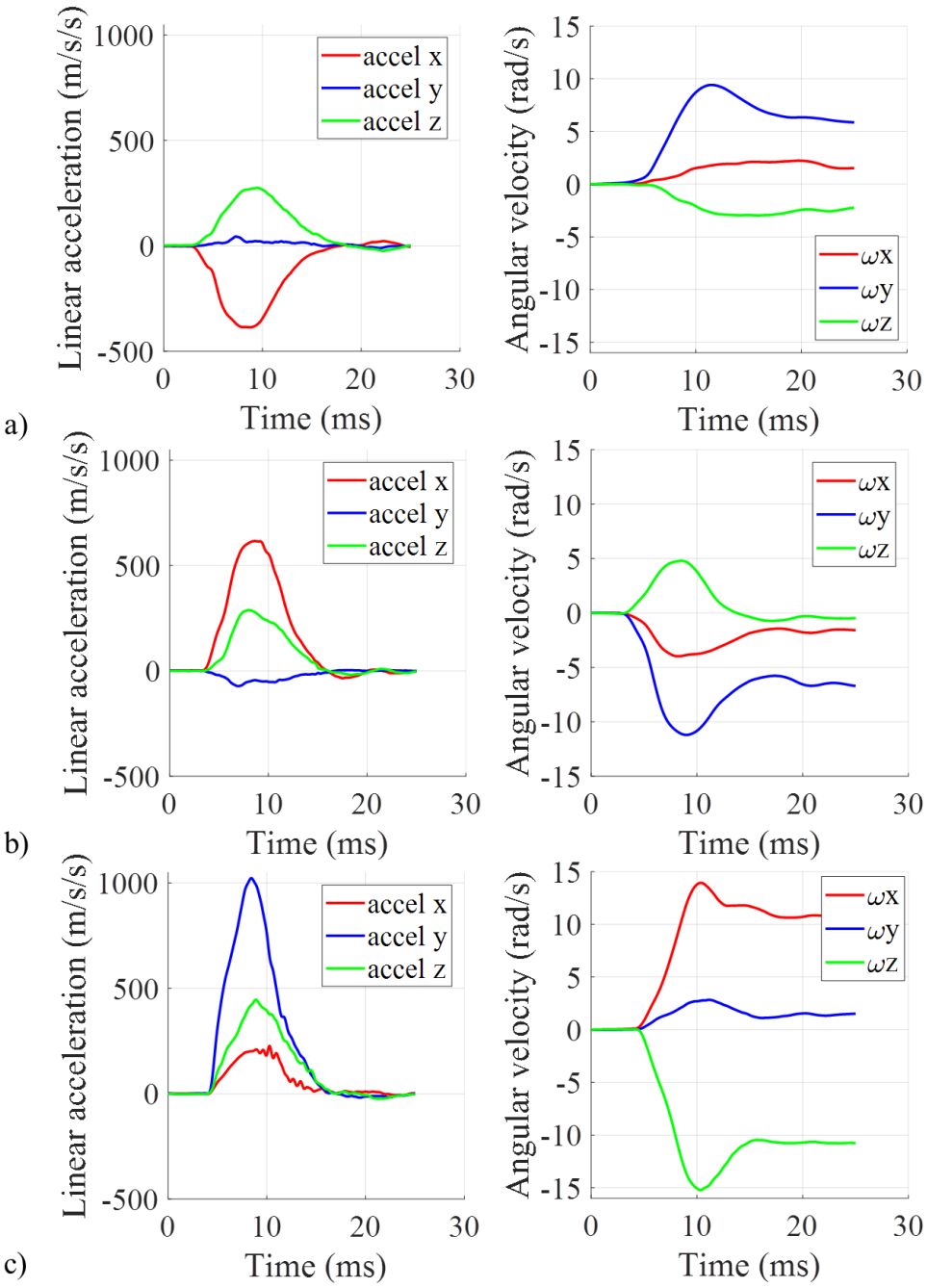

Figure 4.10: Directional linear acceleration (left) and angular velocity (right) for impacts to a helmeted Hybrid III head with no neck for an impact to a hockey helmet a) front, b) back and c) left side. Impact time duration shown here is 25 ms with time scales adjusted to start at time=0, immediately prior to initial impact acceleration.

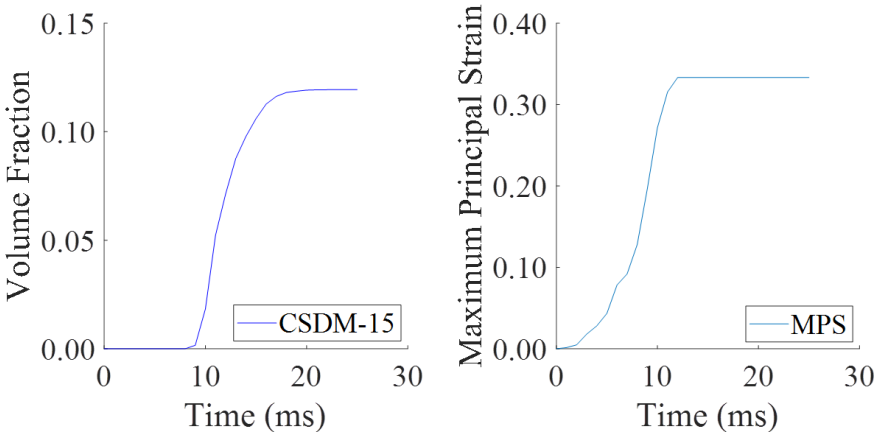

Figure 4.11: SIMon-computed CSDM-15 (left) and MPS (right) plotted against time for a helmeted Hybrid III head with no neck impact to the helmet front for an impact duration of 25 ms.

In limiting the total time that is considered for later analysis to 25 ms for no-neck impacts, it is possible to identify clear peak kinematic values and corresponding peak strain values. Beyond 25 ms, due to the absence of the neck, the head continues to translate and rotate away from the impact site. It is arguably unrealistic to assume these head motions are possible for a human head impact, further justifying kinematic analysis and SIMon simulations be limited to 25 ms.

4.2.2 Statistical analysis for helmeted Hybrid III head and no neck

4.2.2.1 Single kinematics with highest adjusted R^2

The single best kinematic for predicting strain for helmeted impacts with the Hybrid III head and no neck, again defined as the kinematic that simultaneously achieves the highest F-statistic and adjusted R^2, is either resultant change in angular velocity ($\Delta\omega_R$) or peak resultant angular velocity (ω_R). Table 4.7 and Table 4.8 summarize the single kinematic with the highest F-statistic and adjusted R^2 for predicting CSDM-15 and MPS, respectively, for impacts with the Hybrid III head and no neck.

Table 4.7: The single best kinematic for predicting CSDM-15 for helmeted impacts with Hybrid III head with no neck. Bold and italicized variables indicate that they are significant predictors.

Impacts	Variables		Adj R^2	F
Hockey				
All	$\Delta\omega_R$		0.65	487
Front	$\Delta\omega_R$		0.77	316
Back	$\Delta\omega_R$		0.45	75
Side	$\Delta\omega_R$		0.81	320
Football				
All		ω_R	0.91	1128
Crown	$\Delta\omega_R$		0.59	36
Front	$\Delta\omega_R$		0.92	502
Back		ω_R	0.57	32
Side	$\Delta\omega_R$		0.96	451

Table 4.8: The single best kinematic for predicting MPS for helmeted impacts with Hybrid III head with no neck. Bold and italicized variables indicate that they are significant predictors.

Impacts	Variables		Adj R^2	F
Hockey				
All	$\Delta\omega_R$		0.87	1736
Front		ω_R	0.93	1245
Back	$\Delta\omega_R$		0.79	345
Side	$\Delta\omega_R$		0.91	742
Football				
All		ω_R	0.89	970
Crown	$\Delta\omega_R$		0.93	320
Front	$\Delta\omega_R$		0.92	547
Back	α_R		0.90	214
Side	$\Delta\omega_R$		0.97	565

Peak resultant angular velocity (ω_R) is the single kinematic that achieves the greatest adjusted R^2 value for predicting strain metrics for 22% of the impact configurations, while $\Delta\omega_R$ is

favoured for 72%. All impact locations considered together, $\Delta\omega_R$ achieves a greater adjusted R^2 value than angular velocity for CSDM-15 and MPS for hockey helmets. Peak resultant angular velocity, ω_R, however, achieves the greatest adjusted R^2 value for predicting CSDM-15 and MPS for football helmets.

4.2.2.2 Regression models achieving highest F-statistic value

In 83% of impact configurations with the helmeted Hybrid III head with no neck, predicting strain values is statistically most efficient using a single variable model. Table 4.9 and Table 4.10 display the variables required for a model achieving the maximum F-statistic in predicting CSDM-15 and MPS, respectively, for no-neck impacts.

Table 4.9: A summary of multi-variable regression models and the kinematic(s) included in each model achieving the maximum F-statistic for predicting CSDM-15 for helmeted impacts with Hybrid III head and no neck

Impacts	No. of Variables	Variables included in regression model					Adj R^2	F
Hockey								
All	1	$\Delta\omega_R$					0.65	487
Front	1	$\Delta\omega_R$					0.77	316
Back	1	$\Delta\omega_R$					0.45	75
Side	1	$\Delta\omega_R$					0.81	320
Football								
All	1		ω_R				0.91	1128
Crown	1	$\Delta\omega_R$					0.59	36
Front	1	$\Delta\omega_R$					0.92	502
Back	3			ω_x	ω_y	ω_z	0.82	37
Side	1	$\Delta\omega_R$					0.96	451

Table 4.10: A summary of multi-variable regression models and the kinematic(s) included in each model achieving the maximum F-statistic for predicting MPS for helmeted impacts with Hybrid III head and no neck

Impacts	No. of Variables	Variables			Adj R^2	F
Hockey						
All	1		$\Delta\omega_R$		0.87	1736
Front	1			ω_R	0.93	1245
Back	1		$\Delta\omega_R$		0.79	345
Side	1		$\Delta\omega_R$		0.91	742
Football						
All	1			ω_R	0.89	970
Crown	1		$\Delta\omega_R$		0.93	320
Front	2	α_R	$\Delta\omega_R$		0.97	733
Back	2	α_R	$\Delta\omega_R$		0.96	324
Side	1		$\Delta\omega_R$		0.97	565

4.2.2.3 Multi-variable regression models achieving highest possible adjusted R^2

In identifying regression models that achieve the maximum possible adjusted R^2 for predicting strain for helmeted impacts to the Hybrid III head and no-neck, the kinematics to be included appear dependent on the strain metric being predicted. Focusing on models predicting CSDM-15, all models include Peak g and directional angular velocity: either ω_x, ω_y, and ω_z or $\Delta\omega_x$, $\Delta\omega_y$, and $\Delta\omega_z$ (with 3 also including ΔV_R). For models achieving maximum adjusted R^2 for predicting MPS, 6 different variable combinations are presented over the 9 impact configurations. Table 4.11 and Table 4.12 summarize the models achieving maximum adjusted R^2 for predicting CSDM-15 and MPS, respectively, for no-neck impacts.

Table 4.11: A summary of multi-variable regression models and the kinematics included in each model achieving the maximum adjusted R^2 for predicting CSDM-15 for helmeted impacts with Hybrid III head and no neck

Impacts	No. of Variables	Variables included in regression model						Adj R^2	F
Hockey									
All	4	***Peak g***		ω_x	ω_y	ω_z		0.73	179
Front	4	Peak g		ω_x	ω_y	ω_z		0.85	127
Back	5	***Peak g***	ΔV_R	ω_x	ω_y	ω_z		0.77	61
Side	5	***Peak g***	ΔV_R	ω_x	ω_y	ω_z		0.89	124
Football									
All	4	***Peak g***		$\Delta\omega_x$	$\Delta\omega_y$	$\Delta\omega_z$		0.94	475
Crown	4	Peak g		$\Delta\omega_x$	$\Delta\omega_y$	$\Delta\omega_z$		0.80	25
Front	4	***Peak g***		ω_x	ω_y	ω_z		0.95	232
Back	5	Peak g	ΔV_R	ω_x	ω_y	ω_z		0.86	30
Side	4	Peak g		$\Delta\omega_x$	$\Delta\omega_y$	$\Delta\omega_z$		0.98	272

Table 4.12: A summary of multi-variable regression models and the kinematics included in each model achieving the maximum adjusted R^2 for predicting MPS for helmeted impacts with Hybrid III head and no neck

Impacts	No. of Variables	Variables included in regression model								Adj R^2	F
Hockey											
All	4	***Peak g***				ω_x	ω_y	ω_z		0.89	520
Front	4	***Peak g***	V_i	V_R	α_R					0.95	431
Back	4	***Peak g***				ωx	ω_y	ω_z		0.90	200
Side	4	Peak g				$\Delta\omega_x$	$\Delta\omega_y$	$\Delta\omega_z$		0.97	521
Football											
All	5	Peak g		ΔV_R		ω_x	ω_y	ω_z		0.94	374
Crown	3	***Peak g***		ΔV_R					ω_R	0.97	257
Front	2				α_R				$\Delta\omega_R$	0.97	733
Back	2				α_R				$\Delta\omega_R$	0.96	324
Side	2				α_R				$\Delta\omega_R$	0.98	516

Increasing the number of predictor variables in the regression model from the single best kinematic predictor to a multi-variable model achieving the maximum adjusted R^2 increases adjusted R^2 on average by 13% (20% for predicting CSDM-15 and 5% for predicting MPS) and decreases the F-statistic by 37% on average (45% for CSDM-15 and 30% for MPS),

considering all impact locations as a single data set. Similar to impacts with the Hybrid III head and neck, a single-variable model achieves R^2 values similar to a multi-variable model while maximizing F.

4.2.3 Choosing a single kinematic predictor

Adjusted R^2 is similar between multi-variable models and single kinematic models for no-neck impacts, and a single kinematic predicts strain metrics with R^2 as high as 0.91 with F being significant ($p<0.01$). Figure 4.12 compares plots using a single variable model ($\Delta\omega_R$) to predict strain to models based on multiple variables (Peak g, V_i, ΔV_R and $\Delta\omega_R$) to predict strains for hockey helmet impacts. Similarly, Figure 4.13 compares plots using single variable models (ω_R) and multi-variable models (Peak g, V_i, ΔV_R and ω_R) for predicting strain for football helmet impacts.

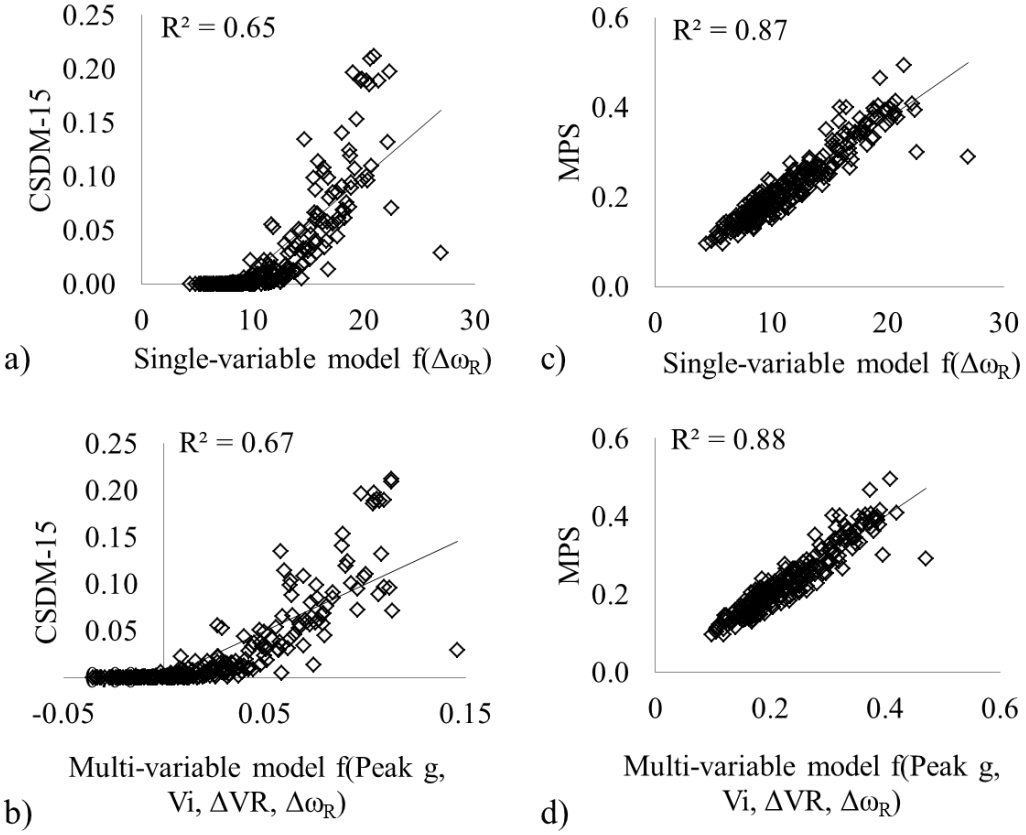

Figure 4.12: Scatter plot comparisons for hockey helmet impacts including a) a single-kinematic model, $\Delta\omega_R$, in units of rad/s, plotted against CSDM-15 and b) a multi-variable model including Peak g, V_i, ΔV_R and $\Delta\omega_R$, in units of volume fraction, plotted against CSDM-15. Similarly, c) a

single-kinematic model, $\Delta\omega_R$, in units of rad/s, plotted against MPS and d) a multi-variable model including Peak g, V_i, ΔV_R and $\Delta\omega_R$, in units of strain, plotted against MPS.

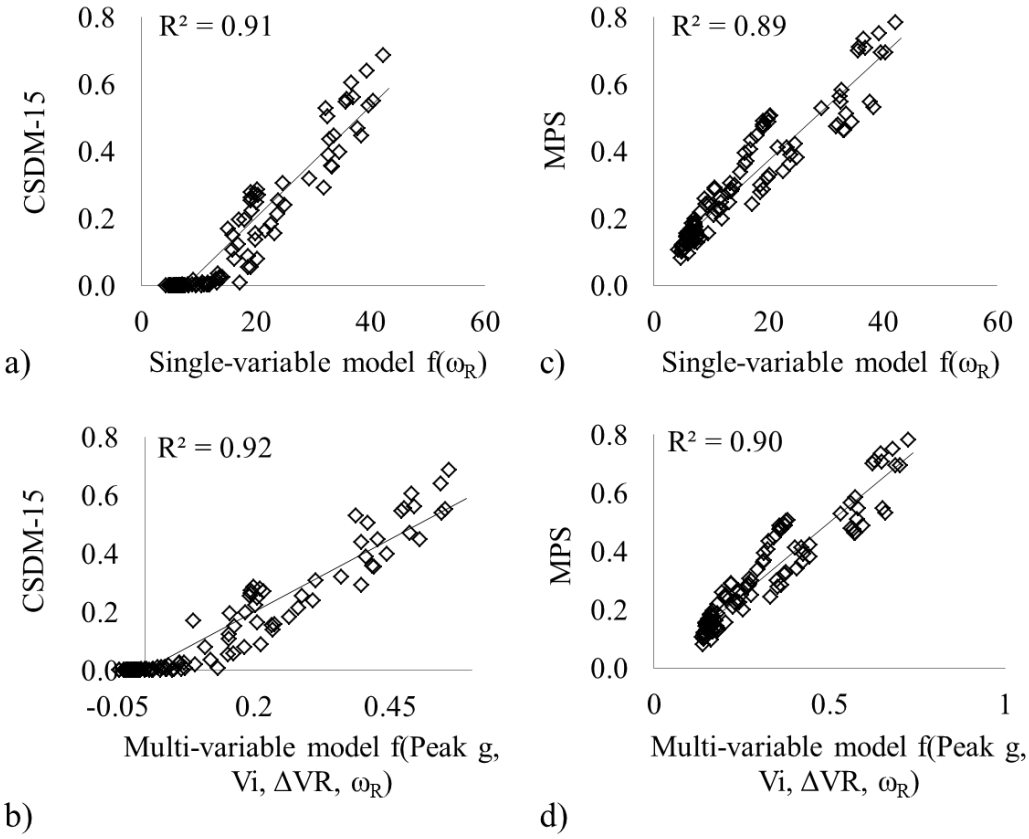

Figure 4.13: Scatter plot comparisons for football helmet impacts including a) a single-kinematic model, ω_R, in units of rad/s, plotted against CSDM-15 and b) a multi-variable model including Peak g, V_i, ΔV_R and ω_R, in units of volume fraction, plotted against CSDM-15. Similarly, c) a single-kinematic model, ω_R, in units of rad/s, plotted against MPS and d) a multi-variable model including Peak g, V_i, ΔV_R and ω_R, in units of strain, plotted against MPS.

It is considered sufficient to use a single kinematic to predict strain metrics for impacts with the Hybrid III head without a neck as significant F-statistics are achieved and R^2 values can reach 0.91 without the need for multiple variables. Similar to the findings for impacts to the Hybrid III head and neck, statistical results indicate ω_R overall achieves the greatest R^2 for considering all impact configurations considering all impact locations together with the Hybrid III head and no neck.

Separately analyzing hockey and football helmet impacts (all locations considered together), angular velocity, ω_R, as a predictor of CSDM-15 or MPS increases adjusted R^2 by 10% on average for no-neck impacts compared to angular acceleration, α_R. For impacts using the

hockey helmet, using ω_R in place of α_R to predict strain increases R^2 by 5% (Figure 4.14), while impacts with the football helmet, show R^2 increases by 15% using ω_R over α_R as an individual predictor (Figure 4.15).

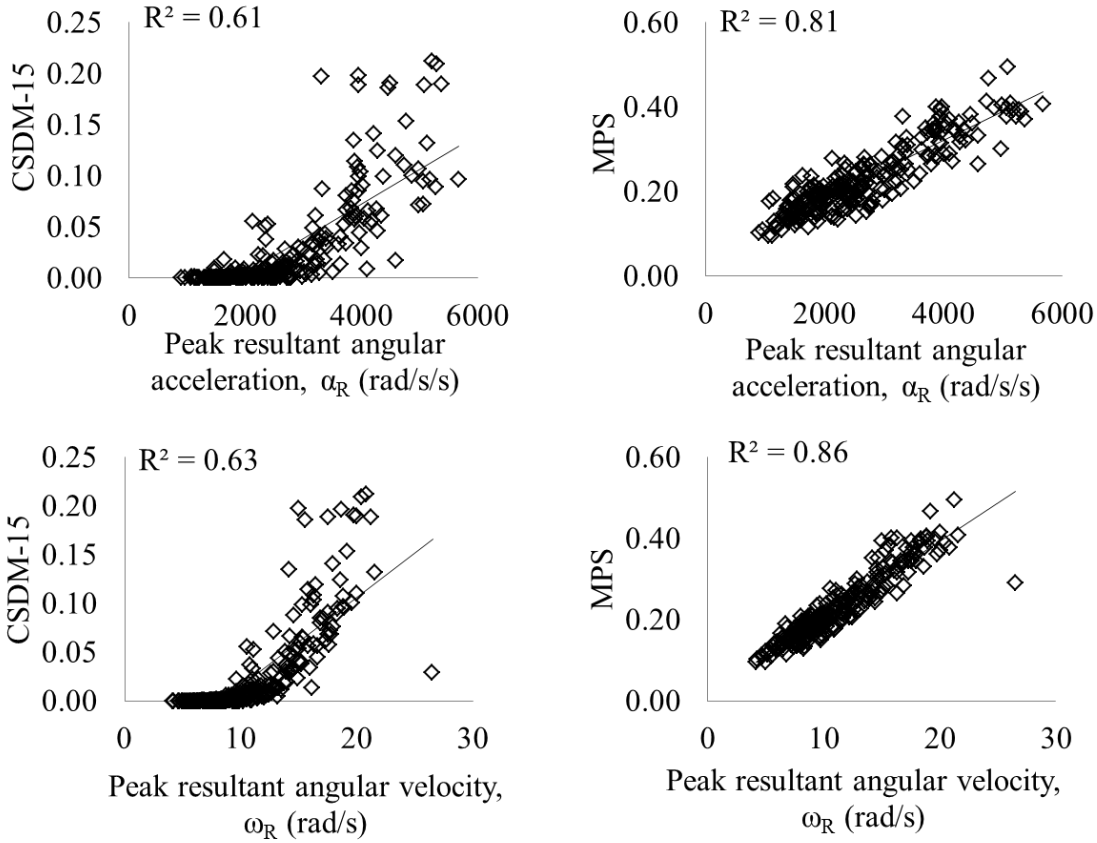

Figure 4.14: Comparison of regression plots for predicting CSDM-15 (left) and MPS (right) for hockey helmet impacts with the Hybrid III head with no neck using peak resultant angular acceleration (top) and peak resultant angular velocity (bottom).

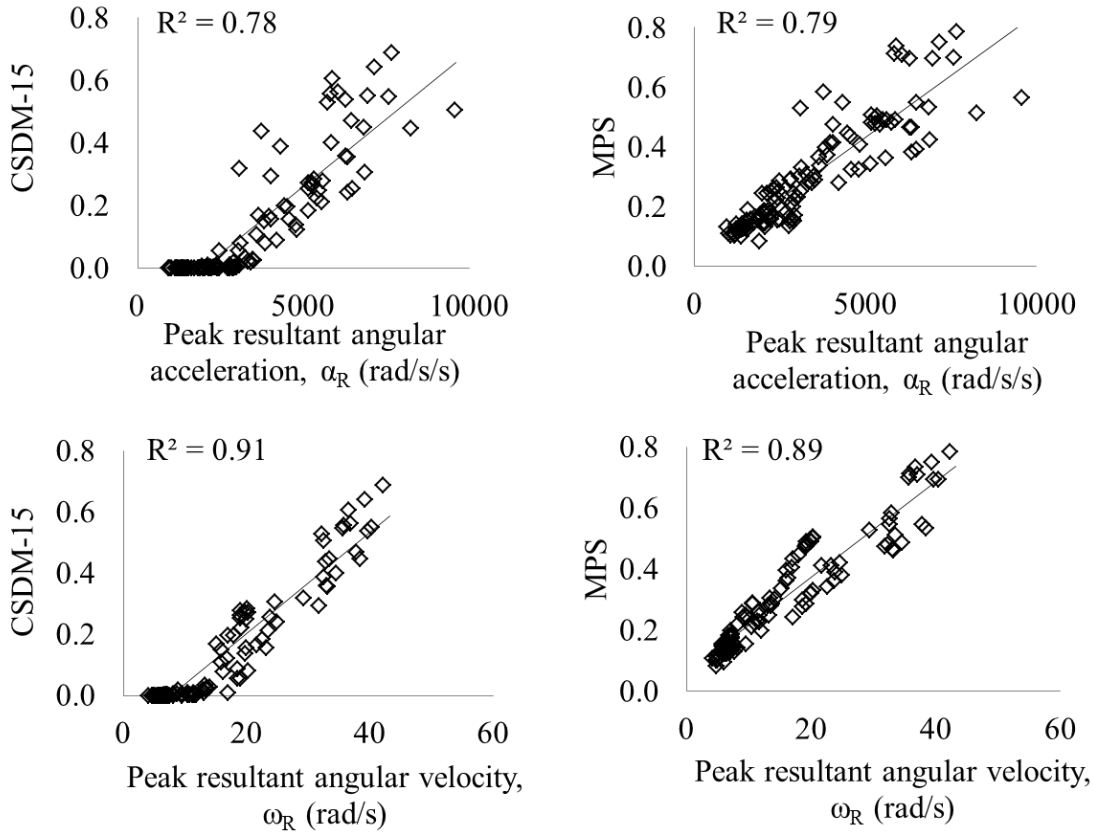

Figure 4.15: Comparison of regression plots for predicting CSDM-15 (left) and MPS (right) for football helmet impacts with the Hybrid III head with no neck using peak resultant angular acceleration (top) and peak resultant angular velocity (bottom).

However, combining hockey and football impacts into a single dataset, as shown in Figure 4.16, ω_R, as a strain predictor, increases R^2 by 17% on average compared to α_R. Therefore, ω_R is the single best kinematic to predict brain strain metrics for impacts with and without the Hybrid III neck.

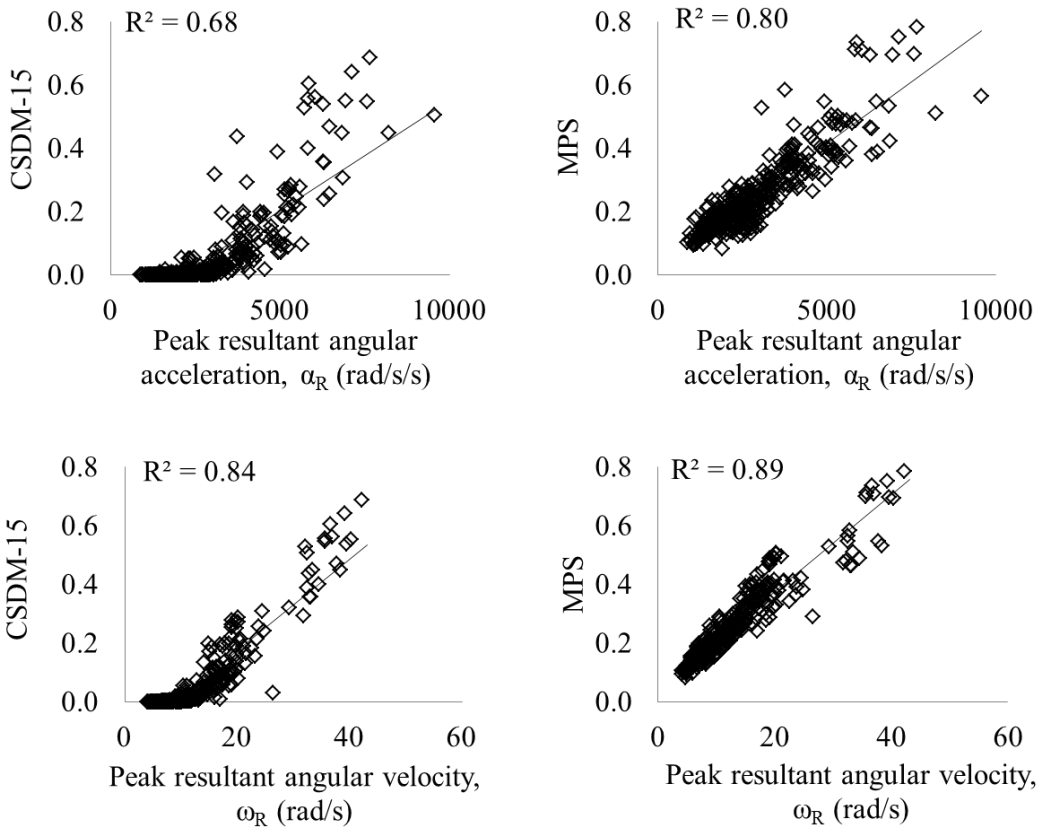

Figure 4.16: Comparison of regression plots for predicting CSDM-15 (left) and MPS (right) for all helmeted impacts with the Hybrid III head with no neck using peak resultant angular acceleration (top) and peak resultant angular velocity (bottom).

It is noted that strain levels, specifically CSDM-15 values for hockey helmet impacts shown in Figure 4.14, were lower for no-neck impacts relative to impacts using the Hybrid III neck. Most ω_R values were also relatively low compared to neck impacts, with only 3% of the no-neck impacts exceeding 25 rad/s (25 rad/s is arbitrarily chosen for comparison though is considered low and is below any ω_R threshold identified here or by previous researchers). Future test protocols for impacts without a neck could consider including oblique impacts with an angled anvil to guarantee sufficient rotation is evaluated for all impact locations. The angular velocities achieved here are considered acceptable for meeting the goal of this thesis work that focuses on the ability of kinematics to predict strain.

4.3 Comparing measured kinematics between cases of helmeted and un-helmeted impact

It is important that any helmet assessment metric be able to differentiate between a protected and unprotected headform. In general, impact kinematics are greater for impacts to an unprotected headform relative to a helmeted headform. Figure 4.17 shows example kinematic-time plots for an unprotected headform and hockey helmeted headform. Figure 4.18 compares peak resultant impact kinematics for the unprotected headform and the headform equipped with a hockey and football helmet during front impacts at matching impact speeds.

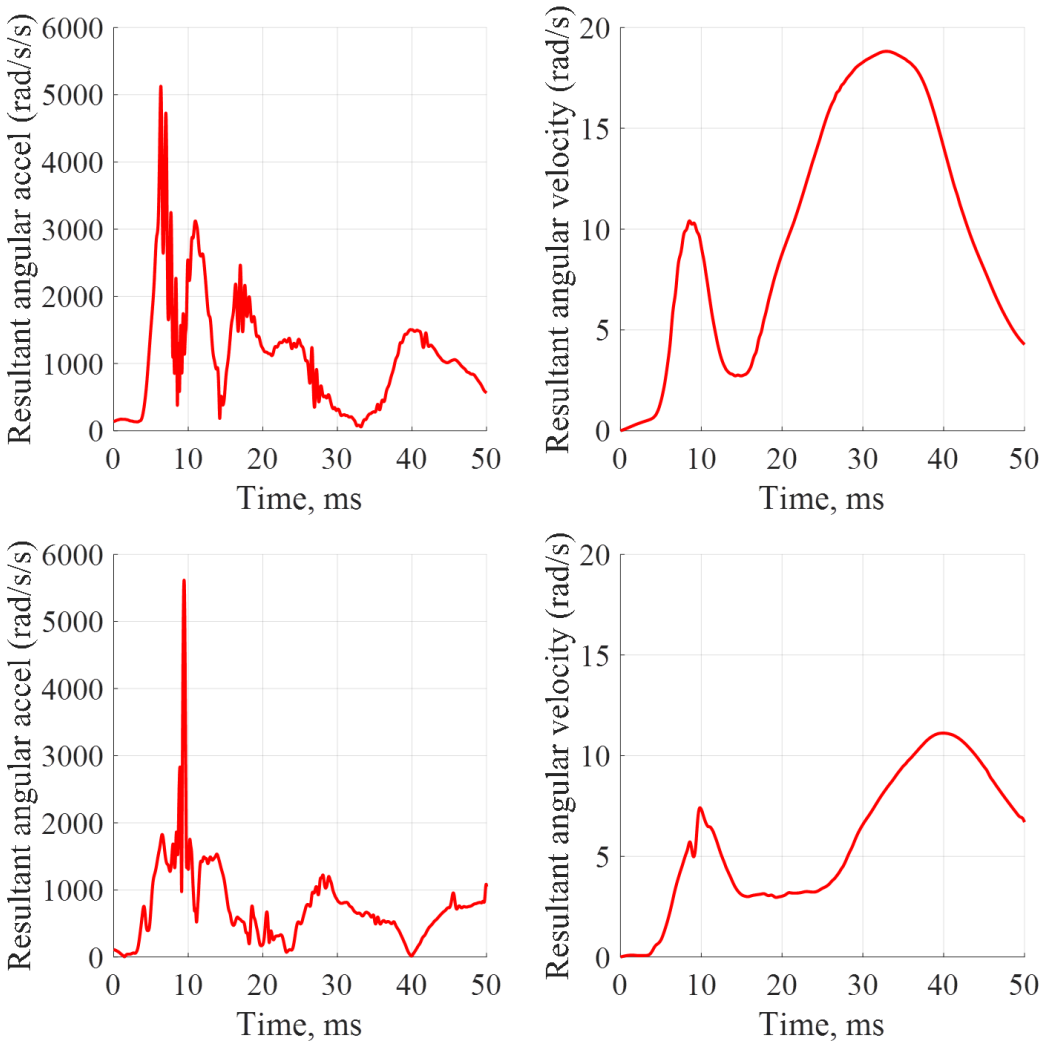

Figure 4.17: Resultant angular acceleration (left) and angular velocity (right) for the unprotected headform (top) and headform equipped with a hockey helmet (bottom) for the same impact speed.

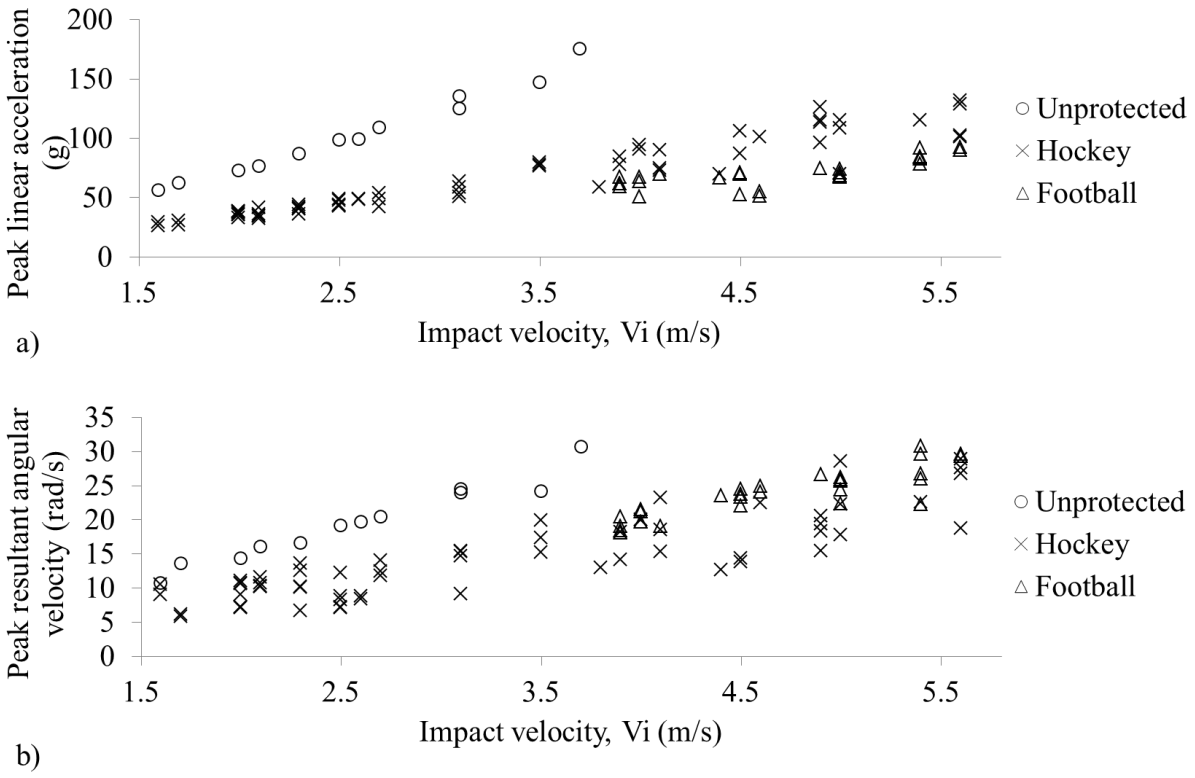

Figure 4.18: a) Peak linear acceleration (peak g) and b) peak resultant angular velocity plotted against impact velocity for impacts to the helmeted and unprotected Hybrid III headform with the Hybrid III neck.

For a front impact, with impact speeds of 3.7 m/s for the unprotected Hybrid III headform and 3.9 m/s for the headform equipped with both a hockey and football helmet, peak g is reduced by 54% and 64% with the use of the hockey and football helmet, respectively. For the same impact, angular velocity is reduced by 47% and 38% with the use of the hockey and football helmet, respectively. Similar trends were observed for back and side impacts.

Helmets overall are effective in lowering angular velocity and linear acceleration during impact. Helmeted impacts, compared to the unprotected headform for impacts using the Hybrid III head and neck, reduce peak g by an average of 52%, while ω_R is reduced on average by 23%.

5 Discussion

The goal of this thesis is to develop a kinematic metric that assesses a helmet based on its ability to limit kinematics that correlate to brain strain metrics. Helmeted impacts were replicated using the Hybrid III head and neck as well as using the Hybrid III head without a neck. Correlations between impact kinematics and the Improved SIMon-computed strain metrics identified key kinematics capable of predicting CSDM-15 and MPS to consider for future helmet assessment.

The data presented in this thesis suggests that, for the experimental configuration and brain model considered, a model based on a single kinematic can be a significantly better predictor than an intercept only model. Further, the data suggest the single kinematic models including angular velocity predict strain better (higher R^2) than peak linear acceleration, which is the current standard assessment metric. For the helmeted Hybrid III headform both with the Hybrid III neck and without a neck, a single angular kinematic, namely ω_R, was able to predict CSDM-15 and MPS. Predicting strain metrics during helmeted impacts can therefore be done by monitoring the select kinematics identified in this study, and in limiting to an identified threshold, brain strain metrics (considered here to be representative of brain injury risk) are also limited.

5.1 Choice of a single kinematic for impacts with and without a neck

One main goal of this thesis is to identify a single kinematic metric that can be universally applied for all helmet types and impact configurations. Specific to this study, this requires choosing the same kinematic metric for impacts with the Hybrid III head with a neck and the Hybrid III head without a neck for impacts with the hockey helmet and with the football helmet. Proposing one kinematic metric for all impact configurations would be similar to the current method of using peak g, in that all standards could adopt the same new metric, potentially simplifying the certification process. Achieving a universal metric eliminates any confusion regarding multiple metrics that depend on impact setup and, in presenting one standard, ensures consistency across all standards organizations.

Additional statistical analysis will be presented below that combines all hockey and football helmet impacts into one data set. Impacts with the Hybrid III neck and the Hybrid III

without a neck will continue to be considered separately. New R^2 and F-statistic values will be investigated and compared for single kinematic metrics ω_R and α_R for the combined helmeted impact data. As ω_R is statistically the best kinematic predictor for strain for the impact setup presented here and α_R is a kinematic commonly referenced as a predictor for brain injury, presently being incorporated into the new NOCSAE football helmet standard, one additional metric is investigated, that is the product of the two, $\omega_R*\alpha_R$.

This opening discussion aims to identify and justify one kinematic metric appropriate for all impact configurations of this study.

5.1.1 Statistical analysis comparing top performing kinematic metrics

Statistically, ω_R is superior to α_R in predicting brain strain metrics for impacts with the Hybrid III head and neck as well as impacts without the Hybrid III neck, achieving a higher R^2 and F-statistic than α_R. Table 5.1 and Table 5.2 below summarize statistical values for linear regressions including ω_R, α_R and $\omega_R*\alpha_R$ predicting strain for impacts with the Hybrid III head and neck (Table 5.1) and Hybrid III head with no neck (Table 5.2).

Table 5.1: Statistical values for all helmeted impacts together using the Hybrid III head and neck

	R^2	F	F significance
CSDM-15			
ω_R	0.83	1829	< 0.001
α_R	0.08	32	< 0.001
$\omega_R*\alpha_R$	0.61	526	< 0.001
MPS			
ω_R	0.81	1569	< 0.001
α_R	0.10	37	< 0.001
$\omega_R*\alpha_R$	0.58	407	< 0.001

Table 5.2: Statistical values for all helmeted impacts together using the Hybrid III head and no neck

	R^2	F	F significance
CSDM-15			
ω_R	0.84	1969	< 0.001
α_R	0.68	779	< 0.001
$\omega_R*\alpha_R$	0.90	3192	< 0.001
MPS			
ω_R	0.89	2970	< 0.001
α_R	0.80	1506	< 0.001
$\omega_R*\alpha_R$	0.82	1747	< 0.001

Overall, $\omega_R*\alpha_R$ does not improve R^2 for all cases compared to ω_R, individually. For predicting CSDM-15, using ω_R increases R^2 by 36% relative to $\omega_R*\alpha_R$ for impacts with the head and neck, while ω_R decreases R^2 by 7% relative to $\omega_R*\alpha_R$ for impacts with the head with no neck. This suggests ω_R could be favored over $\omega_R*\alpha_R$ for predicting CSDM-15. For predicting MPS, ω_R increases R^2 by 40% for impacts with a neck and by 9% for impacts without the neck, presenting ω_R as statistically superior for predicting MPS relative to $\omega_R*\alpha_R$. As this discussion aims to identify one kinematic metric best suited for all impact scenarios, and the product of ω_R and α_R is not statistically preferred, $\omega_R*\alpha_R$ will not be considered further.

5.1.2 Angular acceleration versus angular velocity as a kinematic metric for helmet certification

Angular acceleration has previously been proposed as a predictor for brain injury, also appearing in a future NOCSAE football helmet standard, which considers angular acceleration integrated over time, similar to SI for linear acceleration. However, this thesis work, considering only peak kinematic values for simplification, finds angular velocity to be a better predictor for computed brain strain metrics than angular acceleration. For impacts with the Hybrid III neck, α_R achieves an average R^2 value of 0.09 when plotted against strain. Impacts with the Hybrid III neck result in large angular acceleration magnitudes that occur over short periods of time, providing potentially one explanation for poor correlation between angular acceleration and strain for this setup. It is believed that the stiff properties

of the Hybrid III neck cause rapid changes in direction when the neck is fully compressed during impact, reaching the peak angular acceleration within 1 ms, in some cases, leading to high α_R magnitudes. Though peak α_R is high, the time over which this acceleration magnitude is experienced can be short and, therefore, does not allow time for the brain to deform or experience great strain. As a result, SIMon-computed strain metrics do not reflect corresponding peak α_R magnitudes for impacts with the Hybrid III neck. Previous research by Yarnell and Ommaya link angular acceleration and time duration to risk of injury [11]. Furthermore, Fijalkowski et. al. investigated the effects of angular acceleration duration in rats subjected to head impact and found that increased duration led to increased functional deficits for the same angular acceleration magnitude [89]. Understanding that angular acceleration duration plays a role in brain injury, it may not be a surprise that high angular accelerations over short time durations are associated with low strain magnitudes, and consequently poor correlation, for the helmeted Hybrid III head and neck impacts in this study.

In accounting for time duration, through integration, peak angular velocity is seemingly unaffected by the occasional points of spurious noise in angular acceleration using the Hybrid III neck. In this study's head and neck protocol, angular velocity better correlates to strain than angular acceleration conceivably by accounting for angular acceleration magnitude and duration, both of which have been shown to influence injury. As a result, angular velocity correlates better with computed strain levels than angular acceleration for impacts with the Hybrid III head and neck.

Rapid changes in angular acceleration observed for impacts with the Hybrid III neck are not present, however, for impacts without a neck. The time taken to reach α_R for no-neck impacts appears to provide sufficient time for the brain elements to deform and experience strain proportional to the angular acceleration magnitude as indicated by an average R^2 of 0.74 between strain metrics and α_R. Angular acceleration in no-neck impacts increases to a peak over approximately 5 ms, compared to 1 ms for neck impacts. A longer duration of acceleration has been linked to greater risk of brain injury through the development of both linear and angular acceleration tolerance curves [11], [13]. For the no-neck impacts in this study, angular acceleration magnitudes are applied over longer durations than are typically

applied for neck impacts. It is thought that the angular acceleration pulse duration for no-neck impacts allows α_R to be an effective predictor for strain for impacts without the Hybrid III neck.

Although removing the potential influence of the Hybrid III neck in no-neck impacts improves correlation between angular acceleration and strain, angular velocity remains a superior predictor for brain strain metrics. Research conducted in the 1940s by Holbourn and as recently as 2018 by Gabler et. al. discusses the importance of angular acceleration duration on brain strain magnitudes for short duration impacts, such as direct head impacts [10], [90]. As angular velocity is one way to account for acceleration magnitude and duration, this could provide one explanation for greater statistical measures, R^2 and F, for angular velocity relative to angular acceleration.

Using ω_R to predict strain for helmeted impacts with or without the Hybrid III neck is proposed here. Angular velocity achieves R^2 values on average over 800% greater than angular acceleration for impacts with the Hybrid III head and neck and 17% greater for impacts with the Hybrid III head with no neck, and the F-statistics are significant in all cases (p-value<0.01). In practice, identifying the same single kinematic strain predictor for neck and no-neck impacts provides consistency in helmet certification standards, regardless of the impact setup. In choosing ω_R, one kinematic is proposed for neck and no-neck impacts, allowing European and North American standards to consider the same kinematic metric in helmet assessment and certification. Additionally, measuring angular velocity is advantageous as it could be done with a single rate sensor, limiting the amount of instrumentation required. Therefore, ω_R will perform well in a helmet certification scenario.

5.1.3 Angular velocity as choice kinematic for predicting strain

Peak resultant angular velocity is identified as a strain predictor and assessment metric for helmeted impacts with the Hybrid III head both with the Hybrid III neck and without a neck. Helmeted impacts identify angular velocity, ω_R, as statistically the best predictor for strain and, in practical applications as a helmet assessment tool, ω_R is identified as the single kinematic overall most appropriate for use for all impact scenarios. Similarly, European researchers tend to use a headform without a neck and have found angular velocity to be the

choice kinematic to relate to strain over linear kinematics or angular acceleration. Angular velocity can be applied to impacts with and without a neck to assess helmet ability to mitigate kinematics related to brain strain metrics.

Overall, peak resultant angular velocity, ω_R, was selected as the preferred kinematic to predict strain for helmeted impacts with the Hybrid III headform for the following list of reasons:

- One single kinematic variable was found to be capable of predicting strain
- Choosing a single kinematic maintains simple and straightforward helmet certification.
- ω_R achieves higher R^2 and F than all other single kinematics for helmeted impacts with the Hybrid III head and neck as well as with the Hybrid III head and no-neck and
- Practically, ω_R could allow helmet assessment organizations to consider one kinematic as opposed to more complicated kinematic models.
- ω_R eliminates the need to consider individual impact locations and directions.
- ω_R accounts for angular acceleration magnitude and duration.

The following sections of the discussion will provide additional, in-depth considerations that led to the narrowing of kinematic metrics to simply ω_R or α_R and ultimately selecting ω_R as the chosen kinematic.

5.2 A kinematic metric for the Hybrid III head and neck

Impacts with the Hybrid III head and neck present one possible setup for future helmet certification using equipment that is not unfamiliar to the head impact community. A detailed description of the Hybrid III head response to helmeted impacts, clearly identifying which kinematics are capable of predicting brain strain, had not previously been presented. This work determined peak resultant angular velocity effectively and reliably predicts brain strain during drop impacts.

5.2.1 Identifying a single kinematic for predicting strain

For impacts with the Hybrid III head and neck, nearly all impact scenarios resulted in angular velocity being the variable that was the most effective in achieving the highest adjusted R^2 and angular velocity alone achieved the maximum F-statistic. The form in which angular velocity best predicted strain was not statistically identical for both types of helmets. For hockey helmet impacts, $\Delta\omega_R$ was the preferred form of angular velocity as a strain predictor (average R^2 and F of 0.88 and 1826, respectively), while ω_R was preferred for football helmet impacts (average R^2 and F of 0.74 and 457, respectively). Angular velocity as a key predictor for strain metrics is supported by Takhounts et. al. who developed BrIC with the aim to predict brain injury based on angular velocity [14]. Gabler et. al. investigated the brain's injury tolerance to kinematic loadings and determined that the duration of angular acceleration was a key component [91]. As angular velocity represents the area below an acceleration-time graph, time duration is accounted for by considering angular velocity, thereby showing agreement with work by Gabler et. al. Angular velocity predicts strain metrics as an individual kinematic predictor as well as always increases adjusted R^2 when added to a regression model based on any other kinematics for impacts with the Hybrid III head and neck.

The regression model that achieves the greatest adjusted R^2 is not the same as the model that achieves the greatest F-statistic. This means that statistically the model that correlates best with strain metrics is not the same model that is considered most efficient. Peak g, V_i, ΔV_R and $\Delta\omega_R$ considered together in a regression model achieve the maximum adjusted R^2 for hockey helmet impacts considering all locations together (R^2 of 0.89, F of 525). To achieve the maximum F-statistic, a model includes only $\Delta\omega_R$ (R^2 of 0.86, F of 1629). Determining that different models achieve the maximum adjusted R^2 and the maximum F-statistic is a consistent finding for both hockey and football helmet impacts for all impact locations. It is reasonable that the most efficient (highest F-statistic) model is not the model with the best fit to the data (highest adjusted R^2) as one variable can predict strain and achieve an adjusted R^2 as high as 0.89. Therefore, adding variables to a capable model becomes inefficient. Adding variables always increases adjusted R^2, however, it immediately lowers the F-statistic, or relative efficiency, of a model. It becomes important then to compromise between adjusted

R^2 and F-statistic, based on the goals of this thesis, as both cannot be the highest possible values simultaneously.

Considering a two-variable model that includes one angular and one linear kinematic shows that regardless of the linear kinematic chosen, the adjusted R^2 value depends on the angular kinematic included in the model. Linear kinematics, mainly acceleration, have to date played an important role in the certification of helmets and have been linked to focal injuries while angular kinematics are understood to be a main cause for diffuse injury. Therefore, models including both linear and angular kinematics were considered. Two-variable models with one of either $\Delta\omega_R$ or ω_R and one of either Peak g, ΔV_R or V_R for predicting CSDM-15, considering all impact locations together, give adjusted R^2 values ranging from 0.70 to 0.86 for hockey and football helmeted impacts with the Hybrid III head and neck. Replacing only the linear kinematic in a model with the same angular velocity term, adjusted R^2 changes by a maximum of 2%. For the same linear kinematic term, however, changing the angular velocity term can increase adjusted R^2 by 23%. Angular kinematics have a greater influence than linear kinematics on the adjusted R^2 of the model, and therefore this discussion will narrow the focus to discussing which angular kinematic should be presented as a future metric for helmet certification.

Peak resultant angular velocity, ω_R, is chosen overall to be a better predictor than resultant change in angular velocity, $\Delta\omega_R$, for CSDM-15 and MPS when considering all hockey and football helmeted impacts together. ω_R achieves a consistent adjusted R^2 for CSDM-15 and MPS for both hockey and football helmet impacts, on average resulting in a greater adjusted R^2 than $\Delta\omega_R$ (0.79 for ω_R, 0.72 for $\Delta\omega_R$) when all impact locations were considered together. Should impact locations be considered individually during assessment impacts, i.e. considering separately front, back and side impacts, $\Delta\omega_R$ on average achieves a greater adjusted R^2 value. This thesis aims to present a certification process kept as simple as possible, and therefore will focus on all impacts considered together as a single data set. Currently, helmet standards require helmets be impacted at various locations, but do not certify each location individually and apply the same resultant linear acceleration criteria everywhere. Resultant angular velocity correlates with strain metrics without the need to consider directional components. Therefore, this work presents a kinematic metric that can

be applied as a resultant kinematic for any impact location. All impact locations considered together, for both hockey and football helmets, ω_R is the best predictor for CSDM-15 and MPS.

For impacts using the hockey helmet, a cluster of data points are noted near CSDM-15 = 0. This occurrence is due to measureable impact kinematics that did not result in any (or very few) elements exceeding 15% strain. Specific to angular velocity, up to approximately 10 rad/s, the resulting CSDM-15 values are near zero (see Figure 4.5) and are considered impacts not likely to cause injury. That is not to say that strain values were zero, but rather that they did not exceed 15%. Figure 4.6, for example, confirms that each impact results in a non-zero MPS, though below 10 rad/s, few exceed 15% strain. Where MPS is greater than 15%, though CSDM-15 is near zero, it is due to few elements experiencing strains greater than 15% and the volume fraction (CSDM) is negligible. Therefore, for angular velocity below approximately 10 rad/s, CSDM-15 values were near, or equal to, zero for finite angular velocity and MPS values. Considering regressions without these data points tends to improve R^2 values as a linear regression model better fits the remaining data points. These values were kept in the data set to ensure the minimum sample number was met as defined by equation 3.5. Though regression models better fit the strain data without these "non-injurious" impact data points, the improvements in R^2 are similar from one model to the next and therefore the same conclusions can be drawn.

Using a single kinematic to predict strain is simple and efficient and aligns with current and past certification techniques that focus on a single parameter, however does not include linear acceleration. Perhaps one concern in head injury biomechanics is that considering only angular velocity during helmet certification may not ensure linear kinematics linked to focal injury are also mitigated. Further investigation suggests ω_R may also ensure kinematics linked to focal injury are considered for this study. The following section discusses the possibility of mitigating both focal and diffuse injury risk by limiting linear and angular kinematics simultaneously.

5.2.2 Angular velocity to account for linear acceleration

Limiting angular velocity indirectly limits linear acceleration using today's helmets in impacts with the Hybrid III head and neck and therefore angular velocity may indirectly account for focal injury. Angular velocity is found in this study to correlate with linear acceleration as noted in Figure 4.7. Though variance is noted, a relationship between peak g and ω_R is evident. Ivarsson also identified a correlation between linear acceleration and angular velocity in forehead impacts to the Hybrid III head and neck during mini-sled impacts [92]. As mentioned, a potential concern that arises regarding new helmet metrics that move away from peak linear acceleration, is that kinematics related to focal injury may not be considered. If neglecting to monitor linear acceleration results in high magnitudes of peak g occurring, it is acknowledged that this would indeed lead to increased focal injury risk. However, the findings in this study indicate that there is a relationship between peak g and ω_R, for both hockey and football helmet impacts, and in monitoring angular velocity, peak g is not neglected. Today's helmets limiting peak g are credited with preventing severe focal injury in sport, therefore continuing to limit peak g will ensure helmets continue to provide life-saving protection. Limiting ω_R as a method for reducing risk of diffuse injuries would indirectly limit peak g, continuing to mitigate risk of severe focal injuries linked to linear acceleration.

Helmets including the same basic construction including hard outer shell and soft inner liner are not likely to result in skull fracture-level peak g values, based on the results of this study. A hockey helmet impact resulted in the maximum peak g of all helmeted impacts of 138g, which is well below the 275 g threshold currently set in place by the CSA and ASTM. An injury risk curve was developed by Mertz et. al. that links risk of skull fracture to peak g [93]. A peak g of 138 g, based on this skull fracture risk curve, is associated with a less than 1% risk of skull fracture [93]. It is noted that this curve was developed for bare head impacts and does not perfectly apply to the helmeted impacts conducted in this study. According to Gurdjian et. al., with head protection preventing skull deformation, sustainable linear acceleration is much higher than for a bare skull [34]. If we consider this curve for discussion purposes, any risk factor applied to this work can be assumed to be lowered by the presence of the helmet. Based on the linear relationship between peak g and ω_R, ω_R values

over 60 rad/s would be required to approach 275 g. As will be discussed later in the document, an angular velocity threshold of 34 rad/s is proposed for impacts with the Hybrid III head and neck. Therefore, for this setup, risk of linear acceleration exceeding 275 g by strictly monitoring angular velocity is not anticipated.

The fact that peak g values in this setup remained well below the threshold is likely due to the allowance of head rotation as impact energy was not solely mitigated through linear compression of the helmet's foam liner. The compliance of the Hybrid III neck better represents human head impact than a steel rod in that head rotation is present in real-world impacts. In drop certification methods with the Hybrid III head and neck, where rotation is possible, risk of injuries such as skull fracture is extremely unlikely with contemporary helmets and would require excessive angular velocity values.

Based on this thesis work, identifying angular velocity as a key predictor of strain metrics and noting angular velocity correlates to peak g, one example of a new helmet assessment metric could be simply monitoring and limiting angular velocity. ω_R correlates to CSDM-15 and MPS for hockey and football helmet impacts and allows all impact locations to be considered together. In correlating with peak g, limiting ω_R could also limit peak g and thereby continue to limit peak linear acceleration during impact.

5.3 A kinematic metric for the Hybrid III head with no neck

Impacting the Hybrid III head with no neck provides insights surrounding a second head impact test bed that is currently being considered for helmeted impact assessment. The Hybrid III neck is known to be stiffer than the human neck and while other surrogate necks are being explored [71], one option is to conduct impacts with a free headform with no neck. It is not yet known, however, to what extent the lack of a neck will change impact characteristics and headform or strain response. Therefore, this thesis work explores the resulting impact kinematics and corresponding SIMon-computed strain metrics for impacts with the Hybrid III head without a neck.

5.3.1 Effect of time duration on computed strain

The statistical analyses performed for Hybrid III head and no neck impacts focuses on a 25 ms duration, though evidence suggests that there is more going on beyond this time frame. For impacts with the Hybrid III head and neck, duration beyond 25 ms is required to capture the entire strain event, challenging whether 25 ms is enough time to consider the entire strain event for any head impact. Increasing the impact duration input to SIMon increases resulting CSDM-15 and MPS as more time is given to reach peak strain. Without a deceleration phase of the impact, however, strains often do not reach a stable maximum even up to 200 ms and it is not yet determined the required impact duration necessary to do so. In a real-life impact, the neck would engage after a certain time and the response of the free headform beyond that time becomes unrealistic, justifying the use of a 25 ms duration. This work considers impacts without the Hybrid III neck, and a 25 ms time duration for no-neck impacts has been selected based on kinematic and strain responses. It is important than any research group conducting impacts without a surrogate neck understand the implications of removing the neck and realize the resulting effect on strain responses.

5.3.2 A single kinematic for predicting strain without the Hybrid III neck

Considering all impact locations as a single data set, angular velocity was commonly the kinematic achieving the maximum adjusted R^2 for models based on a single kinematic. A single angular velocity predictor as an effective metric for strain is consistent with the findings for impacts to the Hybrid III head-neck. Whether the Hybrid III head is impacted with or without a neck, angular kinematics are better predictors for strain than peak g.

Comparing the findings for neck and no-neck impacts, both setups present peak resultant angular velocity as a correlate to strain metrics, as discussed above. Applying the proposed threshold technique to be outlined below, impacts with or without the Hybrid III neck suggest angular velocity thresholds within 15% of one another. Further exploration of the effects of time duration during no-neck impacts is recommended, though comparable findings to neck impacts suggest the methods applied here on time duration are valid. It is not known whether the factors of no-neck impacts are troublesome to the results of any study, including this one, but it is important that researchers are aware of the consequences.

5.4 Comparison of this thesis work to others

While a specific kinematic metric for helmet testing is not stated, European researchers recommend adopting a helmet test method that allows for rotation in order to consider kinematics that correlate to strain metrics [94], [95]. In comparing impact configurations for European and United States helmet test methods, Meng et. al. confirmed strains computed using the KTH brain model were up to 6.3 times greater for impacts involving rotation [94]. The work in this thesis focuses solely on impact configurations that include rotation, aligning with the recommendation for rotational testing, and provides a method for implementing a kinematic metric.

A threshold proposed here will focus on identifying a single pass/ fail angular velocity value. Hoshizaki et. al. developed a threshold curve based on angular acceleration, considering various impact scenarios for sport that resulted in TBI, mTBI or no brain injury. Similar to the WSTC, peak kinematic magnitudes and durations were used to create points on a plot to which the curved threshold line was fit [96]. Use of angular acceleration to develop a threshold curve is one other method that may be appropriate for understanding kinematic thresholds for mTBI or concussions. A single value limit can be set on angular velocity during certification, which then also accounts for acceleration magnitude and duration considered in a threshold curve.

For a variety of impact conditions, using two different FE brain models, Gabler et. al. found that metrics with multiple angular kinematics, which also considered direction, achieved the highest R^2 values when correlated to strain metrics [90]. The impacts considered included automotive sled and crash tests with both dummies and cadavers, linear impactor tests for helmeted impacts and human volunteer data. Gabler and colleagues also found that resultant peak angular velocity correlating to strain achieving R^2 greater than 0.6 using both the SIMon and GHBMC brain models [90]. The drop impacts conducted here and the use of only one brain model differs from the impacts and brain FE models used by Gabler et. al., though consistent findings are achieved in that multiple kinematics improves R^2 for predicting strain, while angular velocity alone correlates to strain.

Takhounts et. al. investigated data from available automotive tests and pendulum impact tests using several ATDs, including the Hybrid III, the test device for human occupant restraint (THOR), side impact dummies ES-2, SID-II and WorldSID along with football data from instrumented helmets in the development of brain injury criterion, BrIC, based on angular velocity [14]. The impacts investigated by Takhounts et. al. vary considerably from the drop impacts conducted here, however, both studies identify resultant angular velocity as a representation of strain. The development of BrIC was based primarily on automotive data, with the critical term determined based on AIS 4 brain injury. This work focuses solely on helmeted sport impacts, applying limits on angular velocity for brain injury of lower severity. The results of this thesis work add to that of Takhounts et. al. by confirming that angular velocity is an appropriate predictor for strain, but relevant to certification-style helmeted drops rather than automotive impacts.

Yoganandan et. al. investigated the effect of angular acceleration-deceleration pulses on brain strain responses, considering mono-phase profiles, which included an acceleration or deceleration pulse only [97]. The acceleration pulse had a high peak magnitude and short duration, relative to the deceleration pulse which had a low magnitude and long duration. The change in angular velocity, however, was constant for the acceleration and deceleration pulse. It was found that while the peak angular acceleration or deceleration differed between these pulses, the resulting strains were within 10%, suggesting angular velocity better represents strain response for the mono-phase pulse [97]. Impacts without the Hybrid III neck can be considered mono-phase, as there is no deceleration that follows the acceleration pulse. Considering no-neck impacts to be mono-phase as defined by the work of Yoganadan et. al., angular velocity is confirmed a suitable choice to predict strain.

5.5 Additional rationale for chosen methods

Computing CSDM-15 and MPS conveys two strain metrics that provide unique properties to understand maximum global and local brain strain. Computing MPS conveys the peak strain experienced by any element during the impact and therefore provides insight to local peak strain magnitudes. High MPS values could indicate local tissue damage if such strains were experienced in the human brain, potentially identifying focal injury locations. CSDM-15 considers all elements at each time step, telling the volume fraction of elements exceeding

15% strain. Understanding the strain levels throughout the entire brain provides insight related to diffuse strain and can be extended to potential diffuse injury risk. MPS and CSDM-15 considered alongside one another provides valuable information regarding element deformation during impact, for both local and diffuse strain levels, considered here to represent focal and diffuse injury risk.

Conducting impacts with the Hybrid III headform with and without the Hybrid III neck discovers that kinematic and strain responses are not the same for these two different neck boundary conditions. The Hybrid III neck is found to be stiffer than the human neck under axial compression [98], [99] as well the Hybrid III neck was less compliant than necks of post mortem human subjects during sled tests [100]. Impacts to the Hybrid III head without a neck can then represent a neck with zero stiffness, and it can be assumed the actual stiffness and response of the human neck will fall between the two. The experimental work in this thesis analyzes head kinematics and resulting computed strains for what can be considered opposing neck stiffness levels. By conducting impacts to the Hybrid III headform and comparing impacts using the Hybrid III neck to impacts with no neck at all, this work confirms kinematics and corresponding strain metrics do not respond the same for both scenarios.

This work focused primarily on the individual kinematics in an additive regression form as detailed in the Methods section. Previous functionals, such as HIP, consider products of kinematics as a form for predicting injury. Relating the results of this thesis to the form of HIP, one term of interest could be the product of ω_R and α_R as statistically they each appear effective depending on the use of the Hybrid III neck or no neck. Further exploration of a metric form could be considered for future work on this topic. The final form of a metric for this thesis, however, aimed to simplify the helmet assessment process as much as possible. In determining that a single kinematic was capable of predicting strain metrics, it was decided that one single kinematic could provide a metric that was simple and straightforward.

This work makes significant contributions to helmeted headform impact testing by expanding the knowledge of the influence of the Hybrid III neck on kinematic response and resulting brain FEM computed strain. Researchers are considering other options to the Hybrid III

neck, and using no neck is one of the potential alternatives. This thesis presents some of the consequences of using the Hybrid III headform without a neck.

5.6 Use of injury risk curves to develop a kinematic threshold

To be used as a helmet assessment metric, a threshold must be set on the kinematic metric that is linked to a diagnosable injury at a risk level that is deemed acceptable. Said differently, deciding what brain injury is aimed to be prevented, injury risk curves can allow a corresponding strain metric to be identified that, based on this work, is linked to angular velocity. This section presents one possible method for determining a kinematic threshold, though multiple approaches could be taken. One example of determining a threshold is broken down into the steps outlined below.

5.6.1 Identifying acceptable injury type

The abbreviated injury scale (AIS) for brain injury has a broad spectrum of injuries at each AIS level, ranging from mild concussion with no loss of consciousness (LOC) to a severe DAI, likely causing death. Table 5.3 summarizes the AIS injury scale for brain injuries.

Table 5.3: Abbreviated Injury Scale for brain injury severity [101]

AIS Code	Brain Injury	Loss of Consciousness (LOC)
1	Mild concussion	none
2	Moderate concussion	< 1 hr
3	Severe concussion	1-6 hrs
4	Mild Diffuse Axonal Injury	6-24 hrs
5	Moderate to Severe Diffuse Axon Injury	> 24 hrs
6	Non-survivable	

The first step is to identify an acceptable injury, both type and severity. For example, based on the above table, the acceptable injury could be concussion or DAI. Here, concussion will be selected as the limiting injury and the severity chosen will be “severe”. Therefore, a head injury on the abbreviated injury scale of 3 or higher (AIS 3+) will be used for this example.

AIS 3+ injuries, defined as severe concussions with loss of consciousness from 1 to 6 hours [101], were selected here to represent the upper limit for acceptable injury. Helmets designed to any standard based on the threshold developed using this one possible method will aim to limit the risk of severe concussion.

Here an acceptable injury of 50% risk of AIS 3+ brain injury was used, which perhaps is relatively severe for common brain injuries in football or hockey. It will be important to consider the severity of athlete brain injuries in contact sports to develop a threshold relevant to the most current epidemiology. This method could be considered an initial application of one process for selecting a threshold. Future discussions surrounding a kinematic threshold could consider injuries of lower severity, such as AIS 1 or 2. As CSDM-15 has previously been considered to represent DAI, it may also be appropriate to consider CSDM at lower strain levels for mild diffuse brain injuries, such as concussion.

5.6.2 Identifying acceptable risk

It is important to define the acceptable risk probability that corresponds to the defined injury type. That is, identify the percent likelihood risk of sustaining a severe concussion if the threshold is exceeded. The injury risk level deemed acceptable here is a 50% risk as many injury risk curves (used in the next step) make use of logistic regression.

The chosen threshold will therefore aim to limit the risk of severe concussion (AIS 3) to 50% or less.

5.6.3 Using injury risk curves to identify corresponding strain limit

The next step is to use a risk curve that links the injury deemed acceptable to an impact parameter. In this case, it will be necessary to choose an injury risk curve relating AIS brain injuries to SIMon computed strain CSDM-15. Takhounts et. al. presented injury risk curves that connect CSDM levels to AIS 4+ brain injuries [14]. Scaling factors were also provided by Takhounts et. al. for quantifying risk at other AIS levels [14].

Using the AIS 4+ injury risk curve for CSDM-15, a 50% risk of AIS 4+ corresponds to a CSDM-15 value of approximately 0.79. Therefore, CSDM-15=0.79 is associated with a 50% risk of AIS 4+ injury, or mild DAI. The goal here, however, is to limit injury risk to 50%

risk of AIS 3+. Therefore, the CSDM-15 value corresponding to AIS 4+ must be scaled to represent AIS 3+. The scaling factor defined by Takhounts et. al. to scale from AIS 4+ to AIS 3+ is 0.82 using the equation below.

$$\text{CSDM-15}_{(\text{AIS 3+})} = 0.82*\text{CSDM-15}_{(\text{AIS 4+})} \quad (5.1)$$

After applying the 0.82 scaling factor, it is determined that 50% risk of AIS 3+ occurs for CSDM-15 values of 0.65 and greater.

5.6.4 Translating strain limit to kinematic threshold

The final step in identifying a threshold value requires translating the determined CSDM-15 cut-off value (here, CSDM-15=0.65) to a corresponding threshold on a measurable impact kinematic. Understanding the relationship between CSDM-15 and the kinematic metric, through linear regression, allows a limit to be proposed, such that CSDM-15 values of 0.65 or greater are not likely to occur if the metric threshold is not surpassed. With the kinematic metric identified as angular velocity, a threshold can be determined.

5.6.5 Pass/ fail threshold for helmet certification with the Hybrid III head and neck

This work identifies peak resultant angular velocity, ω_R, as the kinematic most appropriate for future helmet certification and therefore the cut-off value will be determined in reference to ω_R. Figure 5.1, below plots CSDM-15 against ω_R, with lines indicating the CSDM-15 and ω_R limits. An ω_R cut-off value could be determined based on the intersection between CSDM-15=0.65 and the equation of the regression line as one method for choosing the threshold. Alternatively, choosing the minimum ω_R value that results in CSDM-15 of 0.65 is a second method. The latter will be explored here, though it is acknowledged that different approaches could be taken and may change the resulting threshold limit. Selecting the angular velocity threshold based on the minimum value corresponding to CSDM-15 = 0.65 is a conservative choice. By doing so, this suggests a greater number of impacts in the presented data set will be deemed “unacceptable”. However, this strategy also reduces the likelihood that angular velocity below the threshold will produce CSDM-15>0.65, as CSDM-15<0.65 for all impacts below 34 rad/s, in this thesis work.

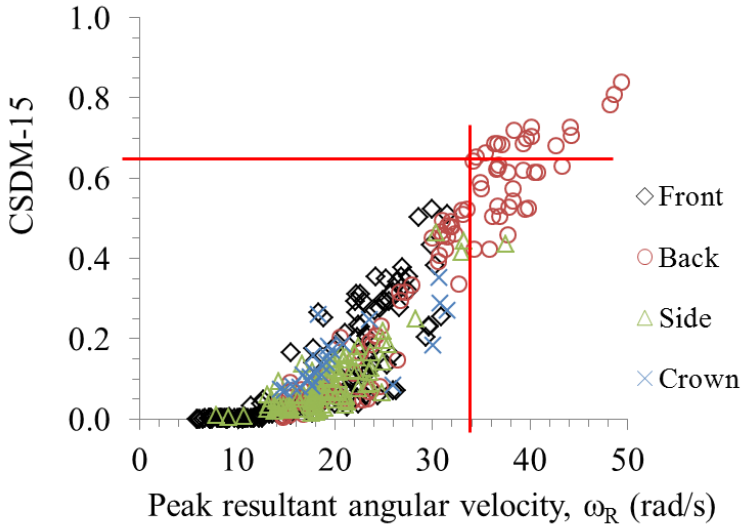

Figure 5.1: CSDM-15 plotted against peak resultant angular velocity for helmeted impacts with the Hybrid III head and neck. The red lines mark the corresponding angular velocity threshold to CSDM-15=0.65, which is considered here to represent 50% risk of an AIS 3+ brain injury.

The minimum ω_R value that results in CSDM-15 equaling 0.65 is 34 rad/s. Therefore, based on the steps outlined here to determine a pass/ fail threshold for helmet assessment, 34 rad/s could be proposed as the kinematic helmet assessment pass/ fail threshold. In combining all impacts together to set a threshold, it can be noted in Figure 5.1 that, regardless of impact location, CSDM-15 does not exceed 0.65 for any impacts with ω_R below 34 rad/s.

It is recognized that there are several ways to identify and apply a threshold for helmet certification. The method presented here should be considered just one example of how a kinematic helmet assessment threshold could be determined for this setup.

5.6.6 Implications for the proposed pass/ fail threshold

While other methods could be used to identify a kinematic threshold, using the steps presented here, 34 rad/s was assigned as the pass/ fail threshold based on the goal to reduce the risk of a severe concussion to 50%. Takhounts et. al. also established critical angular velocity values based on what strain (CSDM or MPS) would result in a 50% risk of a 4th level injury on the abbreviated injury scale (AIS 4+). For impacts with the Hybrid III 50th percentile male, this value was found to be 57.96 rad/s [14]. AIS 4+ injuries are considered traumatic brain injuries resulting in DAI. Margulies et. al. suggested DAI could occur at

changes in angular velocity exceeding 46.5 rad/s [102]. This thesis work takes similar steps to Takhounts et. al. in determining an angular velocity threshold, though aims to mitigate injuries like mTBI and concussion, rather than DAI. As such, the risk curve used here is different from that used by Takhounts et. al. and resulting angular velocity threshold values cannot be directly compared. However, a threshold here should be associated with relatively lower CSDM values corresponding to a lower severity brain injury on the AIS scale and, ultimately, a lower angular velocity threshold. The angular velocity limit established through this thesis work is suitably lower than 57.96 rad/s. Much of the working surrounding brain injury tolerances focuses on severe brain injury, as also pointed out by Stemper and Pintar, in an overview of the biomechanics of concussion [103]. This thesis presents just one possible approach for identifying a threshold for mild brain injury. Considering mTBI, of which concussion is an example, limiting ω_R to less than 34 rad/s during a direct helmeted head impact aims to mitigate risk for severe concussion.

Applying this angular velocity threshold as a pass/ fail helmet assessment metric indicates there is the potential for improvement regarding head and brain protection. Should this example of a possible certification-style assessment method be implemented today, 89% of the helmeted impacts, conducted under these conditions, would "pass", suggesting helmets can limit angular velocity, though improvement is needed to achieve a 100% success rate. An angular velocity limit of 34 rad/s leads to 11% of helmeted impacts exceeding the proposed allowable threshold for this experimental setup. Considering only those impacts that exceed standard level impact velocities (4.5 m/s for hockey and 5.46 m/s for football helmets), 22% of impacts exceed the proposed ω_R threshold of 34 rad/s (18% of hockey helmet impacts and 30% of football helmet impacts). The majority of impacts meeting the proposed threshold suggests that even without certification against angular velocity, helmets are moderately successful in mitigating angular velocity. This can be viewed as a positive result for helmet designers and manufacturers as it does not suggest helmets require a complete redesign. However, as many as 30% of impacts do not meet the suggested ω_R limit and therefore improvements can be made to the basic, multi-impact helmet. Adoption of a helmet standard that requires ω_R be less than 34 rad/s would result in potentially minor changes to today's marketed helmets to ensure all helmets meet this requirement.

It is of interest to note that helmets appear to reduce angular motion of the head, compared to the unprotected headform, though helmets were never designed explicitly for this purpose. One possible explanation for this is relative motion between the helmet and headform. If the helmet is able to rotate separate from the headform, even slightly, this could reduce the magnitude of rotation transmitted to the headform. With the rubber Hybrid III scalp, relative motion is expected to be minimal, though could provide one explanation. The increased inertia of the combined headform and helmet relative to the headform without the mass of the helmet could be another cause for reduced angular velocity. Figure 4.17 compares angular kinematics of an unprotected headform to a hockey helmet for a front impact, showing that for the same impact speed, the area beneath the acceleration-time plot is reduced. An increased inertia, due to an increase in mass, would require reduced angular velocity to achieve the same rotational kinetic energy. Either of these explanations could apply to this experimental setup, as well as real-life impacts during sport, providing possible explanations for a helmets role in reducing angular velocity.

The method for determining a kinematic threshold considered all impact locations together, which eliminates the need for individual, location-specific thresholds. Selecting the minimum ω_R value that corresponded to CSDM-15 = 0.65, with all impacts as a single data set, ensures that all CSDM-15 values exceeding 0.65 are deemed unacceptable, regardless of the impact location. Identifying thresholds for each impact location could result in different kinematic thresholds, however, location-specific thresholds were not considered here as the slope of the regression lines for individual locations are similar. While this setup does not result in impacts exceeding the CSDM-15 limit for each location, with similar slopes, it is expected that limiting ω_R to less than 34 rad/s should limit CSDM-15 to values to less than 0.65 for any location. Furthermore, one goal of this study is to maintain a helmet assessment method that is as simple as possible. Choosing one threshold for all locations eliminates the need to individually assess each impact location. By conservatively choosing one threshold based on the minimum ω_R that results in unacceptable strain levels, all impact locations are expected to achieve acceptable levels of CSDM-15.

5.6.7 Pass/ fail threshold for helmet certification with the Hybrid III head with no neck

Applying the logic and steps detailed above for determining a kinematic threshold, Figure 5.2 shows the correlation between CSDM-15 and ω_R with threshold lines to display chosen limits. While there is variance in the data for no-neck impacts, a CSDM-15 value of 0.65 is reached at 39 rad/s, differing from the limit identified for neck impacts by 15%.

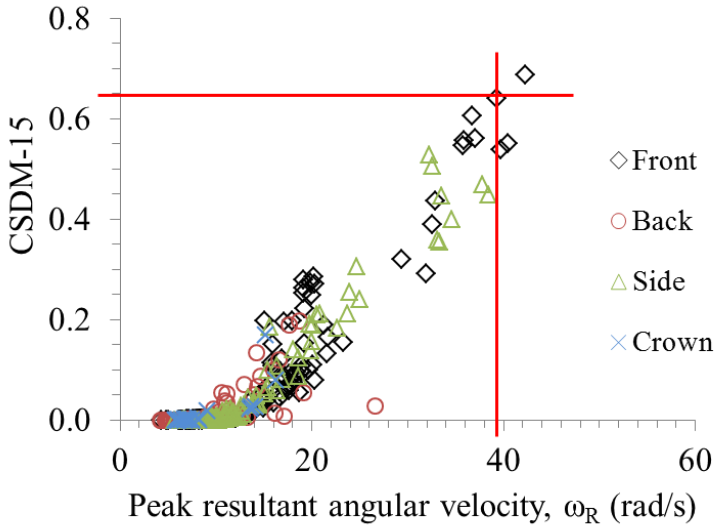

Figure 5.2: CSDM-15 plotted against peak resultant angular velocity where added lines mark the corresponding angular velocity threshold to CSDM-15=0.65, which is considered here to represent 50% risk of an AIS 3+ brain injury.

Identifying a minimum ω_R value corresponding to the chosen CSDM-15 limit presents the ω_R threshold as 39 rad/s for helmeted Hybrid III head and no neck impacts. Impact location does not change the threshold value, as seen in Figure 5.2, based on the method presented here. It is noted, however, that further investigation may be required for no neck impacts as longer time duration results in higher strain magnitudes and ultimately could change the corresponding threshold values.

As mentioned, this method for proposing a kinematic threshold is only one option for doing so. Using this method and considering the lower threshold of 34 rad /s, of all the impacts conducted (both with and without the Hybrid III neck), 8% exceeded a 34 rad/s threshold

theoretically set on angular velocity. It is acknowledged that other methods are viable and could present different limits for angular velocity and this approach should be considered just one possible option.

5.7 Limitations

One limitation of this work is the use of the Hybrid III headform, as it was originally developed for the automotive industry, focusing on frontal impacts. The Hybrid III headform was not validated for back impacts [104], nor for helmeted impacts as it was used in this study. Analysis of the kinematic responses of the Hybrid III headform shows the head is responding realistically, as discussed in section 3.1.3. Previously published works use the Hybrid III head and neck for helmeted impacts at various locations [75], [105], further supporting this setup as one viable option. As well, Cobb et. al. investigated the response of the Hybrid III headform and the NOCSAE headform, which is arguably more biofidelic for helmet use, and in helmeted impacts it was found that the headform responses were comparable [74]. Therefore, relative correlations and the resulting conclusions are expected to be similar for either headform. Future work could investigate responses using different headforms to confirm the results shown here.

The biofidelity of the Hybrid III head and neck is also recognized as a limitation. The Hybrid III head is made of an aluminum skull and rubber scalp, which will inherently respond different to loading than human bone and tissue. Similarly, the Hybrid III neck is known to be stiffer than the human neck as mentioned above. Therefore, head kinematics may not perfectly represent those of a human head. The Hybrid III head and neck allowed for repeatable impacts across all scenarios and is widely used to study head injury in sport [15], [23], [52]. In addition, the concerns regarding the stiffness of the Hybrid III neck were investigated by considering impacts with no neck.

The exclusive use of the Improved SIMon brain model is also considered a limitation of this work. It is recognized that the results of this study are dictated by the model used to compute brain strain metrics and the use of a single brain FEM may not provide the opportunity for direct comparison. However, the use of a different model is expected to produce similar trends. The SIMon model was validated against experimental cadaver data [83], [106], using

the same data for which nearly all brain model calibration work is based [107]. As numerous models were validated against the same data set, it is expected that they should give the same, or similar, responses. In the development of BrIC, Takhounts computed strains using SIMon and the global human body model consortium (GHBMC) and determined that they gave nearly identical results [14]. Additionally, researchers using various models have also found angular velocity to be an important kinematic for predicting strain. Gabler et. al., using both SIMon and GHBMC, assessed kinematic metrics and found angular velocity metrics to correlate to strain metrics computed using either model [105]. Kleiven used a purpose-developed brain finite element model and found that angular velocity represented strain better than HIP and angular acceleration [108]. Though the results here are dependent on the strain metrics computed by SIMon, it is expected that using another brain model should yield similar conclusions.

Injury risk curves developed to date and discussed here are related to unprotected head impacts with a neck. The exact injury thresholds for helmeted head impacts is likely greater than bare heads, as the helmet is shown to mitigate impact kinematics relative to the unprotected headform. Using risk curves for bare cadaver heads to choose thresholds is likely conservative, though this may be positive as selecting thresholds aims to ultimately mitigate injury risk. However, developing a kinematic threshold that is related to a chosen injury risk level for free-head impacts without a neck may require further work to confirm an appropriate limit is identified that reflects the same levels of risk for head and neck impacts.

The results of this study are specific to the test setup used. Here, primary head impacts were conducted using the Hybrid III headform with the Hybrid III neck using a guided rail drop. In addition, head impacts were conducted using the Hybrid III headform without a neck. Hundreds of impacts to the headform including various impact locations and two different helmet types provided a comprehensive data set from which conclusions were drawn.

6 Conclusion

The objective of this thesis was to identify head kinematics that predict finite element model-computed brain strain metrics and develop a kinematic metric that can be used for helmet assessment. Today's helmets are certified on a pass/ fail basis focusing only on linear acceleration during impact, which is not capable of predicting strain experienced by the brain. Previous researchers have developed kinematic functionals to predict brain strain and brain injury, though each equation has limitations related to implementing it as a helmet assessment metric. Current kinematic-based functions and metrics for predicting diffuse brain injury require numerous variables or multiple integrations, which is inefficient and unlikely to be adopted in helmet certification practices. This study identified a simple and efficient method for assessing helmets based on kinematics related to brain strain.

Helmeted head impacts were replicated using a Hybrid III headform and Hybrid III neck or no neck in a drop configuration. Resulting kinematics over the impact duration provided input for the Improved SIMon brain model from which brain strain metrics were computed. Using multiple regression techniques, key kinematics were determined that effectively and efficiently predict the computed strain metrics.

Peak resultant angular velocity alone achieved R^2 and F-statistic values that were overall better than any other kinematics for predicting CSDM-15 and MPS for all helmeted impact scenarios investigated here including hockey and football helmet impacts with the Hybrid III head and neck as well as with the free Hybrid III headform. Angular velocity as a new assessment metric presents a potential protocol for future helmet certification methods. This study found angular velocity to be a key predictor for strain metrics computed using the SIMon brain model for all impact locations considered together, achieving R^2 values of 0.81 or greater and maintaining significant F-statistics when correlated with strain. Using the Hybrid III headform with a neck and without a neck, angular velocity was able to better predict both CSDM-15 and MPS than any other single kinematic.

Strain metrics can be predicted using the single angular kinematic, peak resultant angular velocity, during helmet certification-style drops. Considering multiple kinematic terms does not significantly improve one's ability to predict strain metrics. Additionally, one kinematic

acting as a pass/ fail threshold during helmet assessment is efficient and aligns with historically simple methods. Monitoring angular velocity improves the quality of the helmet assessment, relative to current linear acceleration metrics. Angular velocity correlates to brain strain metrics, which are considered here to be representative of diffuse brain injury. Angular velocity also correlates with linear acceleration, which is linked to focal injury. Therefore, limiting angular velocity succeeds in limiting the single best kinematic correlate to brain strain, while indirectly limiting a linear kinematic linked to focal injury.

One possible method for identifying a certification-appropriate pass/ fail threshold was presented in this thesis. A 50% risk of an AIS 3+ injury was selected as the injury type and risk level to represent the upper limit for identifying a corresponding kinematic threshold. Injury risk curves linking AIS injury to CSDM were used in parallel with the relationship between angular velocity and CSDM to identify a kinematic threshold.

6.1 Contributions and practical applications

As discussed throughout this thesis, previous research has established angular kinematics as a contributor to brain strain. This thesis work is unique in that it clearly identified the single best kinematic correlate to brain strain in a set up deemed reasonable for helmet certification. The main contributions of this thesis work are outlined below.

- Peak resultant angular velocity stands out as the optimum choice for choosing one single kinematic to introduce for helmet certification for both hockey and football helmet impacts to the Hybrid III head with or without the Hybrid III neck. Future discussions surrounding new helmet standards could look at using peak resultant angular velocity as a way of considering diffuse injury during certification.
- It was determined that multiple kinematics are not required to predict strain metrics and one angular kinematic, namely peak resultant angular velocity, is capable of doing so. Considering impact locations and individual kinematic directions separately is not required for angular velocity to effectively predict strain metrics, therefore peak resultant angular velocity is chosen over direction-specific. Furthermore, due to positive correlation between angular velocity and peak g, it could be argued that a certification approach that favored minimizing angular velocity

would also favor helmets that minimize peak g. This could address one concern in the helmet assessment community that centers on assessing helmets based on rotational mechanics. Specifically, some are concerned that minimizing angular kinematics might lead to helmets that give high peak g, potentially leading to ineffective protection against focal injury. Based on the correlation noted, and the helmets in this study, this seems unlikely because reductions in angular velocity are associated with reduced peak g as well.

- This study found that time duration of kinematic responses, particularly for impacts without a neck, affect resulting strain magnitudes and threshold limits and therefore, helmet assessment organizations considering no-neck protocols should examine this when determining their pass/fail thresholds.
- A possible method for identifying a kinematic threshold is proposed based on brain injury risk curves and CSDM-15 limits. The threshold value chosen here, and the method proposed for identifying it can be discussed by standards organizations as one way to identify a failure limit for certification.

6.2 Future work and recommendations

At this stage in head injury biomechanics research, there is overwhelming evidence that evaluating angular kinematics is necessary to estimate risk of brain injury. This thesis presents a simple and effective method for predicting brain strain metrics for helmeted impacts in a drop-style impact using angular velocity. Repeating this study using different impact methods or brain finite element models holds great value in further confirming the results of this study. Creating helmeted head impacts using a linear impactor or pendulum swing impacts, for example, and returning similar findings that support angular velocity as the key predictor would provide additional support for change to the current linear kinematic-based standards.

It will be important to further investigate threshold values to ensure real-life head and brain injury is reflected in the chosen kinematic threshold regardless of impact configuration. The current method makes use of injury risk curves based on automotive and animal injury data and correlations to strains using the Improved SIMon brain model. New risk curves and

additional finite element models could be substituted into the current method to confirm the proposed threshold is reasonable or to propose another appropriate pass/ fail threshold.

Should all researchers agree that angular velocity is the key kinematic for future helmet certification, it is then necessary to implement changes to current standards. This requires governing bodies and helmet manufacturers work together to establish an agreed upon repeatable impact setup to allow angular velocity to be measured. The impact equipment and instrumentation must contain published data regarding proper maintenance and established test reproducibility. Guaranteed consistency from one impact laboratory to another is crucial for implementing a worldwide helmet standard. The current linear drop configuration has achieved this consistency, and it will require extensive discussion to ensure repeatable and reliable methods for future helmet assessments that include angular motion.

Bibliography

[1] Centers for Disease Control and Prevention, 'Report to Congress on Traumatic Brain Injury in the United States: Epidemiology and Rehabilitation', National Center for Injury Prevention and Control; Division of Unintentional Injury Prevention, Atlanta, GA, 2015.

[2] 'CDC Grand Rounds: Reducing Severe Traumatic Brain Injury in the United States', *Cent. Dis. Control Prev.*, vol. 62, no. 27, pp. 549–552, Jul. 2013.

[3] J. Gilchrist, K. E. Thomas, L. Xu, L. C. McGuire, and V. Coronado, 'Nonfatal Traumatic Brain Injuries Related to Sports and Recreation Activities Among Persons Aged≤ 19 Years', *MMWR*, vol. 60, no. 39, pp. 1337–1342.

[4] 'Head Injuries in Canada: A Decade of Change (1994-1995 to 2003-2004)'. Canadian Institute for Health Information, Aug-2006.

[5] F. O. Mueller and R. C. Cantu, 'Annual Survey of Catastrophic Football Injuries', *Am. Footb. Coach. Assoc. Natl. Coll. Athl. Assoc. Natl. Fed. State High Sch. Assoc.*, 2011.

[6] M. Marar, N. M. McIlvain, S. K. Fields, and R. D. Comstock, 'Epidemiology of Concussions Among United States High School Athletes in 20 Sports', *Am. J. Sports Med.*, vol. 40, no. 4, pp. 747–755, Apr. 2012.

[7] K. Flik, S. Lyman, and R. G. Marx, 'American collegiate men's ice hockey: an analysis of injuries', *Am. J. Sports Med.*, vol. 33, no. 2, pp. 183–187, Feb. 2005.

[8] J. M. Hootman, R. Dick, and J. Agel, 'Epidemiology of collegiate injuries for 15 sports: summary and recommendations for injury prevention initiatives', *J. Athl. Train.*, vol. 42, no. 2, pp. 311–319, 2007.

[9] R. A. Wennberg and C. H. Tator, 'National Hockey League reported concussions, 1986-87 to 2001-02', *Can. J. Neurol. Sci. J. Can. Sci. Neurol.*, vol. 30, no. 3, pp. 206–209, Aug. 2003.

[10] A. H. S. Holbourn, 'Mechanics of Head Injuries', *The Lancet*, vol. 242, no. 6267, pp. 438–441, Oct. 1943.

[11] P. Yarnell and A. K. Ommaya, 'Experimental cerebral concussion in the rhesus monkey.', *Bull. N. Y. Acad. Med.*, vol. 45, no. 1, p. 39, 1969.

[12] T. A. Gennarelli, L. E. Thibault, and K. Ommaya, 'Pathophysiologic Responses to Rotational and Translational Accelerations of the Head', in *16th Stapp Car Crash Conference*, 1972.

[13] E. Gurdjian, V. Roberts, and L. Thomas, 'Tolerance curves of acceleration and intracranial pressure and protective index in experimental head injury', *J. Trauma*, vol. 6, no. 5, pp. 600–604, Sep. 1966.

[14] E. G. Takhounts, M. J. Craig, K. Moorhouse, J. McFadden, and V. Hasija, 'Development of Brain Injury Criteria (BrIC)', *Stapp Car Crash J.*, vol. 57, pp. 243–266, 2013.

[15] D. Marjoux, D. Baumgartner, C. Deck, and R. Willinger, 'Head injury prediction capability of the HIC, HIP, SIMon and ULP criteria', *Accid. Anal. Prev.*, vol. 40, no. 3, pp. 1135–1148, Dec. 2007.

[16] J. S. Cheng and K. W. Reichert, 'Adult and Child Head Anatomy', in *Frontiers in Head and Neck Trauma: Clinical and Biomechanical*, N. Yoganandan, F. A. Pintar, and S. J. Larson, Eds. IOS Press, OHMSHA, 1998, pp. 1–15.

[17] K. Cherry, 'A Guide to the Anatomy of the Brain', *Verywell Mind*, 24-Feb-2018. [Online]. Available: https://www.verywell.com/the-anatomy-of-the-brain-2794895. [Accessed: 08-Jan-2018].

[18] L. Wilson *et al.*, 'The chronic and evolving neurological consequences of traumatic brain injury', *Lancet Neurol.*, vol. 16, Oct. 2017.

[19] J. W. Melvin and J. W. Lighthall, 'Brain Injury Biomechanics', in *Accidental Injury - Biomechanics and Prevention*, A. M. Nahum and J. W. Melvin, Eds. New York, USA: Springer, 2002, pp. 277–302.

[20] A. G. Gross, 'A new theory on the dynamics of brain concussion and brain injury', *J. Neurosurg.*, vol. 15, no. 5, pp. 548–561, 1958.

[21] S. Strich, 'Diffuse degeneration of the cerebral white matter in severe dementia following head injury', *J. Neurol. Neurosurg. Psychiatry*, vol. 19, pp. 163–185, 1956.

[22] A. K. Ommaya, A. E. Hirsch, E. S. Flamm, and R. H. Mahon, 'Cerebral Concussion in the Monkey: An Experimental Model', *Science*, vol. 153, pp. 211–212, May 1966.

[23] L. Zhang, K. H. Yang, and A. I. King, 'A Proposed Injury Threshold for Mild Traumatic Brain Injury', *J. Biomech. Eng.*, vol. 126, no. 2, p. 226, 2004.

[24] H. Lee, M. Wintermark, A. D. Gean, J. Ghajar, G. T. Manley, and P. Mukherjee, 'Focal Lesions in Acute Mild Traumatic Brain Injury and Neurocognitive Outcome: CT versus 3T MRI', *J. Neurotrauma*, vol. 25, pp. 1049–1056, Sep. 2008.

[25] L. R. Gentry, J. C. Godersky, B. Thompson, and V. D. Dunn, 'Prospective Comparative Study of Intermediate-Field MR and CT in the Evaluation of Closed Head Trauma', *Am. J. Neuroradiol.*, vol. 9, no. 1, pp. 91–100, 1988.

[26] H. S. Martland, 'Punch Drunk', *J. Am. Med. Assoc.*, vol. 91, no. 15, pp. 1103–1107, 1928.

[27] A. C. McKee *et al.*, 'Chronic Traumatic Encephalopathy in Athletes: Progressive Tauopathy After Repetitive Head Injury', *J. Neuropathol. Exp. Neurol.*, vol. 68, no. 7, pp. 709–735, Jul. 2009.

[28] J. A. Newman, *Modern Sports Helmets: Their History, Science, and Art*. Schiffer Publishing, 2007.

[29] D. J. Pearsall, P. Lapaine, and R. Ouckama, 'Ten years later: Ice hockey helmet impact mechanics change with age', *J. Sports Eng. Technol.*, vol. 230, no. 1, pp. 23–28, 2016.

[30] M. L. Levy, B. M. Ozgur, C. Berry, H. E. Aryan, and M. L. J. Apuzzo, 'Birth and Evolution of the Football Helmet', *Neurosurgery*, vol. 55, no. 3, pp. 656–662, Sep. 2004.

[31] J. J. Crisco *et al.*, 'Frequency and Location of Head Impact Exposures in Individual Collegiate Football Players', *J. Athl. Train.*, vol. 45, no. 6, pp. 549–559, Dec. 2010.

[32] L. L. Brainard *et al.*, 'Gender Differences in Head Impacts Sustained by Collegiate Ice Hockey Players', *Med. Sci. Sports Exerc.*, vol. 44, no. 2, pp. 297–304, Feb. 2012.

[33] P. A. Cripton, D. M. Dressler, C. A. Stuart, C. R. Dennison, and D. Richards, 'Bicycle helmets are highly effective at preventing head injury during head impact: Head-form accelerations and injury criteria for helmeted and unhelmeted impacts', *Accid. Anal. Prev.*, vol. 70, pp. 1–7, Sep. 2014.

[34] E. S. Gurdjian, V. R. Hodgson, W. G. Hardy, L. M. Patrick, and H. R. Lissner, 'Evaluation of the protective characteristics of helmets in sports', *J. Trauma*, vol. 4, pp. 309–324, 1964.

[35] R. C. Cantu and F. O. Mueller, 'Brain Injury-related Fatalities in American Football, 1945-1999', *Neurosurgery*, vol. 52, no. 4, pp. 846–853, 2003.

[36] G. G. Snively, 'Skull Busting for Safety'. Sports Car Illustrated, 1957.

[37] N. Yoganandan, F. A. Pintar, and S. J. Larson, 'Helmet Development and Standards', in *Frontiers in Head and Neck Trauma Clinical and Biomedical*, E. B. Becker, Ed. IOS Press, OHMSHA, 1998.

[38] 'BS 1869:1960 Specification for Protective Helmets for Racing Motorcyclists'. British Standards Institution, 1960.

[39] 'Standards for Racing Crash Helmets'. Snell Memorial Foundation, 1959.

[40] 'CSA Z262.1-09: Standard for Ice Hockey Helmets'. CAN CSA, 01-May-2012.

[41] 'CPSC - Safety Standard for Bicycle Helmets; Final Rule'. Consumer Product Safety Commission (CPSC), 10-Mar-1998.

[42] C. W. Gadd, 'Use of a Weighted-Impulse Criterion for Estimating Injury Hazard', SAE International, Warrendale, PA, 660793, Feb. 1966.

[43] 'Standard Performance Specification for Newly Manufactured Football Helmets, NOCSAE DOC (ND) 002-13m15'. National Operating Committee on Standards for Athletic Equipment, 31-Oct-2015.

[44] J. Versace, 'A Review of the Severity Index', SAE International, Warrendale, PA, 710881, Feb. 1971.

[45] 'FMVSS No. 208'. National Highway Traffic Safety Administration.

[46] 'ECE Reg. 22 Uniform Provisions Concerning the Approval of Protective Helmets and Their Visors for Drivers and Passengers of Motor Cycles and Mopeds'. 2002.

[47] 'FIA Standard 8860-2010'. Federation Internationale de l'Automobile, 2012.

[48] S. P. Broglio, J. J. Sosnoff, S. H. Shin, X. He, C. Alcaraz, and J. Zimmerman, 'Head impacts during high school football: a biomechanical assessment', *J. Athl. Train.*, vol. 44, no. 4, pp. 342–349, 2009.

[49] R. M. Greenwald, J. T. Gwin, J. J. Chu, and J. J. Crisco, 'Head Impact Severity Measures for Evaluating Mild Traumatic Brain Injury Risk Exposure', *Neurosurgery*, vol. 62, no. 4, pp. 789–798, Apr. 2008.

[50] J. A. Newman, 'A Generalized Model for Brain Injury Threshold (GAMBIT)', in *IRCOBI Conference Proceedings*, Zurich, Switzerland, 1986.

[51] J. A. Newman, N. Shewchenko, and E. Welbourne, 'A proposed New Biomechanical head injury assessment function - the maximum power index', *Stapp Car Crash J.*, vol. 44, pp. 215–47, 2000.

[52] J. Newman *et al.*, 'A New Biomechanical Assessment of mild traumatic brain injury. Part 2: Results and Conclusions', in *IRCOBI Conference Proceedings*, Montpellier, France, 2000.

[53] E. G. Takhounts, V. Hasija, S. A. Ridella, S. Rowson, and S. M. Duma, 'Kinematic Rotational Brain Injury Criterion (BRIC)', in *Proceedings of the 22nd International Technical Conference on the Enhanced Safety of Vehicles (ESV)*, Washington, DC, 2011, pp. 11–0263.

[54] H. Kimpara and M. Iwamoto, 'Mild Traumatic Brain Injury Predictors Based on Angular Accelerations During Impacts', *Ann. Biomed. Eng.*, vol. 40, no. 1, pp. 114–126, Jan. 2012.

[55] H. Kimpara, Y. Nakahira, M. Iwamoto, S. Rowson, and S. Duma, 'Head Injury Prediction Methods Based on 6 Degree of Freedom Head Acceleration Measurements during Impact', *Int. J. Automot. Eng.*, vol. 2, pp. 13–19, 2011.

[56] E. G. Takhounts *et al.*, 'Investigation of Traumatic Brain Injuries Using the Next Generation of Simulated Injury Monitor (SIMon) Finite Element Head Model', *Stapp Car Crash J.*, vol. 52, pp. 1–31, Nov. 2008.

[57] B. M. Knowles, S. R. MacGillivray, J. A. Newman, and C. R. Dennison, 'Influence of rapidly successive head impacts on brain strain in the vicinity of bridging veins.', *J. Biomech.*, vol. 59, pp. 59–70, 2017.

[58] E. G. Takhounts, R. H. Eppinger, J. Q. Campbell, R. E. Tannous, E. D. Power, and L. S. Shook, 'On the Development of the SIMon Finite Element Head Model', *Stapp Car Crash J.*, vol. 47, pp. 107–133, Oct. 2003.

[59] L. Zhang, K. H. Yang, and A. I. King, 'Comparison of brain responses between frontal and lateral impacts by finite element modeling', *J. Neurotrauma*, vol. 18, no. 1, pp. 21–30, Jan. 2001.

[60] T. J. Horgan and M. D. Gilchrist, 'Influence of FE model variability in predicting brain motion and intracranial pressure changes in head impact simulations', *Int. J. Crashworthiness*, vol. 9, no. 4, pp. 401–418, Aug. 2004.

[61] H. Mao *et al.*, 'Development of a Finite Element Human Head Model Partially Validated with Thirty Five Experimental Cases', *J. Biomech. Eng.*, vol. 135, no. 11, 2013.

[62] L. F. Gabler, J. R. Crandall, and M. B. Panzer, ‘Assessment of Kinematic Brain Injury Metrics for Predicting Strain Responses in Diverse Automotive Impact Conditions’, *Ann. Biomed. Eng.*, vol. 44, no. 12, pp. 3705–3718, 2016.

[63] D. Sahoo, C. Deck, and R. Willinger, ‘Brain injury tolerance limit based on computational axonal strain’, *Accid. Anal. Prev.*, vol. 92, pp. 53–70, 2016.

[64] S. Kleiven, ‘Predictors for traumatic brain injuries evaluated through accident reconstructions’, *Stapp Car Crash J*, vol. 51, pp. 81–114, 2007.

[65] A. MacAlister, ‘Surrogate Head Forms for the Evaluation of Head Injury Risk’, presented at the Brain Injuries and Biomechanics Symposium, 2013.

[66] ‘ASTM F1045-07: Standard Performance Specification for Ice Hockey Helmets’. 2007.

[67] ‘Impact Machines: Twin Wire Testing Machine’, *Cadex Inc.* [Online]. Available: http://www.cadexinc.com/twin_wire_flying_arm.php. [Accessed: 19-Jan-2018].

[68] B. M. Knowles, H. Yu, and C. R. Dennison, ‘Accuracy of a Wearable Sensor for Measures of Head Kinematics and Calculation of Brain Tissue Strain’, *J. Appl. Biomech.*, vol. 33, no. 1, pp. 2–11, 2017.

[69] J. T. Gwin, J. J. Chu, S. G. Diamond, P. D. Halstead, J. J. Crisco, and R. M. Greenwald, ‘An Investigation of the NOCSAE Linear Impactor Test Method Based on In Vivo Measures of Head Impact Acceleration in American Football’, *J. Biomech. Eng.*, vol. 132, no. 1, pp. 011006–9, Jan. 2010.

[70] E. J. Pellman, D. C. Viano, C. Withnall, N. Shewchenko, C. A. Bir, and P. D. Halstead, ‘Concussion in Professional Football: Helmet Testing to Assess Impact Performance—Part 11’, *Neurosurgery*, vol. 58, no. 1, pp. 78–96, Jan. 2006.

[71] P. Halldin, ‘CEN/TC 158 Working Group 11 Rotational test methods’, ASTM New Orleans, Nov-2014.

[72] P. Halldin and S. Kleiven, ‘The Development of Next Generation Test Standards for Helmets’, in *Proceedings of the 1st International Conference on Helmet Performance and Design*, London, UK, 2013.

[73] B. Rowson, S. Rowson, and S. M. Duma, ‘Hockey STAR: A Methodology for Assessing the Biomechanical Performance of Hockey Helmets’, *Ann. Biomed. Eng.*, vol. 43, no. 10, pp. 2429–2443, Oct. 2015.

[74] B. R. Cobb, A. M. Zadnik, and S. Rowson, ‘Comparative analysis of helmeted impact response of Hybrid III and National Operating Committee on Standards for Athletic Equipment headforms’, *Proc. Inst. Mech. Eng. Part P J. Sports Eng. Technol.*, vol. 230, no. 1, pp. 50–60, Mar. 2016.

[75] T. A. Smith, P. D. Halstead, E. McCalley, S. A. Kebschull, S. Halstead, and J. Killeffer, ‘Angular head motion with and without head contact: implications for brain injury’, *Sports Eng.*, vol. 18, no. 3, pp. 165–175, Sep. 2015.

[76] A. J. Padgaonkar, K. W. Krieger, and A. I. King, ‘Measurement of Angular Acceleration of a Rigid Body Using Linear Accelerometers’, *J. Appl. Mech.*, pp. 552–556, Sep. 1975.

[77] ‘SAE J211 Instrumentation for Impact Test - Part 1: Electronic Instrumentation’. SAE International, 2007.

[78] E. Takhounts *et al.*, ‘Analysis of 3D Rigid Body Motion using Nine Accelerometer Array System’. Injury Biomechanics Research; Proceedings of the Thirty-First International Workshop, 2003.

[79] B. M. Knowles and C. R. Dennison, ‘Predicting Cumulative and Maximum Brain Strain Measures From HybridIII Head Kinematics: A Combined Laboratory Study and Post-Hoc Regression Analysis’, *Ann. Biomed. Eng.*, vol. 45, no. 9, pp. 2146–2158, 2017.

[80] H. Y. Yu, B. M. Knowles, and C. R. Dennison, ‘A Test Bed to Examine Helmet Fit and Retention and Biomechanical Measures of Head and Neck Injury in Simulated Impact’, *JoVE J. Vis. Exp.*, no. 127, pp. e56288–e56288, Sep. 2017.

[81] E. J. Pellman, D. C. Viano, A. M. Tucker, I. R. Casson, and J. F. Waeckerle, ‘Concussion in Professional Football: Reconstruction of Game Impacts and Injuries’, *Neurosurgery*, vol. 53, no. 4, pp. 799–814, Oct. 2003.

[82] M. D. Clark, B. M. Asken, S. W. Marshall, and K. M. Guskiewicz, ‘Descriptive Characteristics of Concussions in National Football League Games, 2010-2011 to 2013-2014’, *Am. J. Sports Med.*, vol. 45, no. 4, 2017.

[83] W. N. Hardy *et al.*, ‘A Study of the Response of the Human Cadaver Head to Impact’, *Stapp Car Crash J.*, vol. 51, p. 17, Oct. 2007.

[84] Andale, ‘F Statistic: Definition and How to find it’, *Statistics How To*. [Online]. Available: http://www.statisticshowto.com/f-statistic/. [Accessed: 07-Oct-2016].

[85] J. Frost, ‘Multiple Regression Analysis: Use Adjusted R-Squared and Predicted R-Squared to Include the Correct Number of Variables’. [Online]. Available: http://blog.minitab.com/blog/adventures-in-statistics/multiple-regession-analysis-use-adjusted-r-squared-and-predicted-r-squared-to-include-the-correct-number-of-variables. [Accessed: 07-Oct-2016].

[86] J. Frost, ‘Understanding Analysis of Variance (ANOVA) and the F-test | Minitab’. [Online]. Available: http://blog.minitab.com/blog/adventures-in-statistics/understanding-analysis-of-variance-anova-and-the-f-test. [Accessed: 07-Oct-2016].

[87] S. E. Maxwell, ‘Sample Size and Multiple Regression’, *Psychol. Methods*, vol. 5, no. 4, pp. 434–458, 2000.

[88] S. B. Green, ‘How Many Subjects Does it Take to Do A Regression Analysis?’, *Multivar. Behav. Res.*, vol. 26, no. 3, pp. 499–510, 1991.

[89] R. J. Fijalkowski, B. D. Stemper, F. A. Pintar, N. Yoganandan, and T. A. Gennarelli, ‘Influence of angular acceleration duration on functional outcomes following mild diffuse brian injury’, in *IRCOBI Conference Proceedings*, Maastricht (The Netherlands), 2007.

[90] L. F. Gabler, J. R. Crandall, and M. B. Panzer, ‘Development of a Metric for Predicting Brain Strain Responses Using Head Kinematics’, *Ann. Biomed. Eng.*, vol. [published online ahead of print], 2018.

[91] L. F. Gabler, J. R. Crandall, and M. B. Panzer, 'Investigating Brain Injury Tolerance in the Sagittal Plane Using a Finite Element Model of the Human Head', *Int. J. Automot. Eng.*, pp. 37–43, 2016.

[92] J. Ivarsson, D. C. Viano, P. Lovsund, and Y. Parnaik, 'Head Kinematics in Mini-Sled Tests of Foam Padding: Relevance of Linear Responses From Free Motion Headform (FMH) Testing to Head Angular Responses', *J. Biomech. Eng.*, vol. 125, pp. 523–532, Aug. 2003.

[93] H. J. Mertz, A. L. Irwin, and P. Prasad, 'Biomechanical and scaling bases for frontal and side impact injury assessment reference values.', *Stapp Car Crash J.*, vol. 47, p. 155, 2003.

[94] S. Meng, A. Cernicchi, S. Kleiven, and P. Halldin, 'The biomechanical differences of shock absorption test methods in the US and European helmet standards', *Int. J. Crashworthiness*, vol. [published online ahead of print], 2018.

[95] P. Halldin, 'CEN/TC 158 Working Group 11 Rotational test methods', ASTM Atlanta, Nov-2017.

[96] T. B. Hoshizaki *et al.*, 'The development of a threshold curve for the understanding of concussion in sport', *Trauma*, vol. 19, no. 3, pp. 196–206, 2017.

[97] N. Yoganandan, J. Li, J. Zhang, F. A. Pintar, and T. A. Gennarelli, 'Influence of angular acceleration-deceleration pulse shapes on regional brain strains', *J. Biomech.*, vol. 41, pp. 2253–2262, 2008.

[98] N. Yoganandan, A. Sances Jr., and F. Pintar, 'Biomechanical Evaluation of the Axial Compressive Responses of the Human Cadaveric and Manikin Necks', *J. Biomech. Eng.*, vol. 111, pp. 250–255, 1989.

[99] A. Sances, Jr., 'Dynamic Comparison of the Hybrid III and Human Neck', in *Frontiers in Head and Neck Trauma: Clinical and Biomechanical*, N. Yoganandan, F. A. Pintar, and S. J. Larson, Eds. IOS Press, OHMSHA, 1998, pp. 73–77.

[100] N. Yoganandan, F. A. Pintar, M. Schlick, J. Moore, and D. J. Maiman, 'Comparison of Head-Neck Responses in Frontal Impacts Using Restrained Human Surrogates', *Annu. Conf. Ann. Adv. Automot. Med.*, vol. 55, pp. 181–191, Oct. 2011.

[101] T. A. Gennarelli and E. Wodzin, 'Abbreviated Injury Scale 2005'. Association for the Advancement of Automotive Medicine, 2005.

[102] S. S. Margulies and L. E. Thibault, 'A proposed tolerance criterion for diffuse axonal injury in man', *J. Biomech.*, vol. 25, no. 8, pp. 917–923, 1992.

[103] B. D. Stemper and F. A. Pintar, 'Biomechanics of Concussion', *Prog. Neurol. Surg.*, vol. 24, pp. 14–27, 2014.

[104] '49 CFR Part 572; Anthropomorphic Test Devices'. National Highway Traffic Safety Administration, 2011.

[105] G. P. Siegmund, K. M. Guskiewicz, S. W. Marshall, A. L. DeMarco, and S. J. Bonin, 'Laboratory Validation of Two Wearable Sensor Systems for Measuring Head Impact Severity in Football Players', *Ann. Biomed. Eng.*, Aug. 2015.

[106] A. Nahum, R. Smith, and C. Ward, 'Intracranial Pressure Dynamics During Head Impact', *SAE Int. Tech. Pap. 770922*, p. 1977.

[107] K.-M. Tse, S. P. Lim, V. B. C. Tan, and H.-P. Lee, 'A review of head injury and finite element head models', *Am. J. Eng. Technol. Soc.*, vol. 1, no. 5, pp. 28–52, 2014.

[108] S. Kleiven, 'Evaluation of head injury criteria using a finite element model validated against experiments on localized brain motion, intracerebral acceleration, and intracranial pressure', *Int. J. Crashworthiness*, vol. 11, no. 1, pp. 65–79, 2006.

Appendices

Appendix A: Repeatability

Two different impact speeds for Front, Back and Side impacts were investigated to confirm repeatability of the system. The plots below show the mean values and standard deviations, using error bars, for three different impacts at each impact speed and location.

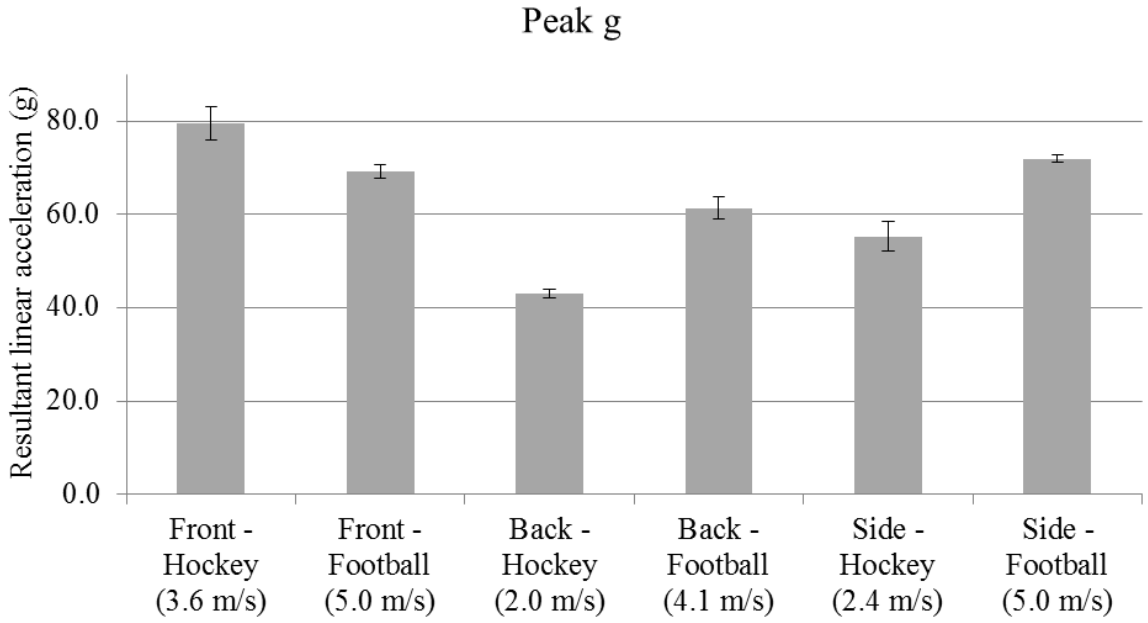

Figure A.1: Mean and standard deviation for resultant peak linear acceleration

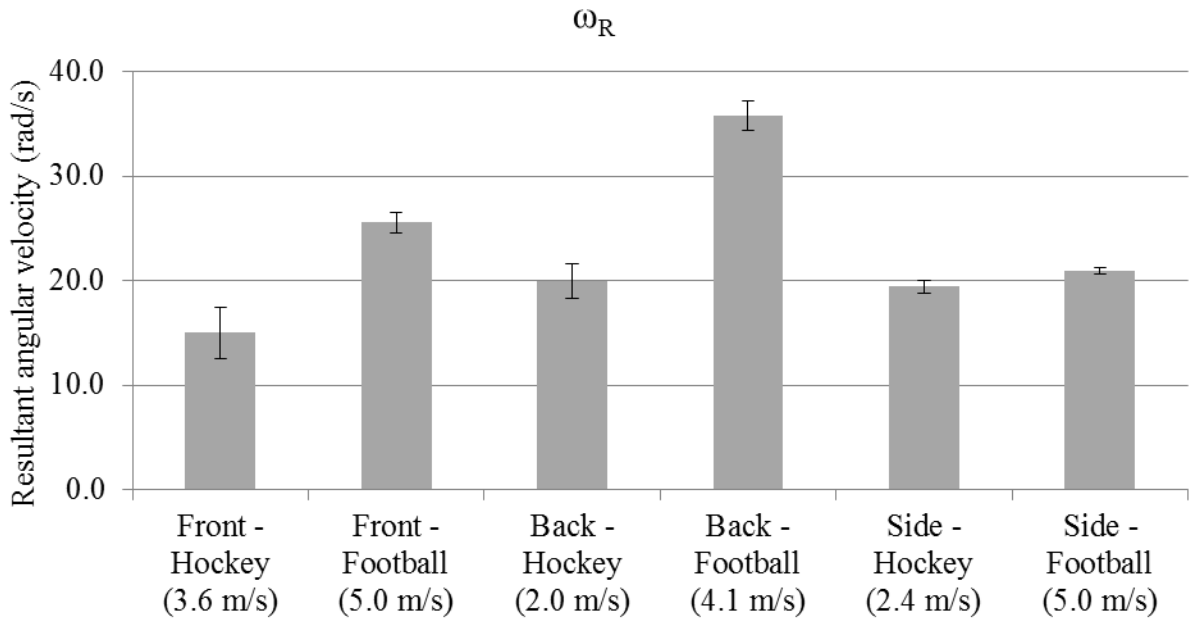

Figure A.2: Mean and standard deviation for resultant peak angular velocity

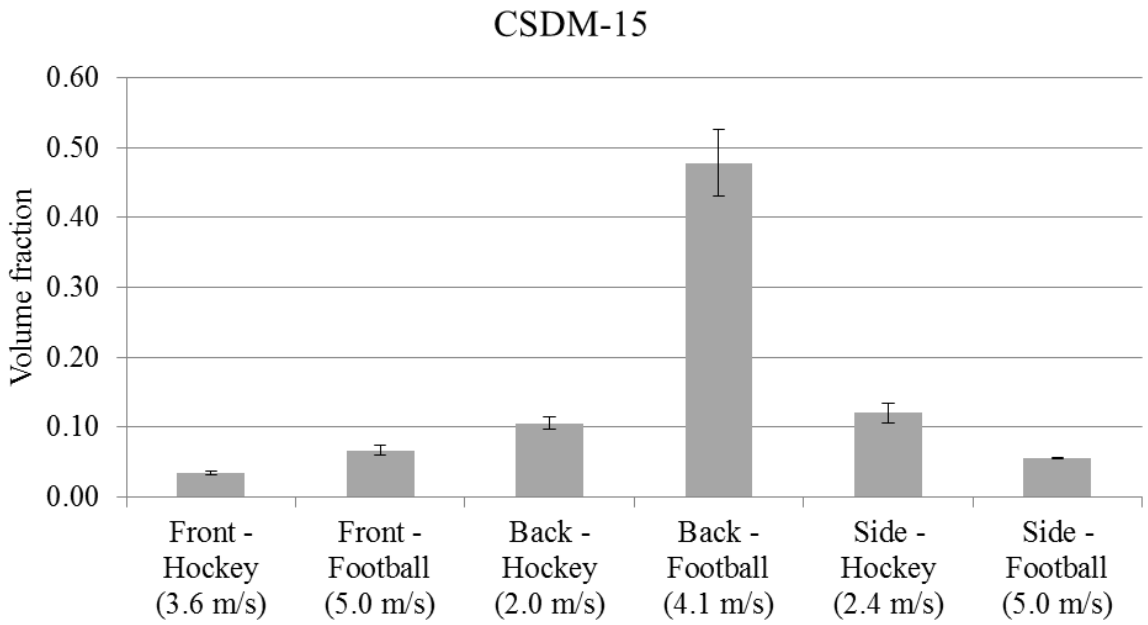

Figure A.3: Mean and standard deviation for resulting CSDM-15

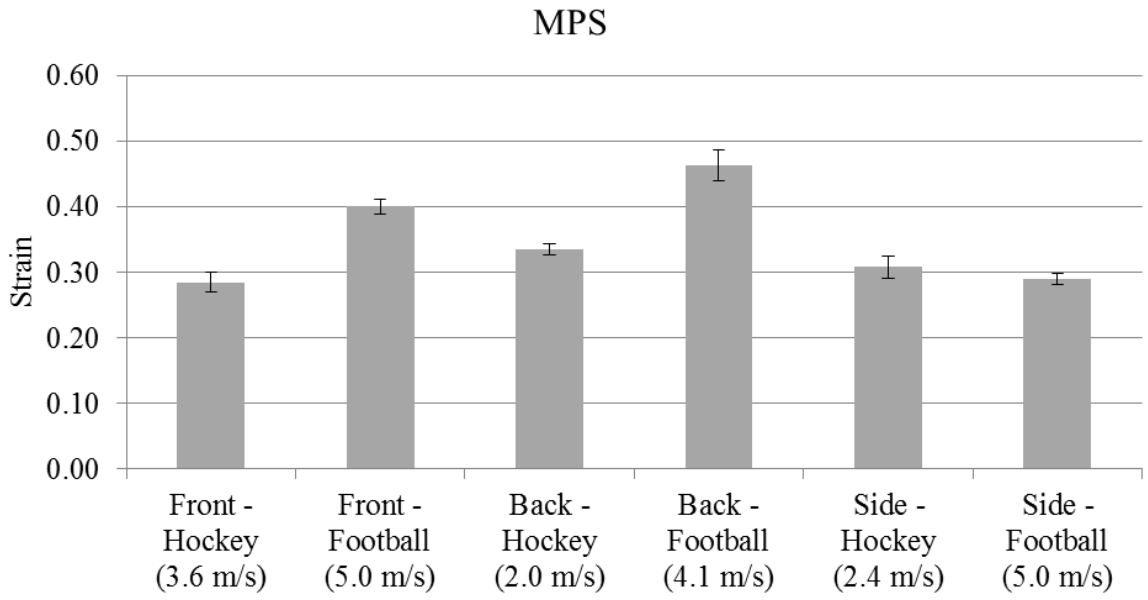

Figure A.4: Mean and standard deviation for resulting MPS

Appendix B: Multiple regression results

Multiple regression results are summarized below for all impact locations considered together, separately presenting data for hockey and football helmets with and without the Hybrid III neck.

Each row contains a unique set of predictor variables and their corresponding regression coefficient (bold and italicized indicates significant predictors with p value < 0.05). The model Adj R^2 and F value are displayed in the right hand columns.

It is noted that angular acceleration (α_R) regression coefficients appear as zero, though are still indicated as significant predictors. The magnitude of the α_R values are in the range of several thousand, and therefore, regression coefficients up to three decimal places are presented as 0.000.

Table B.1: Multiple regression models for predicting CSDM-15 for all hockey helmet impacts with the Hybrid III head and neck.

No. of Variables	Model No.	Peak g	Vi	ΔVR	VR	αR	Δωx	Δωy	Δωz	ΔωR	ωx	ωy	ωz	ωR	Adj R^2	F
1	1	***0.004***													0.36	152
	2		***0.096***												0.40	181
	3			***0.090***											0.44	210
	4				***0.101***										0.46	229
	5									***0.017***					0.86	1629
	6													***0.022***	0.82	1252
	7					***0.000***									0.11	33
2	8	-0.002		***0.120***											0.44	107
	9	***-0.003***			***0.164***										0.48	123
	10	***-0.001***								***0.018***					0.86	841
	11	***0.001***												***0.020***	0.83	658
	12			-0.001						***0.017***					0.86	812
	13			***0.025***										***0.019***	0.85	731
	14				***0.026***									***0.019***	0.84	713
	15				-0.003					***0.017***					0.86	813
	16	***0.005***				0.000									0.37	75
	17			***0.096***		0.000									0.46	106
	18				***0.110***	0.000									0.48	116
	19					***0.000***				***0.017***					0.87	851
	20					0.000								***0.022***	0.83	621
3	21	***-0.003***		***0.052***						***0.017***					0.88	638
	22	***-0.002***		***0.071***										***0.019***	0.86	544
	23	***-0.003***			***0.054***					***0.017***					0.87	619
	24	***-0.002***			***0.072***									***0.019***	0.85	512
	25										***0.012***	***0.016***	***0.006***		0.87	593
	26						***0.011***	***0.014***	-0.002						0.86	525
	27	***-0.002***		***0.134***		0.000									0.46	73
	28	***-0.004***			***0.179***	0.000									0.50	84
4	29	0.000					***0.012***	***0.014***	-0.002						0.86	394
	30	0.000									***0.013***	***0.016***	***0.006***		0.87	443
	31	***-0.002***	0.007	***0.065***										***0.019***	0.86	407
	32	***-0.003***	***-0.060***		***0.111***					***0.016***					0.88	482
	33	***-0.002***	***-0.093***	***0.128***						***0.017***					0.89	525
	34	***-0.002***	***0.049***		0.024									***0.020***	0.85	391
	35	-0.002	***-0.161***	***0.268***		0.000									0.49	60
	36	***-0.003***	***-0.216***		***0.377***	0.000									0.55	78
5	37	***-0.001***		***0.024***							***0.013***	***0.016***	***0.005***		0.87	362

Table B.2: Multiple regression models for predicting MPS for all hockey helmet impacts with the Hybrid III head and neck

No. of Variables	Model No.	Peak g	Vi	ΔVR	VR	αR	Δωx	Δωy	Δωz	ΔωR	ωx	ωy	ωz	ωR	Adj R^2	F
1	1	***0.003***													0.43	192
	2		***0.066***												0.45	206
	3			***0.062***											0.48	234
	4				***0.070***										0.51	260
	5									***0.011***					0.89	2023
	6													***0.014***	0.83	1239
	7					***0.000***									0.17	49
2	8	0.000		***0.060***											0.48	116
	9	-0.001			***0.088***										0.51	132
	10	0.000								***0.011***					0.89	1008
	11	***0.022***												***0.012***	0.85	735
	12			0.002						***0.011***					0.89	1009
	13			***0.020***										***0.012***	0.86	788
	14				***0.022***									***0.012***	0.86	772
	15				0.001					***0.011***					0.89	1008
	16	***0.003***				0.000									0.44	95
	17			***0.064***		0.000									0.49	116
	18				***0.074***	0.000									0.52	129
	19					0.000				***0.011***					0.89	1025
	20					***0.000***								***0.014***	0.84	640
3	21	***-0.001***		***0.014***						***0.011***					0.89	686
	22	0.000		***0.027***										***0.012***	0.86	526
	23	-0.001			0.013					***0.011***					0.89	679
	24	0.000			***0.026***									***0.012***	0.86	514
	25										***0.006***	***0.010***	***0.009***		0.89	720
	26						***0.006***	***0.008***	***0.003***						0.87	556
	27	0.989		***0.000***		0.838									0.49	77
	28	-0.001			***0.092***	0.000									0.52	87
4	29	0.000					***0.005***	***0.008***	0.002						0.87	417
	30	0.000									**0.006**	**0.010**	**0.008**		0.89	541
	31	0.000	0.022	0.009										***0.012***	0.86	397
	32	0.000	-0.022		***0.034***					***0.011***					0.89	514
	33	-0.001	***-0.036***	***0.044***						***0.011***					0.89	530
	34	0.000	***0.043***		-0.016									***0.013***	0.86	398
	35	0.000	***-0.083***	***0.134***		0.000									0.50	61
	36	-0.001	***-0.133***		***0.214***	0.000									0.56	78
5	37	***0.001***		***-0.019***							***0.006***	***0.010***	***0.009***		0.90	447

Table B.3: Multiple regression models for predicting CSDM-15 for all football helmet impacts with the Hybrid III head and neck

No. of Variables	Model No.	Peak g	Vi	ΔVR	VR	αR	Δωx	Δωy	Δωz	ΔωR	ωx	ωy	ωz	ωR	Adj R^2	F
1	1	***0.004***													0.17	29
	2		***0.088***												0.10	17
	3			***0.086***											0.21	37
	4				***0.061***										0.09	14
	5									***0.019***					0.70	320
	6													***0.023***	0.83	679
	7					***0.000***									0.06	7
2	8	0.002		***0.065***											0.22	19
	9	***0.004***			-0.001										0.17	14
	10	0.000								***0.020***					0.70	159
	11	0.000												***0.023***	0.83	337
	12			-0.006						***0.020***					0.70	159
	13			0.008										***0.022***	0.84	341
	14				-0.018					***0.020***					0.71	164
	15				0.008									***0.022***	0.84	341
	16	0.003				0.000									0.08	5
	17			***0.121***		0.000									0.17	11
	18				0.008	0.000									0.05	3
	19					***0.000***				***0.023***					0.59	69
	20					***0.000***								***0.022***	0.83	226
3	21	0.000		-0.006						***0.020***					0.70	105
	22	-0.001		0.018										***0.022***	0.84	229
	23	0.001			-0.026					***0.020***					0.71	109
	24	-0.001			0.019									***0.023***	0.84	230
	25										***-0.006***	***-0.003***	***0.012***		0.29	19
	26						***0.013***	***0.022***	-0.002						0.90	418
	27	-0.001		***0.132***		0.000									0.16	7
	28	0.004			-0.035	0.000									0.07	3
4	29	-0.001					***0.014***	***0.023***	-0.002						0.90	319
	30	***0.006***									***-0.007***	***-0.004***	***0.006***		0.46	29
	31	-0.001	0.034	-0.006										***0.023***	0.84	172
	32	0.000	0.093	-0.075						***0.022***					0.71	81
	33	-0.001	0.026		0.001									***0.023***	0.84	172
	34	0.000	***0.254***		***-0.208***					***0.021***					0.77	114
	35	-0.001	***-0.163***	***0.250***		0.000									0.19	6
	36	0.002	***0.490***		***-0.421***	***0.000***									0.28	10
5	37	***0.003***		***0.087***							***-0.007***	***-0.004***	0.001		0.52	30

Table B.4: Multiple regression models for predicting MPS for all football helmet impacts with the Hybrid III head and neck

No. of Variables	Model No.	Peak g	Vi	ΔVR	VR	αR	Δωx	Δωy	Δωz	ΔωR	ωx	ωy	ωz	ωR	Adj R^2	F
1	1	***0.002***													0.15	24
	2		***0.040***												0.11	18
	3			***0.036***											0.19	32
	4				***0.028***										0.09	15
	5					0.000									0.02	3
	6									***0.007***					0.47	118
	7													***0.009***	0.64	234
2	8	0.001		***0.027***											0.19	16
	9	***0.002***			0.005										0.14	12
	10	0.000								***0.007***					0.46	59
	11	0.000												***0.009***	0.63	116
	12			0.005						***0.007***					0.46	59
	13			0.006										***0.008***	0.64	119
	14				0.008									***0.008***	0.64	120
	15				0.001					***0.007***					0.46	59
	16	0.000				0.000									0.01	2
	17			***0.043***		0.000									0.10	6
	18				0.015	0.000									0.02	2
	19					0.000				***0.005***					0.19	12
	20					0.000								***0.007***	0.46	41
3	21	0.000		0.004						***0.007***					0.46	39
	22	0.000		0.010										***0.008***	0.64	79
	23	0.000			-0.003					***0.007***					0.46	39
	24	0.000			0.013									***0.009***	0.64	81
	25										***-0.003***	0.000	***0.006***		0.28	19
	26						***0.003***	***0.009***	***0.002***						0.81	188
	27	-0.001		***0.059***		0.000									0.11	5
	28	0.000			0.014	0.000									0.01	1
4	29	0.000					***0.003***	***0.009***	***0.003***						0.81	140
	30	***0.002***									***-0.004***	***-0.001***	***0.003***		0.39	23
	31	0.000	***0.052***	-0.027										***0.009***	0.65	63
	32	0.000	***0.110***		***-0.082***					***0.007***					0.52	37
	33	0.000	***0.059***	-0.041						***0.008***					0.47	31
	34	0.000	0.029		-0.008									***0.009***	0.64	61
	35	-0.001	0.031	0.036		0.000									0.11	4
	36	-0.001	***0.239***		***-0.174***	***0.000***									0.30	11
5	37	***0.001***		***0.032***							***-0.004***	***-0.001***	0.002		0.43	22

Table B.5: Multiple regression models for predicting CSDM-15 for all hockey helmet impacts with the Hybrid III head with no neck

No. of Variables	Model No.	Peak g	Vi	ΔVR	VR	αR	Δωx	Δωy	Δωz	ΔωR	ωx	ωy	ωz	ωR	Adj R^2	F
1	1	***0.001***													0.35	140
	2		***0.029***												0.44	207
	3			***0.023***											0.37	150
	4				***0.023***										0.36	149
	5					***0.000***									0.61	404
	6									***0.009***					0.65	487
	7													***0.009***	0.62	429
2	8	0.000		***0.015***											0.37	77
	9	0.000			***0.015***										0.37	77
	10	0.000								***0.008***					0.66	247
	11	***0.000***												***0.008***	0.64	226
	12			0.002						***0.009***					0.65	244
	13			***0.005***										***0.008***	0.63	221
	14				0.002					***0.009***					0.65	244
	15				***0.005***									***0.008***	0.63	221
	16	0.000				***0.000***									0.61	201
	17					***0.000***				***0.006***					0.66	255
	18					***0.000***								***0.005***	0.65	236
	19			0.003		***0.000***									0.61	205
	20				0.003	***0.000***									0.61	205
3	21	0.000		-0.005						***0.008***					0.66	165
	22	***0.000***		-0.003										***0.008***	0.63	150
	23	0.000			-0.005					***0.008***					0.66	165
	24	***0.000***			-0.003									***0.008***	0.63	150
	25										***0.004***	***0.005***	***0.010***		0.73	230
	26						***0.004***	***0.005***	***0.010***						0.73	229
	27	***0.000***		***0.011***		***0.000***									0.62	140
	28	***0.000***			***0.011***	***0.000***									0.62	140
4	29	***0.000***					***0.003***	***0.004***	***0.009***						0.73	177
	30	***0.000***									***0.004***	***0.004***	***0.009***		0.73	179
	31	0.000	***0.030***	***-0.026***						***0.007***					0.66	128
	32	0.000	***0.031***	***-0.025***										***0.007***	0.64	116
	33	0.000	***0.029***		***-0.026***					***0.007***					0.66	128
	34	0.000	***0.030***		***-0.024***									***0.007***	0.64	116
	35	0.000	***0.051***	***-0.030***		***0.000***									0.64	117
	36	0.000	***0.051***		***-0.030***	***0.000***									0.64	116
5	37	0.000		-0.001							***0.004***	***0.004***	***0.009***		0.73	143

Table B.6: Multiple regression models for predicting MPS for all hockey helmet impacts with the Hybrid III head with no neck

No. of Variables	Model No.	Peak g	Vi	ΔVR	VR	αR	Δωx	Δωy	Δωz	ΔωR	ωx	ωy	ωz	ωR	Adj R^2	F
1	1	***0.002***													0.42	188
	2		0.059												0.60	389
	3			***0.047***											0.51	265
	4				***0.047***										0.50	264
	5					***0.000***									0.81	1075
	6									***0.018***					0.87	1736
	7													***0.019***	0.86	1642
2	8	0.000		***0.052***											0.50	133
	9	0.000			***0.052***										0.50	132
	10	0.000								***0.018***					0.87	870
	11	***0.000***												***0.018***	0.87	853
	12			***0.005***						***0.017***					0.87	890
	13			***0.009***										***0.017***	0.87	896
	14				***0.005***					***0.017***					0.87	890
	15				***0.009***									***0.017***	0.87	896
	16	0.000				***0.000***									0.81	541
	17					***0.000***				***0.013***					0.88	973
	18					***0.000***								***0.013***	0.88	947
	19			***0.009***		***0.000***									0.81	569
	20				***0.009***	***0.000***									0.81	569
3	21	***0.000***		***0.013***						***0.017***					0.88	604
	22	0.000		***0.016***										***0.017***	0.88	603
	23	***0.000***			***0.013***					***0.017***					0.88	603
	24	0.000			***0.016***									***0.017***	0.88	603
	25										***0.010***	***0.014***	***0.013***		0.89	673
	26						***0.009***	***0.013***	***0.012***						0.86	550
	27	***-0.002***		***0.043***		***0.000***									0.87	554
	28	***-0.002***			***0.043***	***0.000***									0.87	553
4	29	***0.000***					***0.009***	***0.012***	***0.011***						0.87	421
	30	***0.000***									***0.009***	***0.013***	***0.012***		0.89	520
	31	***0.000***	***0.042***	-0.017						***0.015***					0.88	471
	32	***0.000***	0.027	-0.004										***0.016***	0.88	458
	33	***0.000***	***0.042***		-0.017					***0.015***					0.88	471
	34	***0.000***	0.027		-0.004									***0.016***	0.88	458
	35	***-0.002***	***0.073***	-0.015		***0.000***									0.88	481
	36	***-0.002***	***0.073***		-0.015	***0.000***									0.88	481
5	37	***0.000***		-0.003							***0.010***	***0.013***	***0.012***		0.89	416

Table B.7: Multiple regression models for predicting CSDM-15 for all football helmet impacts with the Hybrid III head with no neck

No. of Variables	Model No.	Peak g	Vi	ΔVR	VR	αR	Δωx	Δωy	Δωz	ΔωR	ωx	ωy	ωz	ωR	Adj R^2	F
1	1	-0.002													0.02	3
	2		***0.109***												0.15	21
	3			***-0.045***											0.03	5
	4				-0.032										0.01	2
	5					***0.000***									0.78	406
	6									***0.017***					0.90	1063
	7													***0.017***	0.91	1128
2	8	-0.001		-0.035											0.03	3
	9	-0.001			-0.019										0.01	2
	10	***-0.001***								***0.017***					0.91	616
	11	0.000												***0.016***	0.91	575
	12			***-0.024***						***0.017***					0.91	601
	13			***-0.018***										***0.016***	0.91	603
	14				***-0.023***					***0.017***					0.91	597
	15				***-0.018***									***0.017***	0.91	606
	16	***-0.002***				***0.000***									0.83	276
	17					0.000				***0.015***					0.90	545
	18					***0.000***								***0.014***	0.91	605
	19			0.000		***0.000***									0.78	201
	20				0.008	***0.000***									0.78	202
3	21	***-0.001***		***-0.014***						***0.017***					0.92	423
	22	0.000		***-0.016***										***0.016***	0.91	399
	23	***-0.001***			***-0.014***					***0.017***					0.92	424
	24	0.000			***-0.017***									***0.016***	0.91	401
	25										***0.012***	***0.010***	***0.011***		0.94	592
	26						***0.012***	***0.010***	***0.010***						0.93	517
	27	***-0.003***		***0.039***		***0.000***									0.85	213
	28	***-0.003***			***0.043***	***0.000***									0.85	223
4	29	***-0.001***					***0.012***	***0.009***	***0.011***						0.94	475
	30	***-0.001***									***0.012***	***0.009***	***0.011***		0.94	470
	31	***-0.001***	-0.039	0.013						***0.018***					0.92	322
	32	0.000	***-0.059***	0.024										***0.019***	0.91	311
	33	***-0.001***	-0.038		0.012					***0.018***					0.92	322
	34	0.000	***-0.053***		0.019									***0.018***	0.91	310
	35	***-0.002***	***0.106***	***-0.046***		***0.000***									0.87	190
	36	***-0.002***	***0.087***		-0.026	***0.000***									0.86	184
5	37	0.000		-0.007							***0.012***	***0.009***	***0.011***		0.94	375

Table B.8: Multiple regression models for predicting MPS for all football helmet impacts with the Hybrid III head with no neck

No. of Variables	Model No.	Peak g	Vi	ΔVR	VR	αR	Δωx	Δωy	Δωz	ΔωR	ωx	ωy	ωz	ωR	Adj R^2	F
1	1	-0.001													0.01	3
	2		***0.122***												0.20	31
	3			-0.029											0.01	2
	4				-0.017										0.00	1
	5					***0.000***									0.79	427
	6									***0.016***					0.89	909
	7													***0.016***	0.89	970
2	8	-0.001		-0.017											0.01	2
	9	-0.001			-0.002										0.00	1
	10	***-0.001***								***0.016***					0.90	499
	11	0.000												***0.016***	0.89	487
	12			-0.009						***0.016***					0.89	458
	13			-0.003										***0.016***	0.89	482
	14				-0.008					***0.016***					0.89	457
	15				-0.004									***0.016***	0.89	482
	16	***-0.002***				***0.000***									0.83	280
	17					***0.000***				***0.013***					0.89	483
	18					***0.000***								***0.012***	0.90	542
	19			0.014		***0.000***									0.79	217
	20				***0.022***	***0.000***									0.79	225
3	21	***-0.001***		0.003						***0.016***					0.89	330
	22	0.000		0.001										***0.016***	0.89	322
	23	***-0.001***			0.002					***0.016***					0.89	330
	24	0.000			0.000									***0.016***	0.89	322
	25										***0.009***	***0.012***	***0.014***		0.94	605
	26						***0.008***	***0.013***	***0.013***						0.93	514
	27	***-0.003***		***0.056***		***0.000***									0.87	268
	28	***-0.003***			***0.059***	***0.000***									0.88	289
4	29	***-0.001***					***0.008***	***0.013***	***0.014***						0.93	404
	30	0.000									***0.009***	***0.012***	***0.014***		0.94	450
	31	***-0.001***	0.016	-0.008						***0.015***					0.89	246
	32	0.000	0.000	0.001										***0.016***	0.89	239
	33	***-0.001***	0.021		-0.012					***0.015***					0.89	247
	34	0.000	0.009		-0.007									***0.015***	0.89	239
	35	***-0.002***	***0.109***	-0.031		***0.000***									0.90	259
	36	***-0.003***	***0.094***		-0.017	***0.000***									0.90	253
5	37	0.001		***-0.017***							***0.008***	***0.013***	***0.013***		0.94	374